Title
Characterizing the Role of Angiopoietin-like 4 in Energy Homeostasis

Author
McQueen, Allison Elizabeth

Publication Date
2017

Peer reviewed|Thesis/dissertation

Characterizing the Role of Angiopoietin-like 4 in Energy Homeostasis

by

Allison Elizabeth McQueen

A dissertation submitted in partial satisfaction of the

requirements for the degree of

Doctor of Philosophy

in

Metabolic Biology

in the

Graduate Division

of the

University of California, Berkeley

Committee in charge:

Professor Jen-Chywan Wang, Chair
Professor Andreas Stahl
Professor James Olzmann
Professor Terry Machen

Fall 2017

Abstract

Characterizing the Role of Angiopoietin-like 4 in Energy Homeostasis

by

Allison Elizabeth McQueen

Doctor of Philosophy in Metabolic Biology

University of California, Berkeley

Professor Jen-Chywan Wang, Chair

The lipoprotein lipase inhibitory function of Angiopoietin-like 4 (ANGPTL4) has been extensively characterized. The purpose of this research is to identify the domain of ANGPTL4 responsible for its lipolytic function and to characterize its physiological and metabolic effects. Also given its lipolytic function, I will try to identify a possible therapeutic role for ANGPTL4.

The introduction outlines the members of the ANGPTL family of proteins. It reviews the physiological functions of ANGPTL4 in metabolism, inflammation, wound healing and angiogenesis. Finally, it examines adipocyte lipolysis and its role in energy expenditure.

The first chapter addresses the *in vivo* effects of overexpression of the ANGPTL4 fibrinogen-like domain on adipose tissue lipolysis and energy expenditure. I hypothesize that the N-terminal coiled-coil domain (CCD) of ANGPTL4 was not required for its lipolytic function. Here I show that the FLD of ANGPTL4 alone stimulates adipocyte lipolysis via the cAMP-PKA pathway. Adenoviral overexpression of ANGPTL4 FLD in mice protects mice against high fat diet induced obesity and ectopic steatosis; increases energy expenditure by inducing beiging of white adipose tissue; and improves glucose homeostasis.

The second chapter addresses the role of ANGPTL4 in glucose homeostasis and seeks to identify the domain responsible for the ANGPTL4-dependent improvement in glucose tolerance in mice. Here I demonstrate that overexpression of ANGTPL4 in mice on high fat diet housed at thermoneutrality and in mice on chow diet improves glucose tolerance by decreasing gluconeogenesis.

The third chapter addresses the role of ANGPTL4 in the regulation of thermogenesis upon cold exposure. Mice lacking ANGPTL4 have lower body temperature and lower energy expenditure when housed at 4°C, room temperature and thermoneutrality. In addition, mice deficient in ANGPTL4 have lower body temperature than wild-type counterparts.

Overall, this study has identified ANGPTL4 as a critical regulator of energy expenditure and as a potential therapeutic target.

For my family, who has been there for all the highs and lows, and especially my parents, Kathleen and David McQueen, who believed in me all along.

Table of Contents

List of Figures

List of Tables

List of Abbreviations

aFAPB	Adipose fatty acid-binding protein
AGPAT2	1-Acylglycerol-3-Phosphate O-Acyltransferase 2
AKT	Protein kinase B
AMPK	Adenosine monophosphate-activated protein kinase
ANGPTL	Angiopoietin-like
ATGL	Adipose triglyceride lipase
AUC	Area under the curve
BAT	Brown adipose tissue
BMI	Body mass index
BMP	Bone morphogenic protein
CaCl2	Calcium chloride
CaMK1	Calcium/Calmodulin Dependent Protein Kinase I
cAMP	Cyclic adenosine monophosphate
CCD	Coiled-coil domain
cDNA	Complimentary deoxyribonucleic acid
CD36	Cluster of differentiation 36
ChREBP	Charbohydrate-responsive element-binding protein
CIDEA	Cell Death-Inducing DFFA-Like Effector A
CLAMS	Comprehensive Laboratory Animal Monitoring System
Cpt1a	Carnitine Palmitoyltransferase 1A
CREB	cAMP response element-binding protein
CRC	Colorectal cancer
CXCR4	C-X-C motif chemokine receptor 4
DEXA	Dual energy X-ray absorptiometry
DGAT2	Diglyceride acyltransferase
DIO	Diet induced obesity
Dio2	Iodothyronine Deiodinase 2
DMEM	Dulbecco's modified eagle medium
ECAR	Extracellular acidification rate
ECM	Extracellular matrix
EGFRvIII	Epidermal growth factor receptor variant type III
EGF	Endothelial growth factor
Elovl3	Elongation Of Very Long Chain Fatty Acids
EMT	Epithelial-to-mesenchymal transition
ERK	Extracellular signal-regulated kinase
eWAT	Epididymal white adipose tissue
FAK	Focal adhesion kinase
FAO	Fatty acid oxidation
FAS	Fatty acid synthase
FFA	Free fatty acid
FGF21	Fibroblast growth factor 21
FGF21	Fibroblast growth factor 19
FIAF	Fasting induced adipose factor
FLD	Fibrinogen-like domain

G6PASE	Glucose-6-phosphatase
GTT	Glucose tolerance test
HDL	High density lipoprotein
HFARP	Hepatic fibrinogen/angiopoietin-related protein
HFD	High fat diet
HOXB4	Homeobox B4
HSC	Hematopoietic stem cell
ITT	Insulin tolerance test
iWAT	Inguinal white adipose tissue
JAK	Janus kinase
KCl	Potassium chloride
KO	Knockout
KRB	Krebs-Ringer buffer
LILRB2	Leukocyte immunoglobulin-like receptor B2
LPL	Lipoprotein lipase
MAG	Monoacylglycerol
MAPK	Mitogen-activated protein kinase
MGL	Monoglyceride lipase
MgSO4	Magnesium sulfate
MMP	Matrix metalloproteinase
mRNA	Messenger ribonucleic acid
NaCl	Sodium chloride
NEFA	Non-esterified fatty acid
NF-κB	Nuclear factor kappa-light-chain enhancer of activated B cells
OCR	Oxygen consumption rate
PAK1	p21 activated kinase 1
PI3K	Phosphatidyl inositol kinase-3
PKA	Protein kinase A
PC	Proprotein convertase
PEPCK	Phosphoenolpyruvate carboxykinase
PGAR	PPARγ angiopoietin-related protein
PGC-1 α	Peroxisome proliferator-activated-γ co-activator-1 α
PKC	Protein kinase C
PPAR	Peroxisome proliferator-activated receptor
Prdm16	PR domain containing 16
PTT	Pyruvate tolerance test
RIFL	Refeeding induced in fat and liver
SCD1	Stearoyl-CoA desaturase-1
SEM	Standard error of the mean
SERCA2	Sarco/endoplasmic reticulum Ca^{2+}-ATPase
SHP2	Src homology region 2 (SH2)-containing protein tyrosine phosphatase 2
SLUG	Snail family transcriptional repressor 2
SNP	Single nucleotide polymorphism
SP1	Specificity protein 1
SREBP-1c	Sterol regulatory element-binding protein 1

STAT3	Signal Transducer and Activator of Transcription
TG	Triglyceride
TGF-β2	Transforming growth factor-beta 2
UCP1	Uncoupling protein 1
VEGF	Vascular endothelial growth factor
VLDL	Very low density lipoprotein
WAT	White adipose tissue
WT	Wild type

Acknowledgements

Throughout graduate school, I have been surrounded by an incredible support system of both family and friends, without whom this would have been a very lonely journey.

I would like to start by thanking my advisor, Jen-Chywan (Wally) Wang for all the advice and encouragement he has provided throughout the years. Wally has been an incredibly supportive mentor—he has always made himself available and willing to discuss experiments, guided me through the publication process, encouraged and gave me the opportunity to go to conferences and meetings and listened to my own thoughts and opinions.

I would also like to thank Suneil Koliwad, our collaborator at UCSF. Suneil has essentially served as a second advisor and has provided so much valuable advice throughout the last several years, in addition to supporting many of my experiments and allowing me to work in his laboratory. Perhaps most importantly, Suneil patiently taught me that there is an art to making figures and made me the figure snob I am today. His enthusiasm and mentorship have been instrumental throughout the publication process.

I am grateful for the help of Dr. Christophe Paillart, who helped me to run the CLAMS and the DEXA machines; Donghui Wang, who performed many, many flawless tail vein injections on my mice; and Martin Valdearcos Contreras and especially Daniel Stifler for their willingness to help me with experiments while I was at UCSF, keep an eye on things when I wasn't, and remotely locate a key when I was locked out of lab.

I would like to thank the members of my dissertation committee—Dr. Andreas Stahl, Dr. James Olzmann and Dr. Terry Machen—for their guidance and insight throughout the years.

I was lucky to have had several wonderful labmates who have become friends during my time in the Wang lab—Dr. Deepthi Kanamaluru, Rebecca Lee and Damian Costello. Thank you for your willingness to share your knowledge, lend a helping hand, and taste-test my baked goods. In particular, a big thank you to Damian for accompanying me on so many UCSF (mis)adventures and providing a lot of laughs along the way.

I would be remiss if I did not thank the many talented undergrads I have worked with throughout the years—in particular, Adeeba Hasan, Kimberly Yan, and Mei-lan Li. My students have played integral parts in helping me gather useful and informative data, in addition to making our time in lab together fun and memorable.

To my Nutritional Sciences and Toxicology department mates—Kevin Tharp, Diyala Shihadih, and especially Vanessa de la Rosa—thank you for your advice, support, encouragement and (often) reagents, but mostly for your friendship.

To my friends Leah, Tara and Jonathan—thank you for choosing me as your roommate, cheering me up after a bad day in lab and always eating my brownies with enthusiasm. To the South Bay crew (especially Kim)—thank you for the laughs, the music, the Thanksgivings, and sharing your pool when Berkeley was unbearably hot. To Francesca, in particular—thank you for all the

delicious dinners, constructive talks, advice, insight and just generally being a wonderful friend over the last three years.

To Jon Dempersmier—thank you for listening to and critiquing too many 292 practices to count, your willingness to give me advice, sharing reagents, sitting through the worst practice oral qualifying exam in history, editing my manuscript and generally teaching me how to be a better scientist. Words cannot express how grateful I am.

Finally, to my parents, Kathy and Dave, and my sisters, Stephanie and Sandra—thank you for always (cautiously) picking up the phone when I call, believing in me and supporting me in everything I do. I could not have done this without you.

Introduction

Introduction

Angiopoietin-like Proteins

The angiopoietin-like (ANGPTL) proteins, a family of proteins quite structurally similar to the four-member angiopoietin family of proteins has been identified over the last two decades. The family is made up of eight proteins, ANGPTL 1-8. All of the ANGPTLs contain an N-terminal coiled coil domain (CCD), while only ANGPTL 1-7 contain a C-terminal fibrinogen-like domain (FLD). While all angiopoietin proteins bind and activate the Tie1 and Tie2 receptor tyrosine kinase (the classic angiopoietin receptors), ANGPTL proteins do not bind these receptors and have therefore been considered orphan ligands (1). Despite the fact that ANGPTLs do not bind the typical angiopoietin receptors many groups have shown that ANGPTLs can in fact regulate angiogenesis. Other groups have also shown that ANGPTLs also play key roles in lipid, glucose and energy metabolism as well as in inflammation, hematopoiesis and cancer—functions that distinguishes them from their angiopoietin counterparts (2,3). Here, I will briefly outline the ANGPTL family of proteins before providing an in depth review of current ANGPTL4 literature.

Angiopoietin-like 1

Angiopoietin-like 1 (ANGPTL1), also known as angioarrestin, was the first member of the ANGPTL family to be identified. It has been shown to be a strong regulator of angiogenesis. Specifically, it plays a key anti-angiogenic role by inhibiting cell proliferation and migration, tubular network formation and adhesion to extracellular matrix proteins (4). In a screen of patients with lung cancer, ANGPTL1 was found to be inversely correlated with invasion and lymph node metastasis (5). *In vitro*, ANGPTL1 suppressed migratory, invasive and metastatic capabilities of both lung and breast cancer cell lines, as well as reduced metastasis in ANGPTL1 overexpressing mice injected with cancer cell lines. Ectopic expression of ANGPTL1 in cancer cells suppressed epithelial-to-mesenchymal transition (EMT), a process by which cells de-polarize and gain migratory and invasive properties which can lead to the initiation of metastasis for cancer progression. This occurred by inducing miRNA630 and subsequently reducing expression of the zinc finger protein SLUG in an $\alpha_1\beta_1$/FAK/ERK/SP1 pathway–dependent manner (5). Additionally, another group reported that downregulation of ANGPTL1 is associated with vascular invasion, tumor thrombus, metastasis and poor prognosis in hepatocellular carcinoma (HCC) (6). *In vitro* and *in vivo* ectopic expression of ANGPTL1 in HCC cells decreased tumorigenicity, cell motility and angiogenesis, while depletion of ANGPTL4 had the opposite effects. Here, once again, ANGPTL1 interacts with the integrin $\alpha1\beta1$ receptor to suppress downstream FAK/Src-JAK-STAT3 signaling (6). Finally, ANGPTL1 mRNA has been shown to be downregulated in colorectal cancer (CRC) tissues (7). By contrast, high ANGPTL1 expression levels are associated with better survival in CRC patients. *In vitro* overexpression of ANGPTL1 in CRC cell lines suppressed migration and invasion and prolonged survival in mouse models *in vivo*. When ANGPTL1 knockdown in CRC cells enhanced migration and invasion. MicroRNA-138 positively correlated with ANGPTL1 expression in CRC tissues and upregulated ANGPTL1 in CRC cells. Inhibition of microRNA-138 reversed the ANGPTL1 inhibition of CRC cell migration (7). Taken together, ANGPTL1 has been identified as a biomarker and potential therapeutic agent in certain cancers as well as has a positive correlation with survival in patients with cancer.

Angiopoietin-like 2

Angiopoietin-like 2 (ANGPTL2) is a circulating glycosylated protein expressed in the heart, adipose tissue, skeletal muscle, kidney and some hematopoietic stem cells (8-10). Circulating levels of ANGPTL2 correlate with adiposity, insulin resistance and inflammation in both mice and humans (10). In a Japanese population, ANGPTL2 levels correlated with age as well as with vascular inflammatory markers, indicating atherosclerotic development in patients with no history of cardiovascular disease (9). In patients with chronic heart failure, ANGPTL2 was elevated in the cardiac tissue and secretion levels of the protein from cardiac tissue increased with age (11). In mice, elevated levels of ANGPTL2 impairs cardiac contractility and induces cardiac dysfunction, while endurance exercise reduces ANGPTL2 expression and ANGPTL2 knockout mice can resist the development of heart failure (11). The detrimental effects of ANGPTL2 on the heart are mediated by its inactivation of AKT-SERCA2a signaling in cardiomyocytes, leading to a decrease in cardiac contractility (11). In severely obese patients, bariatric surgery decreased plasma ANGPTL2 levels which correlate with an improvement in both glucose and insulin homeostasis as well as inflammatory markers (12). In several colorectal cancer (CRC) cell lines, ANGPTL2 expression was highly elevated (13). In human patients, serum ANGPTL2 concentrations were also correlated with development of colorectal cancer, suggesting a potential role for ANGPTL2 as a predictive biomarker for CRC (13). Interestingly, ANGPTL2 expression has been shown to be suppressed by glucocorticoid treatment (14). In both human lung cancer cell lines and tumor samples, ANGPTL2 is highly expressed along with the LILRB2 receptor and this expression pattern adversely correlates with patient prognosis. ANGPTL2 binds LILRB2 to promote lung cancer cell proliferation via SHP2/CaMK1/CREB signaling (15). Overall, ANGPTL2 has been implicated as a mediator in development of insulin resistance in an obese phenotype, development of cardiovascular disease, and proliferation of certain types of cancers. Suppression of ANGPTL2 has emerged as a potential strategy to target insulin resistance and as a potential biomarker in certain cancers.

Angiopoietin-like 3

Angiopoietin-like 3 (ANGPTL3) is a secreted, glycosylated protein expressed mainly in liver (16). The N-terminal CCD is released from the C-terminal FLD and activated when it is cleaved at its linker region by proprotein convertases (17). Its activity is regulated by ANGPTL8 (18). In KK/San mice, low plasma TG levels were identified as the result of a mutation in *Angptl3* (19). Overexpression of ANGPTL3 in these mice increased plasma TG levels. (17). Injection of recombinant ANGPTL3 into C57BL/6 mice increased plasma triglyceride levels, a phenotype attributable to ANGPTL3's reversible reduction in lipoprotein lipase (LPL) catalytic activity (17,20). This LPL inhibitory effect is enhanced when the ANGPTL3 CCD alone is injected into mice (17). The ANGPTL3 hypertriglyceridemic effect occurs mainly in the fed state, indicating that ANGPTL3 manly affects lipid uptake in a post-prandial manner (21). In fasted and refed *Angptl3* KO mice, white adipose tissue (WAT) uptake of TGs from VLDL is disrupted, and uptake of VLDL TGs by WAT, skeletal muscle and BAT was not changed by refeeding, indicating that ANGPTL3 plays a key role in promoting uptake of TGs by WAT (rather than other oxidative tissues) in the fed state (22).

Genome wide scans in European populations indicate a positive correlation between plasma ANGPTL3 and TG levels (23). In individuals affected by familial combined hypolipidemia, it has been shown that the low plasma TG phenotype is due to a loss of function mutation in the *Angptl3* gene (24). *Angptl3* deficient patients demonstrate enhanced insulin sensitivity, LPL activity and decreased plasma free fatty acids, indicating a role in lipid and glucose metabolism (25). ANGPTL3 has also been implicated as having a role in development of atherosclerosis. One group has shown that knockdown of ANGPTL3 in apoE-deficient mice protects mice against development of atherosclerosis (26). In a phase I clinical trial, human subjects were dosed with antisense oligonucleotides targeted to *Angptl3* mRNA (27). Those who received the treatment displayed reduced levels of ANGPTL3 protein and several atherogenic lipoproteins--including plamsa TG, LDL cholesterol, VLDL cholesterol, and non-HDL cholesterol (27).

Angiopoietin-like 5

Angiopoietin-like 5 (ANGPTL5) was identified during a large scale DNA sequencing of the human fetal brain and has been found to be expressed mainly in the human heart (28). To date, ANGPTL5 has only been identified in humans, with no orthologs identified in other species (3). One report has shown that ANGPTL5 stimulates *ex vivo* expansion of hematopoieic stem cells, a proliferative effect that is synergized when HSCs are treated with both ANGPTL5 and IGF binding protein (29).

HSCs were cultured with ANGPTL5 *in vitro* and then engrafted into immunodeficient (NOD-*SCID Il2rg*$^{-/-}$, or NSG) mice where they maintained the capacity for long term engraftment in both neonate and adult recipients (30). Interestingly, ANGPTL4 can similarly maintain this repopulation capacity of HSCs engrafted into NSG mice (31). In an RNAseq analysis, ANGPTL5 was identified as a biomarker in stage III lung adenocarcinoma (32). In the Dallas Heart Study population, subjects with plasma TG in the lowest quartile had a loss of function mutation in either ANGPTL5, ANGPTL3 or ANGPTL4, indicating that in humans, ANGPTL5 plays a non-redundant role in TG metabolism (33).

Angiopoietin-like 6

Angiopoietin-like 6 (ANGPTL6) (also known as angiopoietin-like growth factor, AGF) is produced and secreted by the liver (34). It has been identified as an angiogenic factor which promotes chemotaxis in endothelial cells and induces vascularization and vascular leakiness, although the receptor that mediates this function is unknown (34). Like other ANGPTL proteins, ANGPTL6 has metabolic effects. While complete ablation of ANGPTL6 is mostly embryonic lethal, surviving *Angptl6* -/- mice display marked obesity; lipid accumulation in liver, skeletal muscle and brown adipose tissue (BAT); lowered whole body oxygen consumption and insulin resistance. Conversely, *Angptl6* transgenic mice were leaner with enhanced energy expenditure and increased insulin sensitivity (35). In a model of deficient mitochondrial oxidative phosphorylation function, in both mice and cultured adipocytes, upregulation of ANGPTL6 has been identified to increase PPARα expression. This subsequently increases FGF21 expression and β-oxidation, indicating that ANGPTL6 expression is regulated by mitochondrial function and is required for FGF21 production in adipocytes and adipose tissue (36). In human subjects, ANGPTL6 levels positively correlate with serum thyroid stimulating hormone and negatively with

thyroxine levels. Similarly, subjects with hypothyroidism had higher serum levels of ANGPTL6 (37). More recently, in an analysis of candidate genes in European children with severe early onset obesity, higher numbers of rare variants in *Angptl6*, a gene known to be associated with obesity, were identified in obese subjects (38).

Angiopoietin-like 7

Genomic analyses have revealed that Angiopoietin-like 7 (ANGPTL7) mRNA is expressed in neural tissues, melanotic melanoma, and uterus endometrial cancer. In mice, ANGPTL7 mRNA is expressed in the four cell embryo, synovial fibroblasts, thymus, uterus and testis (39). As observed with other ANGPTLs, ANGPTL7 promotes HSC and progenitor cell expansion as well as increases repopulation activity of human hematopoietic progenitors in xenografts in immunodeficient mice. RNA sequencing revealed that ANGPTL7 mediates HSC expansion through CXCR4/HOXB4/Wnt downstream signaling (40). While the role of ANGPTL7 in inflammation has not been extensively characterized, one group has shown that increased expression of ANGPTL7 in macrophages lead to increased gene expression of inflammatory markers and antagonized the effects of anti-inflammatory factors. These effects were mediated by the P38 mitogen-activated protein kinase (MAPK) signaling pathway (41). Human microarray studies have identified ANGPTL7 as being downregulated in colorectal cancer tumors (42). Human ANGPTL7 has been characterized as a potent target gene of the WNT/beta-catenin signaling pathway and thus has been identified as an oncological therapeutic target (39). In another bioinformatics study, ANGPTL7 has been identified as a marker (along with two other protein coding genes and two long non-coding RNAs) whose high expression level correlates with poor prognosis in patients with esophageal carcinoma (43). In a study in which obese and non-obese patients were subjected to three months of physical activity, circulating ANGPTL7 was increased in obese patients and its levels correlated with plasma TG levels. However, physical activity reduced circulating and adipose tissue ANGPTL7 levels in those patients (44).

Angiopoietin-like 8

Angiopoietin-like 8 (ANGPTL8) (also known as "refeeding induced in fat and liver, RIFL; lipasin) is an unusual member of the ANGPTL family in that while it has an N-terminal CCD, it lacks a C-terminal FLD (18,45). ANGPTL8 is mainly expressed in WAT, BAT and liver (45). Its expression is upregulated by cold exposure and high fat diet and downregulated by fasting (45). *Angptl*8-/- mice have reduced plasma TG compared to controls while ANGPTL8 levels are increased in ob/ob mice (46). Interestingly, several groups have shown that exerts its effects coordinately with ANGPTL3. While there was no change in mice expressing ANGPTL3 alone, Expression of ANGPTL8 alone increases plasma TG and coexpression of ANGPTL3 and 8 results in a synergistic increase in plasma TG and mice develop hypertriglyceridemia (18). ANGPTL8 expression hepatocytes increases the presence of cleaved ANGPTL3 in the media indicating that ANGPTL8 activates ANGPTL3 (18). ANGPTL8, similar to ANGPTL3 and 4, inhibits lipoprotein lipase activity *in vitro* and consequently adenoviral overexpression of ANGPTL8 in mice increases plasma TG levels (47). In human adipocytes cultured in a medium of liposaccharide-stimulated macrophages, ANGPTL8 mRNA is suppressed by the induction of microRNA-221-3p (48). In mice, ANGPTL8 in WAT is induced by insulin and inhibits lipolysis (49). Consistently, knock-

down of ANGPTL8 in cultured adipocytes reduced cellular TG levels and led to increased release of non-esterified fatty acids into the medium (49).

Angiopoietin-like 4

Structure, Expression and Transcriptional Regulation of ANGPTL4

Initially, ANGPTL4 (also known as fasting induced adipose factor, FIAF; hepatic fibrinogen/angiopietin-related protein, HFARP; PPARγ angiopoietin-related protein, PGAR) was identified as a secreted glycoprotein in the plasma. In humans, ANGPTL4 is most highly expressed in liver and adipose tissue, but is also detectable in thyroid, brain and small intestine, as well as circulates in plasma (50). In mice, ANGPTL4 is most highly expressed in white and brown adipose tissue, liver and placenta (51-53). The *Angptl4* gene is highly conserved, maintaining approximately a 77% amino acid sequence similarity with that of mice (54).

A ≈45 kDa protein, ANGPTL4 consists of an amino-terminal coiled coil domain (CCD) and a carboxyl-terminal fibrinogen like domain (FLD) connected by a cleavable linker region, structurally similar to ANGPTLs 1-7. ANGPTL4 contains a signal sequence for protein secretion, a highly hydrophobic sequence of amino acids, which is located within the N-terminal domain (51).

ANGPTL4 levels are altered depending on nutritional status and is controlled by a variety of factors. Namely, ANGPTL4 is upregulated by fasting and caloric restriction, in obese and diabetic states (in both mice and humans) during cold exposure, by glucocorticoids, by thyroid hormone, under hypoxic conditions and by free fatty acids (53,55-61). Conversely, ANGPTL4 is downregulated by insulin signaling, in a fed state, and during high fat diet feeding (52,62,63).

Transcriptional regulation of ANGPTL4 is complex and several transcription factors have been identified in the regulation of *Angptl4* mRNA. In the fasted state, upregulation of ANGPTL4 is mediated by glucocorticoids, whereas in a state of caloric restriction its expression is increased by an increase in circulating free fatty acids, which in turn activate PPARα and PPARβ/δ transcription factors to increase *Angptl4* mRNA transcription (50,61). ANGPTL4 has also been identified as a transcriptional target of PPARγ in adipocyte differentiation (53). In both human fetal and rat neonatal cardiomyocytes, hypoxia and subsequent upregulation of hypoxia-inducible factor 1α (HIF-1α) led to upregulation of *Angptl4* mRNA via PPARα (64). PPARα and hypoxia can also lead to synergistic activation of transcription of Angptl4 mRNA in cardiomyocytes (64).

Processing of ANGPTL4

As the functions of ANGPTL4 have become better understood, so has understanding of the processing of the protein itself. As already mentioned, ANGPTL4 is made up of an N-terminal CCD and a C-terminal FLD. Proteolytic processing of ANGPTL4 is tissue dependent. In medium from cultured liver cells, secreted ANGPTL4 is detected in three forms: full length, the carboxy-terminal FLD and the amino-terminal CCD (65). Additionally, in both human and mouse plasma, ANGPTL4 is detected in both its full length and truncated forms indicating tissue-dependent processing mechanisms (57). Initially, in Huh7 cells, a human liver cell line transfected with

plasmid for full length ANGPTL4, ANGPTL4 appeared in the media and the cleaved products appeared during incubation, indicating that cleavage occurs outside the cell (65). Full length ANGPTL4 is cleaved at a proprotein convertase (PC) consensus site within the linker region between the N- and C-termini (65). Only certain PCs are capable of cleaving ANGPTL4 including furin, PC5/6, paired basic amino acid cleaving enzyme 4 and PC7 (65). White adipose tissue (WAT), on the other hand, secretes mainly full length ANGPTL4 (57). In order to perform its functions, ANGPTL4 may be proteolytically cleaved. Full-length ANGPTL4 can oligomerize to higher order structures via disulfide bonds formed between ANGPTL4 N-terminal domains (66). Upon oligomerization, ANGPTL4 can form either dimers or tetramers and this oligomerization is required for its ability to inhibit lipoprotein lipase (67). The C-terminal domain of ANGPTL4 is not capable of oligomerization (66).

ANGPTL4 ***and lipid metabolism***

ANGPTL4 has perhaps been the most extensively characterized in the context of lipid metabolism. Initially, discovery of ANGPTL4 as a transcriptional target of PPARs indicated a potential role within lipid metabolism. To date, ANGPTL4 has been identified as having two distinct roles in lipid metabolism: inhibition of extracellular lipoprotein lipase (LPL) and induction of intracellular lipolysis.

Initially, experiments involving intravenous administration of recombinant ANGPTL4 in mice revealed a marked increase in plasma triglyceride (TG), non-esterified fatty acids (NEFA), and non-HDL cholesterol (68). Further *in vitro* experiments demonstrated that ANGPTL4 inhibits LPL, providing an explanation for the hyperlipidemic effect (68). In another study, adenoviral mediated overexpression of ANGPTL4 caused a similar hyperlipidemic effect (69). However, increased ANGPTL4 levels did not increase plasma VLDL levels, a phenotype that would suggest ANGPTL4 either increased VLDL output from the liver or inhibited VLDL clearance (69). While ANGPTL4 had no effect on VLDL secretion, it did in fact delay VLDL clearance from the plasma due to inhibition of LPL (69). Various other studies have confirmed the role of ANGPTL4 in LPL inhibition: hepatic adenoviral overexpression of full length ANGPTL4 resulted in hyperlipidemia and enlarged and fatty liver, as well as increased plasma TG, FFA and cholesterol levels in both chow- and high fat diet-fed C57BL/6 mice and in a diabetic (db/db) mouse model (70,71). *Angptl4*$^{-/-}$ mice have reportedly higher LPL mRNA expression in muscle in addition to overall increased LPL activity as well as lower fasting plasma TG and cholesterol levels compared to WT controls (21,72-74). Interestingly, treating WT mice with an anti-ANGPTL4 antibody mimics the *Angptl4*$^{-/-}$ lipid phenotype (75). Male *Angptl4* $^{-/-}$ mice display increased weight gain as a result of increased epididymal fat pad size; however, female *Angptl4*$^{-/-}$ mice displayed no difference in weight gain, indicating that this may be a sex-specific phenotype (76).

Initially, it was reported that the CCD alone is sufficient to form oligomeric structures (77). Further site-directed mutagenesis revealed that two cysteine residues within the CCD are required for oligomerization. This mutated form of CCD, when expressed in mice, attenuates the increased plasma TG levels that are observed in mice overexpressing WT ANGPTL4. Also within the CCD is a highly conserved hydrophobic amino acid sequence which, when mutated, abolishes the LPL inhibitory effect (67). Interestingly, treatment with a peptide consisting of only the CCD's conserved amino acid motif mimics the ANGPTL4 LPL inhibitory effect (67).

There are conflicting reports regarding how ANGPTL4 exerts its LPL inhibitory function. Initially, it was reported that ANGPTL4 inhibits LPL by binding transiently to LPL, causing the catalytically active dimerized LPL subunits to separate, irreversibly, into inactive monomers (78). More recently, it has been suggested that, rather than a catalytic inhibitor of LPL, ANGPTL4 reversibly forms an LPL-ANGPTL4 complex to act as a nonocompetitive inhibitor to prevent TG hydrolysis by the enzyme (79). This model is also consistent with an *in vivo* study in which ANGPTL4-LPL complexes were identified in the plasma of ANGPTL4 overexpressing mice (71,80).

ANGPTL4 has also been identified as an inducer of intracellular lipolysis within adipocytes. In one study, treatment of isolated adipocytes from WT and *Angptl4* $^{-/-}$ mice with purified human ANGPTL4 promoted lipolysis (81). Fasting-induced *ex vivo* glycerol release (a marker of lipolysis) and intracellular TG hydrolysis was reduced in both epididymal and inguinal fat pads from *Angptl4*$^{-/-}$ mice (81). Mechanistically, it has been shown that this induction of lipolysis occurs through increased cAMP signaling (81). *Angptl4*$^{-/-}$ mice also display decreased phosphorylation of perilipin and hormone sensitive lipase (two proteins that mediate lipolysis) upon fasting compared to controls, consistent with decreased ANGPTL4-mediated lipolysis (81). Consistent with a lipolytic effect, several *in vivo* studies have reported increased plasma FFA in mice overexpressing ANGPTL4 (70,71,81). Similarly, in humans, plasma ANGPTl4 also correlates with increased plasma non-esterified fatty acids, indicative of increased lipolysis (82).

Given its role in inhibition of LPL and the fact that ANGPTL4 expression is upregulated during fasting indicated that ANGPTL4 may play a role in shunting lipids away from adipose tissue in times of energy deficit. This role was validated in a study in which Angptl4 mRNA was upregulated early in fasting (before a long term-fasted catabolic state is induced) (83). Radiolabeled chylomicrons administered to fasted WT and *Angptl4*$^{-/-}$ mice were cleared more quickly in *Angptl4*$^{-/-}$ mice; the adipose tissue of the *Angptl4*$^{-/-}$ mice displayed the highest levels of radiolabeled TG; and LPL activity was increased during fasting in *Angptl4*$^{-/-}$ mice indicating that ANGPTL4 diverts TG away from adipose tissue by inhibiting LPL in the fasted state (83). There are two limitations to this study. First, the role of ANGPTL4 in other tissues during fasting has not yet been fully elucidated. ANGPTL4 is induced in other tissues such as liver, heart and skeletal muscle upon fasting, although to lower levels than in adipose tissue. A tissue-specific knockout would be useful to study these other roles. Second, this study does not examine the second function of ANGPTL4—lipolysis—in the context of fasting. One hypothesis is that if ANGPTL4 were inhibiting LPL as well as inducing lipolysis in adipocytes during fasting, that the lipids could then be shunted to other tissues. This is the case in a second study examining the role of ANGPTl4 in mice during cold exposure. During cold exposure, ANGPTL4 is downregulated in brown adipose tissue (BAT) during long term cold exposure which promotes LPL activity and subsequent uptake of plasma TG whereas in WAT, ANGPTL4 is upregulated (55). This divergent regulation leads to a net shift toward lipid uptake by BAT, presumably to drive thermogenesis (55). This concerted response is likely due to differential activation of AMPK (55). Overall, it is likely that ANGPTL4, with its dual LPL inhibitory and lipolytic inducing functions, drives a concerted mechanism in both the fasted and cold exposed states to divert lipids from accumulation and storage in WAT to other tissues for utilization.

ANGPTL4 ***and glucose homeostasis***

Given that regulation of its expression is altered by nutritional status, it was initially hypothesized that ANGPTL4 also played a role in glucose homeostasis (53). Hepatic overexpression of ANGPTL4 in chow-fed and high fat diet-fed C57BL/6 mice improved glucose tolerance and decreased blood glucose levels in both fasted and fed states (70,71). In a diabetic mouse model, ANGPTL4 overexpression alleviates hyperinsulinemia, hyperglycemia and glucose intolerance. Interestingly, qPCR analysis revealed that expression of two gluconeogenic genes—*PEPCK* and *G6Pase*—were lowered in the livers of ANGPTL4 overexpressing mice, while several lipogenic genes, including FAS and SCD1, were increased, indicating a potential diversion of substrates to lipogenesis from gluconeogenesis. Additionally, adenoviral expression of ANGPTL4 in rat primary hepatocytes suppressed glucose production and enhanced insulin sensitivity. This suggests a potential mechanism that ANGPTL4 may suppress glucose output in the liver (70). There is evidence for a similar correlation in humans, as ANGPTL4 levels are decreased in patients with type two diabetes and have inversely correlated levels of plasma glucose (70).

ANGPTL4 ***and food intake***

There are conflicting reports regarding the effect of ANGPTL4 and food intake. ANGPTL4 is expressed in the brain—specifically in the ipsilateral cortex and the hippocampus (84).
In mice, adenoviral overexpression of ANGPTL4 two weeks after tail vein injection did not affect food intake or body weight (70). In another study, hypothalamic Angptl4 mRNA expression was decreased during fasting and increased upon food intake, indicating differential expression of ANGPTL4 in the central versus peripheral axes dependent upon nutritional state (76). While there was no observed difference in food intake between *Angptl4*$^{-/-}$ and wild-type mice fed ad libitum, *Angptl4*$^{-/-}$ mice had increased food intake after a fast (76). Administration of either full length ANGPTL4 or the ANPGTL4 FLD directly to the hypothalamus decreased food intake indicating that the FLD is responsible for this phenotype (76). Consistently, both full length ANGPTL4 and FLD administration to the hypothalamus also resulted in reduced weight gain. This effect is mediated by suppression of hypothalamic AMPK activity (76). To date, it has not been shown that ANGPTL4 can cross the blood brain barrier, so this could potentially explain the discrepancies in food intake based on central or peripheral administration. More research is needed to fully understand the differential effects of ANGPTL4 on food intake.

ANGPTL4 ***and energy expenditure***

Agents that increase energy expenditure has become an increasing attractive target in the treatment of obesity. *Angptl4* -/- mice have reduced energy expenditure while central administration of full length ANGPTL4 increases energy expenditure in C57BL/6 mice (76). This phenotype is likely due to a suppressive effect on hypothalamic AMPK by ANGPTL4. To date, no study has studied the effects of ANGPTL4 on energy expenditure in the context of peripheral overexpression or injection. One way to increase energy expenditure is in response to a cold environment. Studies have shown that cold exposed rodents can also activate non-shivering thermogenesis, a process performed by activated brown adipose tissue, leading to increased energy expenditure (85). Interestingly, the study that identified the role of ANGPTl4 in shunting plasma TG to BAT during cold exposure did not examine energy expenditure, although the process is governed by differential

activation of AMPK. Further studies should be performed to identify whether ANGPTL4 affects energy expenditure during cold exposure as this could be a novel therapeutic target.

ANGPTL4 ***and the gut microbiome***

Over the last decade, there has been mounting evidence of the link between the gut microbiome and metabolic disorders. Several potential factors involved in metabolic regulation have been identified as being modulated by gut microbiome composition—in particular, ANGPTL4. As already addressed, ANGPTl4, in addition to adipose tissue and liver, is expressed in the intestine, and is in fact produced and secreted by entero-endocrine cells that line the intestine, and is a potent inhibitor of lipoprotein lipase (86). Initial studies first identified ANGPTL4 as being selectively suppressed in the intestinal epithelium of mice that had a normal gut microbiome composition compared to germ free mice (87). When a normal gut microbiome was introduced into germ free mice, this led to the suppression of *Angptl4* mRNA expression in the small intestine, but not in adipose tissue or liver (87). As also previously mentioned, PPARα controls Angptl4 gene expression. Interestingly, absence of PPARα in either a germ free or normal gut microbiome-reintroduced mouse model did not affect microbiome suppression of Angptl4, indicating that PPARα does not mediate this response (87). Further work indicated that when *Angptl4*$^{-/-}$ mice were rederived as germ free, these mice lost their resistance to diet induced obesity when fed a high fat diet (88). These mice also had reduced expression of Pgc-1α, a PPAR coactivator, as well as various other fatty acid oxidation genes (88). In WT germ-free mice compared to control WT mice with normal gut microbiota, elevated ANGPTL4 levels in the intestine increased expression of Pgc-1α (88). Essentially, "normal" microbial colonization of the gut of germ-free mice leads to increased processing of dietary polysaccaharides to monosaccharides which are then taken up by the liver to be utilized in hepatic lipogenesis. Simultaneously, these bacteria downregulate Angptl4 expression to upregulate LPL activity. Both of these pathways lead to increased TG storage in the adipose tissue. This establishes ANGPTl4 as a mediator of the microbiome as a potential factor that can lead to obesity. This upregulation of ANGPTL4 is likely due to an increase in short chain fatty acids—in particular, C4, the production of which, is due to an increase of C4 producing bacteria (89,90).

ANGPTL4 ***Variants***

Several single nucleotide polymorphisms (SNP) in ANGPTL4 have been identified. Of these, the two most physiologically relevant (and beneficial) appear to be the ANGPTL4 E40K mutation, in which the glutamic acid at position 40 is replaced with a lysine and the ANGPTL4 T266M mutation, in which a threonine at position 266 is replaced by a methionine. In several separate studies, human carriers of the ANGPTL4 E40K mutation had lower plasma triglyceride levels than non-carriers and this point mutation was also associated with protection against coronary artery disease (91-93). Consistent with these findings, while overexpression of wild-type ANGPTL4 in mice causes marked hypertriglyceridemia, overexpression of ANGPTL4 E40K eliminates the hypertriglyceridemic effect (77). This is due to the fact that the ANGPTL4 E40K mutant can no longer inhibit lipoprotein lipase (77). ANGPTL4 E40K has also been associated with lowered risk for cardiovascular disease (94). More recently, GWAS studies identified a second mutation within the CCD, denoted ANGPTL4 E15K (92). This mutation occurs in ~3% of Caucasian populations and is, interestingly, also associated with lowered plasma TG levels and reduced risk of coronary

heart disease. Experiments using recombinant ANGPTL4 E15K revealed that this mutant has impaired ability to inhibit LPL (95).

The ANGPTL4 T266M mutation occurs more frequently than that of E40K; however, conflicting reports indicate that T266M is either not associated with plasma triglyceride levels or that T266M, while being associated with lowered plasma TG levels compared to WT ANGPTL4, has a lessened effect on lowering plasma TG levels compared to E40K (94,96). This is consistent with the fact that the T266M mutation is in the carboxy-terminus of ANGPTL4, while the LPL inhibitory function is associated with the amino-terminal fragment. Interestingly, unlike E40K which has not been shown to affect plasma glucose levels, carriers of T266M administered an oral glucose tolerance test cleared the glucose more slowly than non-carriers (96). Unfortunately, no animal studies have been performed to further elucidate the physiological effects of the T266M mutation.

Until recently, the majority of SNPs identified have been associated with metabolic disorders. However, T266M has recently been linked to reduced tumor invasiveness (97). In this study, binding affinity of the recombinant cANGPTL4 T266M variant to $\alpha 5\beta 1$ integrin was reduced compared to wild-type cANGPTL4, leading to reduced downstream PI3K/PKBα and ERK signaling which lead to anoikis resistance and invasiveness. Treatment of human hepatoma cells (HepG2) with T266M (versus WT control) reduces tumor cell proliferation. Upon injection of HepG2 cells expressing either the T266M variant or WT c-terminal ANGPTL4 into immunodeficient mice, tumors resulting from the T266M derived cells were much smaller tumors as well as more apoptotic cells compared to controls (97). Finally, treatment with recombinant T266M in cANGPTL4 deficient HepG2 cells did not restore glucose uptake to the same extent as treatment with WT c-terminal ANGPTL4, an effect due to reduced *Glut2* expression (97).

ANGPTL4 ***and inflammation***

Obesity and high fat diet have long been linked with inflammation. Given its role in lipid metabolism, it stands to reason that ANGPTL4 would play some role in inflammation as well. Interestingly, much of the work linking ANGPTL4 to inflammation indicates a protective role.

When placed on a high fat diet, mice lacking ANGPTL4 develop a severe phenotype characterized by fibrinopurulent peritonitis and fluid in the peritoneal cavity, inflammation that originates from enlarged mesenteric lymph nodes (98). These mice develop foam cells and inflammation within mesenteric lymph node macrophages (98). Treatment of macrophages loaded with chyle (fluid consisting of fat droplets and lymph that passes to the lymphatic system during digestion) with recombinant ANGPTL4 prevented lipid uptake and reduced inflammation as evidenced by a reduction in inflammatory markers (98). Treatment with ANGPTL4 also reduced chyle-induced ER stress in macrophages and formation of foam cells (98). In mice, ANGPTL4 deficiency exacerbates colonic inflammation in a dextran sulfate sodium salt-induced colitis model by driving the development of a colonic inflammatory gene expression profile as well as increasing infiltration of immune cells (99). *In vitro*, the c-terminus of ANGPTL4 upregulates tristetraprolin expression via CREB and NF-κB to regulate chemokine transcript stability and protect against acute colonic inflammation (99). Lipid accumulation in macrophages significantly contributes to the development of atherosclerosis. Macrophage derived ANGPTL4 has been shown to play a protective role in the development of atherosclerosis (100).

Hematopoietic-specific deficiency of ANGPTL4 promotes development of atherosclerosis and leukocytosis, which is associated with increased cardiovascular risk in humans (100). Hematopoetic ANGPTL4 prevents lipid overloading in macrophages and development of foam cells (100).

ANGPTL4 ***in keratinocyte migration and wound healing***

Relatively recently, it was discovered that ANGPTL4 interacts with proteins of the cell matrix to regulate wound healing. In keratinocytes, Angptl4 has been identified as a target gene of PPARß/δ and as being secreted by wound keratinocytes in mice (101). On the keratinocyte cell surface, the C-terminus of ANGPTL4 interacts with two extracellular matrix proteins, vitronectin and fibronectin (an interaction disrupted upon treatment with an anti-C-terminal ANGPTL4 antibody) but does not impair their ability to bind their integrin receptor, ß5 (101). Through this interaction, ANGPTL4 delays the degradation of the matrix proteins (101). *Angptl4*$^{-/-}$ mice display impaired wound re-epithelialization as well as keratinocyte specific impairment of cell adhesion and migration (101,102). By mediating the binding of vitronectin and fibronectin to their receptors, ANGPTL4 mediates signaling of the integrin-FAK-14-3-3-PKC pathway to induce keratinocyte migration (101). In addition, ANGPTL4 has been identified as *directly* interacting with ß1 and ß5 integrins even in the absence of matrix proteins leading to the subsequent activation of the FAK-Src-PAK1 pathway resulting in cell migration (102). Given the role of ANGPTL4 in keratinocyte migration and wound healing combined with its roles in lipid and glucose metabolism, it has been suggested that ANGPTL4 could have a promising role in wound healing in diabetic patients who often experience impaired wound healing (103).

ANGPTL4 ***and angiogenesis—Evidence for both a stimulatory and a suppressive role in tumorigenesis***

Angiogenesis is important in tumorigenesis and cancer progression. Given the structural similarity between the angiopoietins and the angiopoietin-like proteins, ANGPTL4 has been studied for its potential role in angiogenesis. Early on, the role of ANGPTL4 in angiogenesis and vascular permeability was somewhat controversial. Early studies indicated that *in vitro* treatment of vascular endothelial cells with ANGPTL4 inhibited VEGF-induced proliferation, chemotactic activity and tubule formation in addition to decreased vascular leakiness (104). *In vivo*, mice implanted with pellets containing VEGF and ANGPTL4 in the cornea displayed inhibited growth of capillary pellets compared to mice implanted with only VEGF (104). Later on, it was shown that full length ANGPTL4 accumulates in the extracellular matrix (ECM) of vascular endothelial cells in response to hypoxia *in vitro*, where it binds and interacts with heparin and heparan sulfate proteoglycans to inhibit endothelial cell adhesion to the ECM and inhibit endothelial cell migration (105). ANGPTL4 has further been shown to prevent metastasis by inhibiting vascular activity as well as tumor cell motility and invasiveness *in vivo* (106).

More recently, however, a pro-angiogenic role has been identified for ANGPTL4. Upregulation of ANGPTL4 has been observed in several types of cancer and is frequently associated with metastasis. As already addressed, *Angptl4* mRNA is upregulated in endothelial cells under hypoxic conditions (107). In tumors, ANGPTL4 is produced in necrotic regions (107). ANGPTL4 has been identified as a marker of conventional renal cell carcinoma indicating a potential new role as

a therapeutic target (107). ANGPTL4 is upregulated by a mutant form of epidermal growth factor receptor variant type III (EGFRvIII) in glioblastomas and promotes tumor angiogenesis both *in vivo* and *in vitro* via the ERK/c-Myc pathway (108). Knockdown of *Angptl4 in vivo* suppressed tumor growth in malignant glioma (108). Prostaglandin E(2) and hypoxia synergistically promote ANGPTL4 expression which in turn promotes colorectal cancer growth via STAT1 signaling both *in vivo* and *in vitro* (109). Elevated levels of both ANGPTL4 and STAT 1 are both detected in human colorectal cancer specimens as well (109). Upregulation of ANGPTL4 by TGFβ in mammary tumor cells primes the cancer cells for metastasis to the lungs by mediating endothelial disruption which allows the cells to pass through tight lung endothelial junctions (110). In a giant cell tumor model in bone, ANGPTL4 is highly expressed (111). In this model, TGF-β2 released by osteoclasts leads to induction of ANGPTL4 expression which in turn promotes tumor progression; while knockdown of Angptl4 in giant cell tumor stromal cells suppressed tumor growth and giant cell formation *in vivo (111)*. In head and neck squamous cell carcinoma, ANGPTL4 expression is induced by endothelial growth factor (EGF) (112). Upregulation of ANGPTL4 by EGF promotes tumor-endothelial cell interaction and resistance to anoikis (112). Mechanistically, ANGPTL4 binds to integrin β1 to upregulates several matrix metalloproteinases (MMPs) to promote cell metastasis (112). Other groups have also that MMP expression is also dependent upon ANGPTL4 and correlates with cancer metastasis in colorectal cancer and melanoma (113,114).

At the site of a bone fracture, which develops hypoxia at the site of the damage, ANGPTL4 is upregulated (115). Cultured osteoblasts also had increased Angptl4 mRNA levels under hypoxic conditions and treatment of osteoblasts with ANGPTL4 increased osteogenic gene expression in addition to *Vegf* (vascular endothelial growth factor, an angiogenic factor) expression, indicating a role for ANGPTL4 not only in angiogenesis, but also in osteogenesis (115).

One drawback of these studies is that the majority of these studies investigate the effect of full length ANGPTL4, not which domain in particular might be responsible. Interestingly, in metabolic studies in which ANGPTL4 is overexpressed in mice, no tumor development has been observed. Overall, ANGPTL4 could be a link between hypoxia-induced angiogenesis and metabolic disease.

ANGPTL4*: No Longer Entirely an "Orphan Ligand"*

Notably, like other members of the ANGPTL family of proteins and unlike the angiopoietins, ANGPTL4 does not bind to the Tie1 or Tie2 receptors (51). Until recently, ANGPTL4 was considered an "orphan ligand" as its receptors were unknown. Over the past decade, however, integrins ß1 and ß5 have been identified as receptors for ANGPTL4 on the keratinocyte cell surface (102). In addition, receptors for ANGPTL4 have been identified on both human and mouse hematopoietic stem cells (HSC)-- immune-inhibitory receptor human leukocyte immunoglobulin-like receptor B2 (LILRB2) and paired immunoglobulin-like receptor (PIRB), respectively (116). Binding of ANGPTL4 to these receptors results in *ex vivo* expansion of HSCs. In mice, binding and activation of the PIRB receptor supports the development of leukemia (116). In terms of its metabolic roles, though, ANGPTl4 may still be considered an orphan ligand as its receptors in the liver and adipose tissue are yet to be identified. Given the prolific role of ANGPTL4 in lipid and glucose metabolism, identification of its receptor in both adipose tissue and liver would go a long way toward clarifying lingering questions regarding its metabolic effects.

Lipolysis, PKA and Energy Expenditure

Lipolysis in adipocytes

White adipose tissue is the major site of energy storage in the body whereas brown adipose tissue (BAT) is the major site for cold-induced non-shivering thermogenesis, characterized by its hallmark protein, uncoupling protein-1 (UCP1). In both tissues, lipids are stored mainly as triacylglycerol (TAG) within lipid droplets inside adipocytes. Lipolysis, the hydrolysis of TAG to glycerol and free fatty acids (FFA), for the purpose of releasing FFAs to be utilized for energy by other organs, is a characteristic specific to adipocytes. During lipolysis, sequential hydrolysis occurs, generating first diacylglycerol (DAG), then monoacylglycerol (MAG), which is finally hydrolyzed to glycerol and a free fatty acid. Several enzymes are involved in this process. Hormone sensitive lipase (HSL) can hydrolyze both TAG and DAG, although, at least in vitro, HSL has been shown to be more active when utilizing DAG as a substrate as opposed to TAG (117). Desnutrin (also known as ATGL) is considered to be the major TAG-specific lipase, expressed most highly in adipose tissue, but also at lower levels in cardiac and skeletal muscle (118). TAG hydrolases have also been discovered as lipases that mediate TAG lipolysis in an HSL-independent manner in adipose tissue and in the liver, where they may play a role in synthesis of VLDL (119,120). Adiponutrin, another lipase expressed highly in adipose tissue, is also responsible for TAG hydrolysis, although, unlike other lipases, is highly upregulated upon refeeding (121). Hydrolysis of TAG results in a FFA and DAG. As already mentioned, HSL is highly specific for DAG. To date, it is the only lipase that has been identified that acts upon DAG (122). Finally, the resulting MAG is hydrolyzed by monoglyceride lipase (MGL) (123).

Lipolysis occurs through a similar mechanism in brown adipose tissue (BAT) when activated by cold exposure. Cold triggers the β3 adrenergic receptor, upregulating cAMP-PKA signaling in brown adipocytes and and phosphorylation of the lipases ATGL, HSL and MGL (124,125). This cascade leads to the hydrolysis of TAG (126). Whereas FFAs generated by lipolysis in WAT can served as substrates for oxidative phosphorylation in a variety of tissues, liberated FFAs in BAT activate UCP1 and act as substrates so that the organ may produce heat (127). Indeed, lipolysis within BAT has been found to be crucial for development of a non-shivering thermogenic phenotype. Mice globally lacking ATGL were unable to defend their body temperatures upon cold exposure and displayed dramatically attenuated lipolysis in BAT which led to TG accumulation and hypertrophy of BAT (128).

In addition to a variety of lipase enzymes that control hydrolysis of TAG, there are also several proteins associated with the lipid droplets themselves which control access of the enzymes to their TAG substrates. Perilipin is found at the surface of lipid droplets and functions as a barrier to the TAG inside to prevent lipases from unchecked basal lipolysis. Upon stimulation of lipolysis, perilipin is phosphorylated and changes configuration so that the lipases may access and hydrolyze the TGs. Adipose fatty acid-binding protein (aFABP) is a cytosolic lipid binding protein that transport fatty acids in adipocytes (129). aFABP transports FAs from the adipocyte upon their release by lipolysis (130). Caveolin-1 is highly expressed in adipose tissue and has been shown to play roles in modulation of lipid droplet formation and lipolysis. Mice lacking caveolin-1 have reduced lipolytic activity as well as reduced phosphorylation of perilipin. Lipid droplet structure was also severely altered in these mice (131).

Nutritional and hormonal control of lipolysis

Lipolysis in WAT is a tightly regulated process under both nutritional and hormonal control. During fasting, lipolysis is activated via catecholamine signaling through beta-adrenergic receptors on the adipocyte plasma membrane (132). Activated G-coupled beta-adrenergic receptors signal to adenyl cyclase to produce cyclic AMP (cAMP) which in turn binds and activates protein kinase A (PKA). Subsequently, PKA phosphorylates hormone sensitive lipase (HSL), activating it and causing its translocation from the cytosol to the lipid droplet (117,122,133). PKA also phosphorylates perilipin, a lipid droplet-associated protein, changing its conformation and exposing lipids to the enzymes that mediate lipolysis (134). There is also evidence from HSL deficient mice that catecholamine-stimulated lipolysis may also involve other TAG lipases as well. Isoproterenol-treated adipocytes isolated from HSL-deficient mice still show increased lipolysis, albeit at a lower level compared to WT controls (135). Lipolysis in brown adipocytes is induced by norepinephrine stimulation upon cold exposure, activating a similar pathway (127).

Lipolysis is inhibited upon refeeding, mainly via insulin signaling. Refeeding stimulates the secretion of insulin which then binds and causes dimerization and autophosphorylation of its receptor tyrosine kinase. Subsequently, the p85 subunit of phosphatidyl inositol kinase-3 (PI3K) binds and is activated (136). Activated PI3K autophosphorylates its p85 and p110 subunits. Protein kinase B (PKB/AKT) is then phosphorylated and activated and in turn phosphorylates and activates phosphodiesterase 3B which degrades cAMP in adipocytes. This signaling pathway results in decreased PKA activity and a subsequent decrease in lipolysis as activation of HSL is reduced and perilipin reverts back to its original conformation. Separate from the cAMP pathway, lipolysis is also reduced by insulin signaling via activation of protein phosphatase-1 which dephosphorylates HSL, leading to reduced lipolysis (137).

Targeting lipolysis for a therapeutic role

In recent years, there has been much interest in developing obesity therapeutics that target upregulation of fat mobilization and increased energy expenditure. Increasing lipolysis in adipose tissue could be a potential therapeutic option for targeting obesity. However, unchecked lipolysis and chronic elevated levels of free fatty acids in the plasma could lead to unwanted metabolic effects such as dyslipidemia, insulin resistance and fatty liver (138,139). Indeed, insulin resistance has been observed in response to dysregulated and excessive lipolytic activity, elevated plasma FFAs, and impaired suppression of plasma FFAs by insulin signaling (140-143). If released from the adipocytes to the plasma, they can serve as an energy source for other tissues (122). However, excessive lipolysis can lead to ectopic accumulation of TGs in tissues not meant to store them, namely skeletal muscle and liver. Alternatively, these FFAs can also be used by the adipocytes themselves, to either again be stored as TG or to serve as a substrate in oxidative metabolism.

More recently, however, lipolysis has been identified as a therpautic target to reduce body weight *if* it can be coupled to oxidation of the liberated FFAs (144). In one study, increasing lipolysis by overexpressing desnutrin (adipose triglyceride lipase, ATGL) in mice decreases diet induced obesity; improves insulin sensitivity; increases thermogenesis and energy expenditure; and increases fatty acid oxidation (145). Indeed, several other studies have also shown that increased

lipolysis in mice leads to reduced adiposity, increased energy expenditure and increased fatty acid oxidation in adipocytes (146,147). It is when the rate of lipolysis and fatty acid release is higher than that of oxidation that ectopic accumulation and subsequent development of insulin resistance can occur (146).

cAMP-PKA signaling, beiging and energy expenditure

A variety of studies link increased adipocyte lipolysis with increased whole-body energy expenditure (145-147). As already mentioned, catecholamines, upregulated upon cold exposure, activate the β3 adrenergic receptor on both brown and white adipocytes to stimulate lipolysis via a cAMP-PKA-p38MAPK dependent pathway to phosphorylate lipases including ATGL, HSL and MGL and stimulate lipolysis (124,125). In addition, the induction of cAMP-PKA triggers increased transcription of *UCP1* and peroxisome proliferator-activated (PPAR)-γ co-activator-1 α (PGC-1 α) which in turn activates PPARα, a nuclear receptor responsible for upregulating lipid and glucose oxidation and thermogenic genes in BAT (126). The free fatty acid products of lipolysis can then activate UCP1 and act as oxidative substrates for UCP1 to generate heat during thermogenesis.

Within (mainly) subcutaneous white adipose tissue exist precursor cells which, upon stimulation by certain ligands including catecholamines (via cold exposure), induce their differentiation into so-called "beige" or "brite" adipocytes (148-151). These adipocytes have an activated thermogenic program, express UCP1, and thus are capable of burning free fatty acids to generate heat (152,153). Inducing "beiging" in WAT depots has also been targeted as a potential therapeutic mechanism by which energy expenditure can be increased, although the contribution by beige adipocytes is thought to be relatively small. While it is estimated that beige adipocytes only contribute about one fifth of the thermogenic capacity generated by BAT, at least in rodents, the physiological contribution of beige fat is still thought to be important, even if not the predominant contributing factor (153). Increasing beiging of WAT in rodents has been shown to increase energy expenditure, improve glucose tolerance and display anti-obesity effects in a number of rodent models (150,154-156).

Clinical Relevance of BAT/Beige adipose tissue and increased energy expenditure

For a long time, the overarching belief was that BAT existed only in mammals and in newborn humans. However, more recently, positron emission tomography (PET) imaging has made it apparent that adult humans also have metabolically active BAT, which takes up glucose and which can be activated by mild cold exposure (157-159). Interestingly, there is an inverse correlation between human BAT mass and BMI and adiposity (160).

With the ultimate goal of identifying factors capable of inducing a beige phenotype in humans to treat metabolic disorders, the important question to ask is whether humans are in fact capable of such a phenomenon. Several studies have now identified that there two relatively distinct gene expression profiles in classical vs beige adipocytes. In newborn humans, BAT depots expressing genes from the classical brown profile are found in the intrascapular region (161). However, in adult humans, samples collected from the supraclavicular region provide evidence that what had initially been thought to be a classical BAT, in fact expressed a gene profile more reminiscent of

beige adipocytes (161). Genome-wide analysis on human-derived UCP1 positive adipocytes isolated from BAT depots further revealed that these adipocytes display a gene expression profile more similar to beige than brown adipocytes, indicating that adult "BAT" depots are in fact mainly comprised of beige adipocytes that could potentially be recruited (162). In several studies on human subjects, daily mild, short-term (two hour, 19°C) cold exposure increased energy expenditure, reduced fat mass and improved insulin sensitivity due to increased recruitment and activation of supraclavicular BAT made up of beige adipocytes(163,164). Consistently, BAT mass is higher in adults during winter months compared to summer (165). Aside from recruitment during cold exposure, a variety of endocrine factors have been identified and have become attractive options to induce beiging in human adipose tissue. To name a few, bone morphogenic proteins 4 and 7 (BMP4, BMP7), FGF19 and FGF21, prostaglandins, and VEGF have all been shown to increase energy expenditure, protect against weight gain and improve glucose homeostasis (166-171). Identification and development of therapies utilizing of novel regulators of human BAT metabolism that do not pose negative side effects could go a long way toward combatting the ever-growing problem of metabolic disease.

Chapter 1: The C-terminal Fibrinogen-like Domain of Angiopoietin-like 4 Stimulates Adipose Tissue Lipolysis and Promotes Energy Expenditure

Chapter 1: The C-terminal Fibrinogen-like Domain of Angiopoietin-like 4 Stimulates Adipose Tissue Lipolysis and Promotes Energy Expenditure

Abstract

Angiopoietin-like 4 (Angptl4) is a circulating protein secreted by white and brown adipose tissues and the liver. Structurally, Angptl4 contains an N-terminal coiled-coil domain (CCD) connected to a C-terminal fibrinogen-like domain (FLD) via a cleavable linker, and both full-length Angptl4 and its individual domains circulate in the bloodstream. Angptl4 inhibits extracellular lipoprotein lipase (LPL) activity and stimulates the lipolysis of triacylglycerol stored by adipocytes in the white adipose tissue (WAT). The former activity is furnished by the CCD, but the Angptl4 domain responsible for stimulating adipocyte lipolysis is unknown. We show here that the purified FLD of Angptl4 is sufficient to stimulate lipolysis in mouse primary adipocytes and that increasing circulating FLD levels in mice through adenovirus-mediated overexpression (Ad-FLD) not only induces WAT lipolysis *in vivo*, but also reduces diet-induced obesity without affecting LPL activity. Intriguingly, reduced adiposity in Ad-FLD mice was associated with increased oxygen consumption, fat utilization, and the expression of thermogenic genes (*Ucp1* and *Ppargc1a*) in subcutaneous WAT. Moreover, Ad-FLD mice exhibited increased glucose tolerance. Chronically enhancing WAT lipolysis could produce ectopic steatosis, due to an overflow of lipids from the WAT to peripheral tissues; however, this did not occur when Ad-FLD mice were fed a high-fat diet. Rather, these mice had reductions in both circulating triacylglycerol levels and the mRNA levels of lipogenic genes in the liver and skeletal muscle. We conclude that separating the FLD from the CCD-mediated LPL-inhibitory activity of full-length Angptl4 reveals lipolytic and thermogenic properties with therapeutic relevance to obesity and diabetes.

Introduction

Angiopoietin-like 4 (Angptl4; also known as fasting induced adipose factor, FIAF) is a circulating protein expressed in and secreted by white and brown adipose tissues (WAT and BAT, respectively) and the liver (51,52,54,55). Angptl4 is a part of the 8-member angiopoietin-like family of structurally related proteins, and the human *ANGPTL4* gene is highly conserved among mammals, sharing a 77% amino acid sequence similarity with that of mice (3,54). Structurally, Angptl4 contains an N-terminal coiled-coil domain (CCD) connected to a C-terminal fibrinogen-like domain (FLD) via a cleavable linker (54,172). Both full-length and truncated forms of Angptl4 circulate in the bloodstream, and the processing of Angptl4 may be tissue dependent: the liver secretes mainly truncated forms, while WAT secretes mainly the full-length form (57,81). The expression of Angptl4 can be induced by several stimuli, including fasting, glucocorticoids, non-esterified fatty acids (NEFAs), thyroid hormone and relative hypoxia (57,59,61,107,173) .

The CCD of Angptl4 is responsible for the ability of Angptl4 to inhibit lipoprotein lipase (LPL) (67,69), the enzyme responsible for hydrolyzing circulating lipoprotein-associated triacylglycerol (TG) to produce free fatty acids (FFAs) for uptake by surrounding tissues. Adenoviral overexpression of full-length human ANGPTL4 in mice causes severe hypertriglyceridemia and hepatic steatosis, whereas mice lacking the gene encoding Angptl4 (*Angptl4*$^{-/-}$) have much lower plasma and liver TG levels than wild-type (WT) controls (21). This hypolipidemic phenotype

correlates with human genetic data supporting a key role for ANGPTL4 in maintaining plasma TG levels (93,174).

Most notably, ~3% of European Americans harbor a single nucleotide polymorphism in which the glutamic acid at position 40 of ANGPTL4, within the CCD, is replaced by a lysine (E40K), decreasing the ability of ANGPTL4 to inhibit LPL (91-93). Indeed, people expressing E40K have reduced plasma levels of TG and LDL-cholesterol, and elevated levels of HDL-cholesterol, although it is not associated with altered body mass index (BMI) or adiposity.

The E40K mutation in ANGPTL4 was initially viewed as the human equivalent of *Angptl4*$^{-/-}$ mice, however it is now known that ANGPTL4 is a bi-functional protein that stimulates adipocyte lipolysis in addition to inhibiting LPL activity (81,175). However, the domain of ANGPTL4 responsible for stimulating adipocyte lipolysis is unknown. One possibility is that FLD might carry out this function.

Prior studies showed that FLD binds β1, β3 and β5 integrins (102,176,177), activates the integrin-dependent focal adhesion kinase (FAK)-Src-p21-activated kinase 1 (PAK1) cascade required for keratinocyte migration (102), interacts with vitronectin and fibronectin to induce the activation of integrin-dependent FAK, 14-3-3 proteins, and PKC during wound healing (101), and stimulates NADPH oxidase-dependent O_2^- production to protect cancer cells from anoikis and apoptosis (177). By contrast, the role of FLD in metabolism has not been explored.

We showed that purified ANGPTL4 directly induces adipocyte lipolysis by increasing intracellular cAMP levels. Moreover, lipolysis induced by fasting or glucocorticoid treatment is reduced in *Angptl4*$^{-/-}$ mice (81). Here, we show that the FLD of Angptl4 alone stimulates adipocyte lipolysis through a mechanism structurally distinct from that by which Angptl4 inhibits LPL. We retained the pro-lipolytic activity of Angptl4 while eliminating its LPL-inhibitory activity by using adenoviral delivery to specifically increase circulating FLD levels in mice (Ad-FLD). Remarkably, doing so increases WAT lipolysis, lowers adiposity by increasing energy expenditure in conjunction with beige thermogenesis, prevents ectopic tissue steatosis, and improves glucose homeostasis under conditions of dietary excess.

Results

The FLD of Angptl4 is sufficient to stimulate adipocyte lipolysis

Prior studies showed that the CCD of Angptl4 can inhibit extracellular LPL activity (67). To determine whether the CCD is required to stimulate intracellular TG hydrolysis in adipocytes, we used adenovirus to express a FLAG-tagged mutant form of human ANGPTL4, which retains both the signal sequence needed for secretion and the intact FLD, but which lacks amino acids 38-165 of the CCD (Ad-FLD), in the livers of adult mice (Figure 1A). Controls included mice overexpressing either FLAG-tagged human full-length ANGPTL4 (Ad-ANGPTL4) or LacZ (Ad-LacZ) (Figure 1B). Immunoblot analysis of plasma collected from mice 3 weeks after adenoviral injection (anti-FLAG) confirmed the presence of FLAG-tagged FLD or ANGPTL4 in the

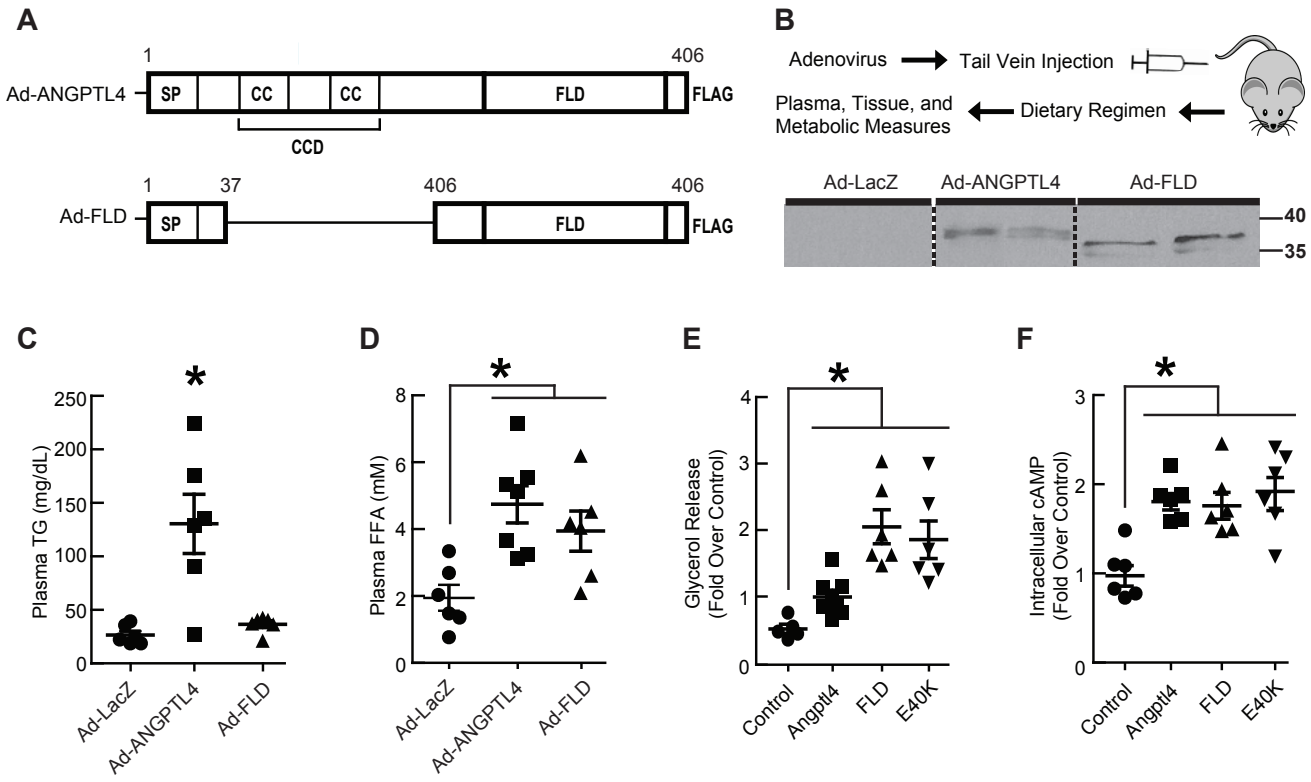

Figure 1. FLD exerts effects on lipid homeostasis, *in vivo* and *in vitro*, that are distinct from those of full length Angptl4. A. Graphical depiction of the Ad-ANGPTL4 and Ad-FLD constructs. **B.** (top) Schematic, showing adenoviral strategy to generate Ad-ANGPTL4, Ad-FLD, and Ad-LacZ mice. (bottom) Immunoblot using anti-FLAG M2 antibody (Sigma, 1:1000) and a corresponding ANTI-FLAG affinity gel, showing increased FLD abundance in the plasma of both Ad-ANGPTL4 and Ad-FLD mice (blot was cropped). **C.** Plasma TG and **D.** FFA measurements, showing that Ad-ANGPTL4 mice fed a standard chow diet have increased levels of both TG and FFAs vs. Ad-LacZ controls, whereas Ad-FLD mice have elevated FFA levels without concomitant hypertriglyceridemia (n = 5-6 mice per group for A-D; *p<0.05 vs. Ad-LacZ). **E.** Glycerol release and **F.** intracellular cAMP levels measured from primary mouse adipocytes treated for 1 hour with purified ANGPTL4, FLD, or the E40K mutant form of ANGPTL4, showing that each stimulates adipocyte lipolysis with similar potency (n = 7 per group; *p<0.05 vs. PBS-treated controls).

appropriate mice (the FLAG-tag is located at the C-terminus in each case). Notably, full-length ANGPTL4 is normally post-translationally cleaved into both CCD and FLD forms (11, 47, 48), accounting for our seeing FLAG-detected proteins from the plasma of Ad-FLD and Ad-ANGPTL4 mice running at similar molecular weights (Figure 1B). As expected, no signal was detected in the plasma of Ad-LacZ mice (Figure 1B). Plasma TG levels were increased in Ad-ANGPTL4 mice (vs. Ad-LacZ) but were not altered in Ad-FLD mice, consistent with the role of CCD in LPL inhibition (Figure 1C). Plasma FFA levels, on the other hand, were markedly increased in both Ad-ANGPTL4 and Ad-FLD mice, suggesting that FLD alone is sufficient to promote WAT lipolysis (Figure 1D).

To directly test this, we treated isolated primary adipocytes with 20 nM of either purified ANGPTL4 or FLD for 1 hour. Both ANGPTL4 and FLD treatments increased adipocyte glycerol release (Figure 1E), indicating enhanced lipolysis. Seeing that FLD alone is sufficient to stimulate intracellular lipolysis by adipocytes led us to predict that this ability would be retained by the c-

terminal E40K mutant form of ANGPTL4, which cannot properly inhibit LPL. Indeed, purified E40K ANGPTL4 also stimulated glycerol release from primary adipocytes (Figure 1E). Moreover, ANGPTL4, FLD and E40K treatment each significantly increased cAMP levels in adipocytes, supporting the concept that each stimulates a common pro-lipolytic pathway (Figure 1F). Together, these findings demonstrate that the FLD of ANGPTL4 is sufficient to stimulate intracellular adipocyte lipolysis.

Ad-FLD mice are protected from diet-induced obesity (DIO)

Given the ability of FLD to stimulate adipocyte lipolysis, we used Ad-FLD and Ad-LacZ mice to determine whether increasing plasma FLD levels in mice would reduce adiposity. Immunoblot analysis of plasma collected from mice 10 days after adenoviral injection (anti-FLAG) confirmed the presence of FLAG-tagged FLD in the appropriate mice (Figure 2A, left). No signal was detected in the plasma of Ad-LacZ mice (Figure 2A, left). To estimate the plasma concentration of exogenous FLD expression in Ad-FLD mice, similar immunoblots were performed on 20.5 ng of purified FLAG-FLD protein run alongside 3μl of plasma from Ad-FLD mice. By comparing the relative intensity of the bands produced by these immunoblots, we calculated that the plasma samples from Ad-FLD mice contained approximately 2ng/μl, or 61.5 nM, of FLAG-FLD (Figure 2A, right).

In accordance with this degree of FLD overexpression, Ad-FLD mice fed a HFD gained less weight than Ad-LacZ mice, with a divergence beginning after one week on the diet (Figure 2B), despite having food intake similar to control (Figure 2C).

Analyzing this protection against DIO revealed that Ad-FLD mice fed a HFD have a pervasive reduction in body fat that includes the inguinal, epididymal and brown adipose tissue (iWAT, eWAT and BAT) depots, which weighed 37%, 46% and 36% less, respectively, than those from Ad-LacZ mice (Figures 2D and 2E). By contrast, hepatic, cardiac, and gastrocnemius muscle weights were similar between Ad-FLD and Ad-LacZ mice (Figure 2E), indicating that increasing systemic FLD levels lowers body weight by specifically reducing adiposity. This specificity was confirmed by monitoring body composition (DEXA) 21 days after adenoviral injection; the lean mass of Ad-FLD mice was increased compared to Ad-LacZ controls, whereas the fat mass of Ad-FLD mice was reduced by 67% vs. Ad-LacZ controls (Figure 2F).

Given that Ad-FLD mice had elevated plasma FFA levels and unaffected plasma TG levels when fed a standard chow diet, we hypothesized that we would see a similar pattern of dyslipidemia when Ad-FLD and Ad-LacZ mice were fed a HFD. Indeed, plasma TG levels in the context of a HFD were not different between Ad-FLD and Ad-LacZ mice, consistent with the role of CCD in LPL inhibition (Figure 3A). Moreover, plasma FFA levels were elevated in Ad-FLD mice fed a HFD, just as when the mice were fed a chow diet, further supporting that FLD alone is sufficient to promote WAT lipolysis (Figure 3B).

We hypothesized that chronic, FLD-mediated WAT lipolysis enhances the flux of mobilized FFAs to ectopic tissues such as the liver and skeletal muscle, where they might be stored as TG, resulting in tissue steatosis. However, we found surprisingly that that the protection against DIO seen in the context of increasing systemic FLD levels occurred without inducing non-adipose tissue steatosis.

Indeed, TG levels in the livers and skeletal muscle of Ad-FLD mice were 24% and 44% lower, respectively, than in Ad-LacZ mice (Figure 3C).

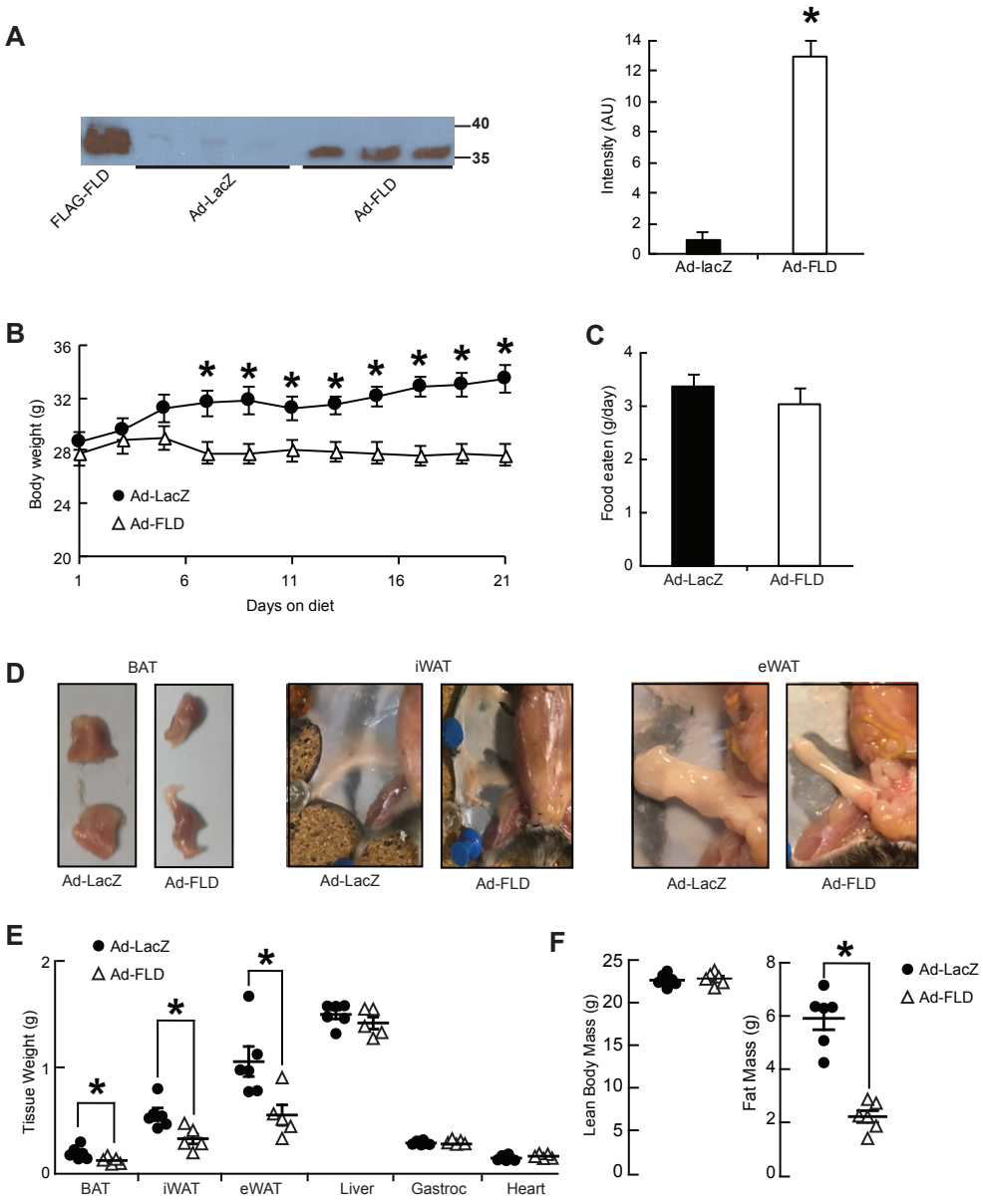

Figure 2. Increasing circulating levels of FLD in isolation limits DIO in mice. A. Immunoblot (left) and quantification (right) of purified (20.5ng) FLAG-FLD proteins and plasma samples (3µl) from Ad-LacZ and Ad-FLD mice, using an anti-FLAG M2 antibody (Sigma, 1:1000). Plasma was isolated from both Ad-LacZ and Ad-FLD mice 10 days after infection. **B.** Body weight curves and **C.** average food intake values for Ad-LacZ and Ad-FLD mice fed a HFD for 3 weeks. **D.** Representative images, showing the reduction in BAT, iWAT, and eWAT masses induced by FLD overexpression in the context of a HFD. **E.** Quantification of C, as well as equivalent weight values for other tissues represented in percentage of body weight in Ad-LacZ and Ad-FLD mice fed HFD for 3 weeks. **F.** Respective lean and fat masses represented in percentage of body weight in the mice mentioned above, as determined by DEXA, showing the specific reduction in fat mass seen in Ad-FLD mice fed a HFD for 3 weeks. In all cases, n = 6 mice per group and *p<0.05 vs. Ad-LacZ.

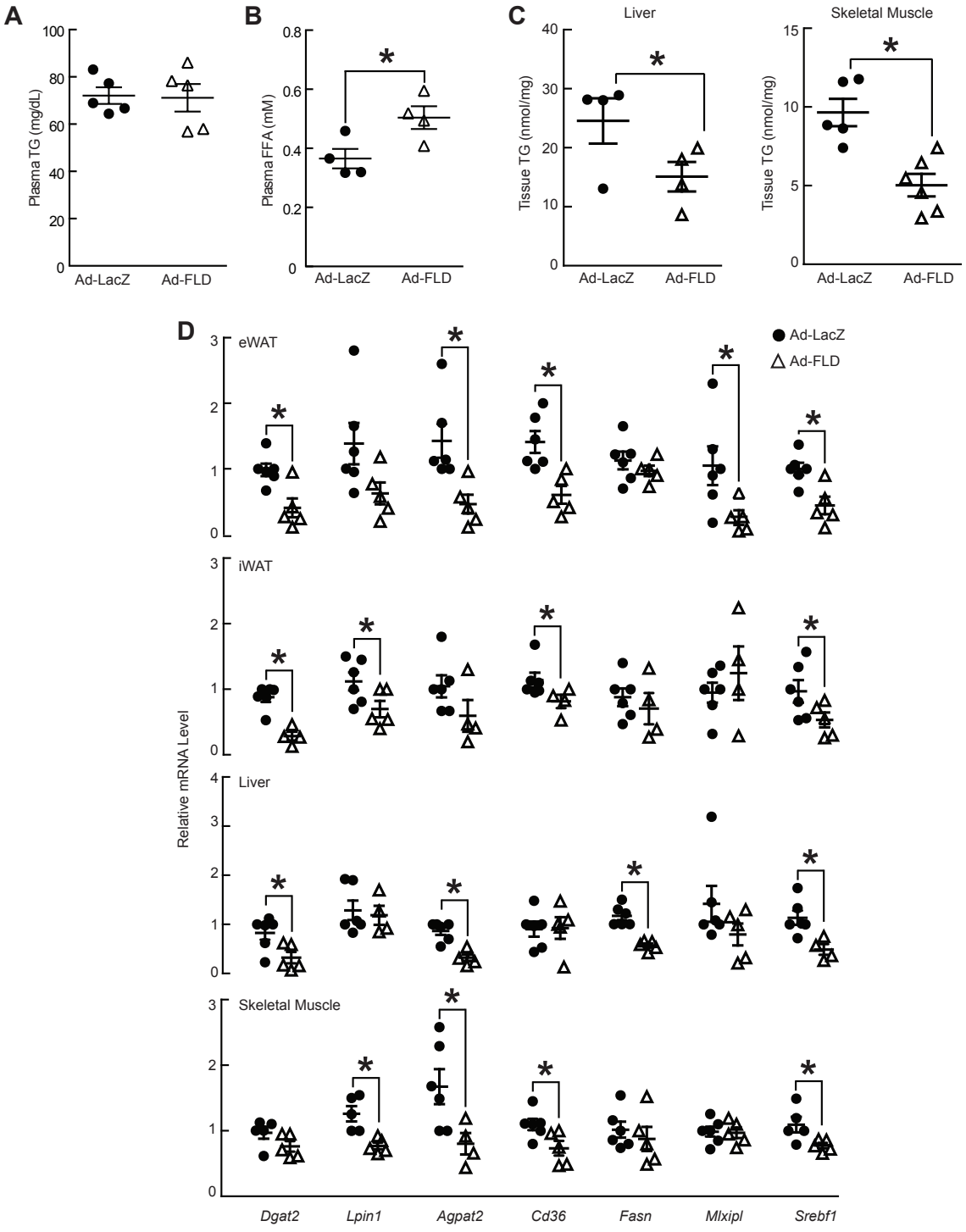

Figure 3. Increasing circulating levels of FLD reduces indicators of fat uptake, synthesis, and storage. Measurements of **A.** Plasma TG and **B.** plasma FFA concentrations, showing that Ad-FLD mice fed a HFD have elevated FFA levels vs. Ad-LacZ controls without concomitant hypertriglyceridemia (n = 4-5 mice per group; *p<0.05 vs. Ad-LacZ.) **C.** Liver and skeletal muscle (gastrocnemius) TG content, showing reduced values for Ad-FLD mice fed a HFD in both tissues (n = 6 mice per group and *p<0.05 vs. Ad-LacZ). **D.** qPCR data, showing markedly lower mRNA levels of genes involved in glycerolipid synthesis, FFA uptake, lipogenesis, and the transcriptional control of these processes, in the iWAT, eWAT, livers, and skeletal muscles (gastrocnemius) of Ad-FLD mice vs. Ad-LacZ controls (n = 5-6 mice per group; *p<0.05 vs. control).

One possible mechanism for the lack of steatosis in Ad-FLD mice fed a HFD is that these mice have enhanced fatty acid oxidation (FAO) in non-adipose tissues. However, the mRNA levels of genes involved in FAO were not different between genotypes (data not shown). Another possibility is that Ad-FLD mice fed a HFD have reduced TG synthesis, storage, or fat uptake in the liver and skeletal muscle. Examining this possibility revealed that the mRNA levels of genes encoding proteins involved in TG synthesis [e.g. *Dgat2* (DGAT2), *Lpin1* (Lipin-1), and *Agpat2* (AGPAT2)], transcriptional control of lipogenesis [*Srebf1* (SREBP-1c) and *Mlxipl* (ChREBP)], and fatty acid uptake and synthesis [*Cd36* (FAT/CD36) and *Fasn* (FAS)] are on the whole markedly lower in the livers, gastrocnemius muscles, as well as in the iWAT and eWAT of Ad-FLD mice vs. Ad-LacZ controls (Fig. 3D). Thus, the potential impact of FLD-induced WAT lipolysis on hepatic and muscle steatosis may be offset by the transcriptional down-regulation of fat synthesis and storage programs in these tissues.

Ad-FLD mice have enhanced cold-inducible energy expenditure

Beyond linking increased adipocyte lipolysis with decreased adiposity in the WAT, we explored how Ad-FLD mice are protected from DIO more mechanistically. To do so, we fed singly housed Ad-FLD and Ad-LacZ mice a HFD for 21 days, then placed them into a Comprehensive Laboratory Animal Monitoring System (CLAMS) to perform indirect calorimetry. Ad-FLD mice fed a HFD had 9.9% higher oxygen consumption (VO_2) and 8.3% higher carbon dioxide production (VCO_2) during the dark period than did Ad-LacZ mice (Figures 4A-D). There were no differences in VO_2 or VCO_2 between groups during the light period. In accordance with these findings, the respiratory exchange ratios (RERs) of Ad-FLD mice fed a HFD were reduced vs. control mice (Figure 4E), and were present during both the light period (6.8% reduction) and the dark period (1.8% reduction). These results indicate that Ad-FLD mice rely more on fat to fuel metabolic processes than do control mice, and correspond with the ability of FLD to induce WAT lipolysis and raise plasma FFA levels. Overall, these results strongly support the concept that increasing circulating FLD levels in mice augments energy expenditure and thus lowers adiposity by coordinately coupling enhanced WAT lipolysis to greater fat utilization.

After establishing the ability of FLD to stimulate energy expenditure at room temperature (22-23ºC), which prior studies indicate is cold enough to stimulate reactive thermogenesis in mice (178), we examined Ad-FLD mice at thermoneutrality to eliminate any such thermogenic stress. Ad-FLD and Ad-LacZ mice fed a HFD for 21 days were placed into a CLAMS maintained at 30ºC, and indirect calorimetry was performed. Interestingly, measuring VO_2 and VCO_2 in this setting eliminated the excess energy expenditure that had been seen in Ad-FLD mice at room temperature (Figure 5A-5D), indicating that FLD drives energy expenditure in mice by potentiating their non-shivering thermogenic response to cold. Notably, the temperature dependence of FLD-stimulated energy expenditure was not reflective of its impact on fuel utilization; RER was 5.3% lower in Ad-FLD (light period) even at thermoneutrality (Figure 5E).

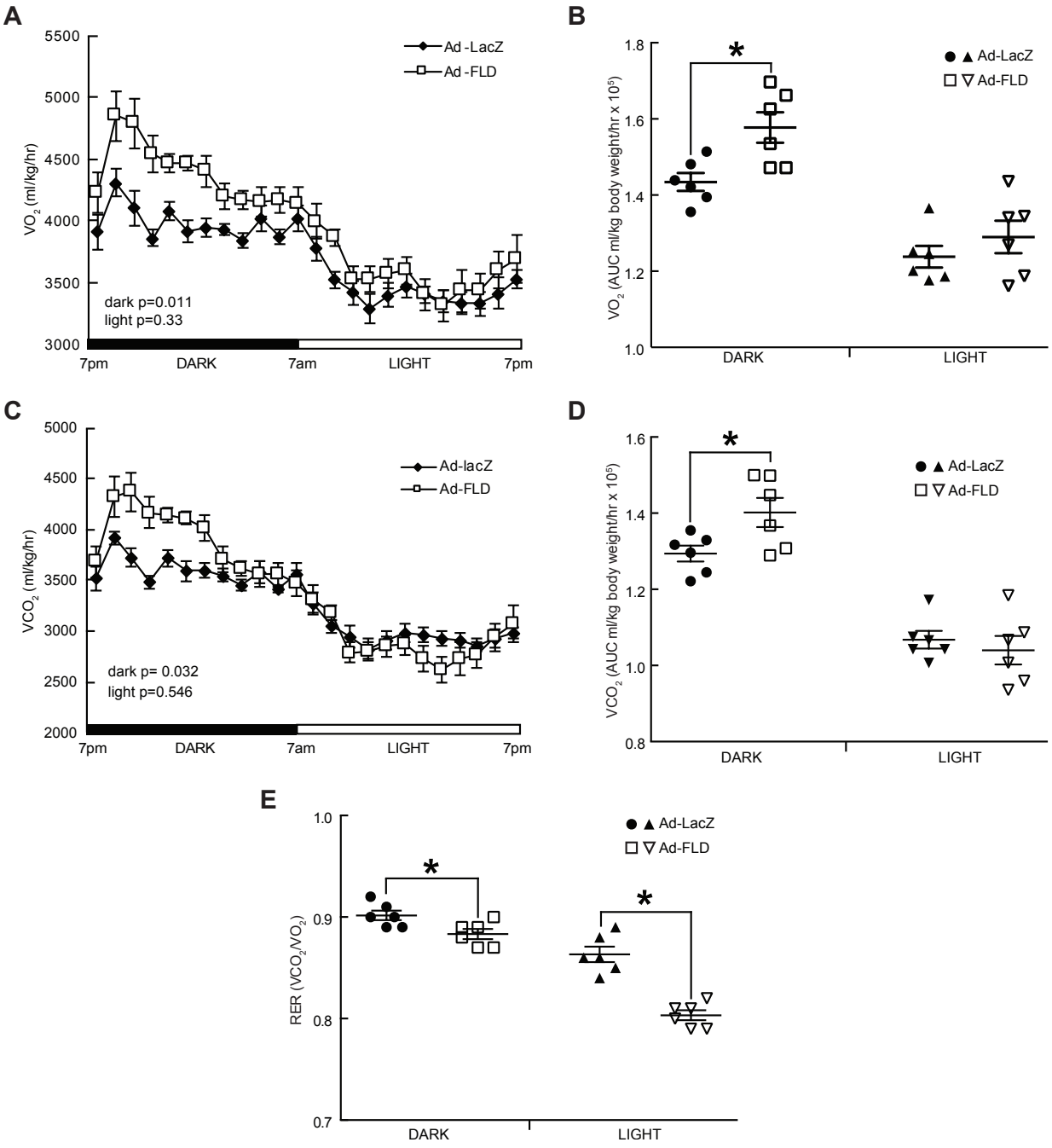

Figure 4. Increasing circulating levels of FLD in isolation enhances energy expenditure in mice fed a HFD. **A.** Whole-body oxygen consumption (VO_2) measured at 23ºC over a 24-hour period in Ad-LacZ and Ad-FLD mice (n = 6 per group) fed a HFD for 3 weeks. **B.** Average VO_2 during the light and dark periods for the data in A. **C.** Carbon dioxide production (VCO_2) measured over 24 hours from the mice in A. **D.** Average VCO_2 during light and dark periods for the data in C. **E.** Respiratory exchange ratios (RERs) measured at 23ºC and during light and dark periods from the mice in A. *p<0.05 vs. Ad-LacZ in all cases.

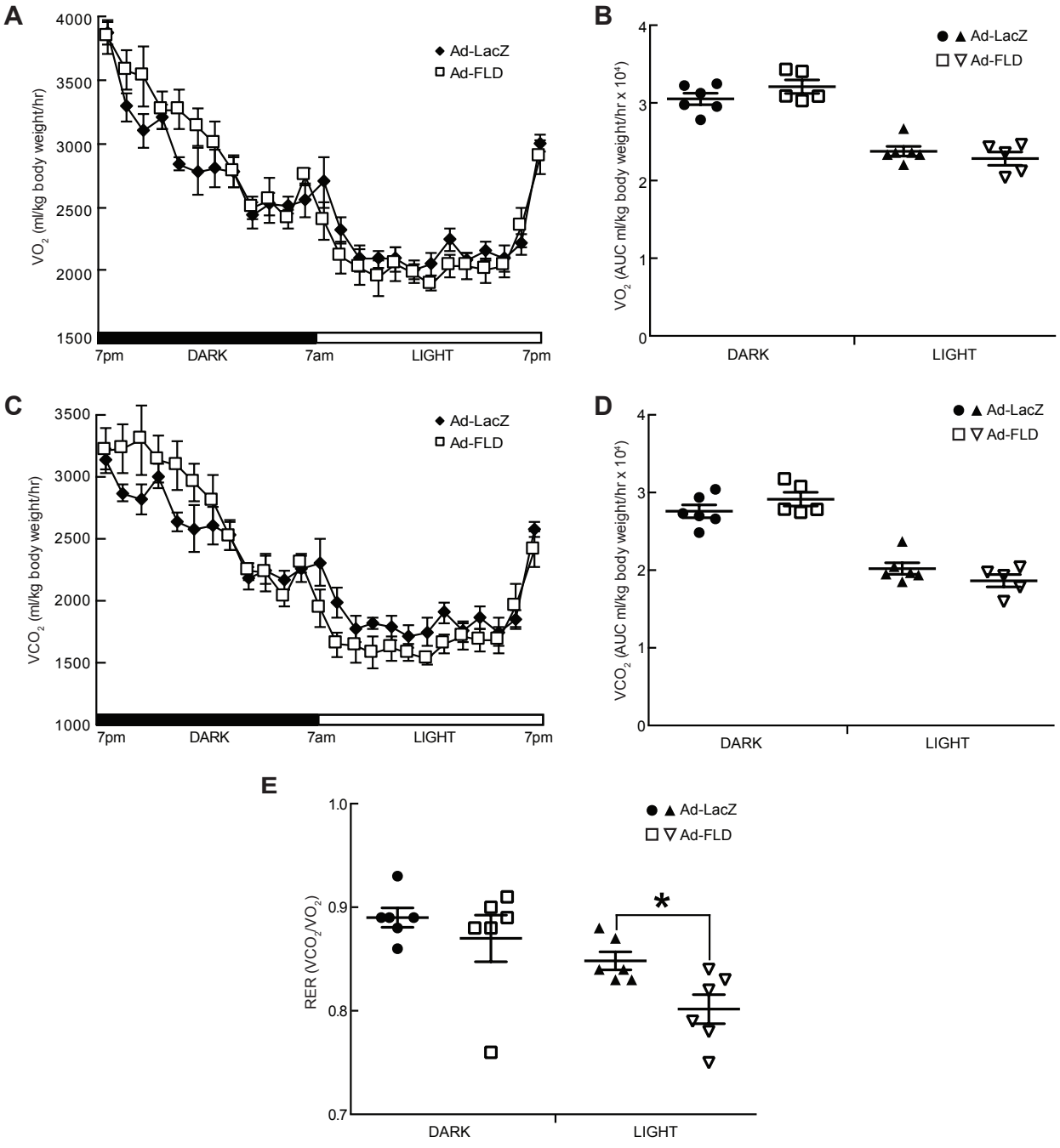

Figure 5. Ad-FLD mice fed a HFD at thermoneutrality do not have enhanced energy expenditure. A. Whole-body oxygen consumption (VO_2) measured at 30ºC over a 24-hour period in Ad-LacZ and Ad-FLD mice (n = 6 per group) fed a HFD for 3 weeks. **B.** Average VO_2 during the light and dark periods for the data in A. **C.** Carbon dioxide production (VCO_2) measured over 24 hours from the mice in A. **D.** Average VCO_2 during light and dark periods for the data in C. **E.** Respiratory exchange ratios (RERs) measured at 30ºC and during light and dark periods from the mice in A. *$p<0.05$ vs. Ad-LacZ in all cases.

Increasing systemic FLD levels induces beige conversion in the WAT

To test whether the ability of FLD to enhance cold-inducible energy expenditure in Ad-FLD mice results from the activation of BAT or beige conversion within the iWAT, we isolated iWAT and BAT from Ad-LacZ and Ad-FLD mice fed a HFD for 3 weeks. Oxygen consumption, which we monitored in each of these tissues *ex vivo*, was increased 2.5-fold in the iWAT of Ad-FLD mice (Figure 6A), but was similar in the BAT of Ad-LacZ and Ad-FLD mice (Figure 6B). Similarly, extracellular acidification rate (ECAR), indicative of glucose utilization, was 2.9-fold higher in the iWAT of Ad-FLD mice vs. control (Figure 6C), but was not altered in the BAT (Figure 6D). Therefore, increasing systemic FLD levels enhances cellular respiration and increases glucose utilization specifically in the iWAT, highlighting the role of this specific fat depot in FLD-stimulation of systematic energy expenditure.

We also monitored OCR and ECAR in the iWAT and BAT of Ad-LacZ and Ad-FLD mice at thermoneutrality. Again, although OCR and ECAR remained elevated in the iWAT of Ad-FLD mice vs. control, these elevations were greatly diminished (46% for OCR and 43% for ECAR) when compared to values taken at standard room temperature (Figures 6A and C). These data support the temperature-dependent nature by which increased systemic FLD levels stimulate energy utilization in the iWAT. Notably, whereas OCR values in the BAT were similar in Ad-FLD and Ad-LacZ mice whether the mice were housed at 23ºC or 30ºC, ECAR in the BAT of Ad-FLD mice fell by 34% in response to thermoneutrality (Figures 6B and D).

Certain WAT depots contain so-called "beige" adipocytes that can acquire a phenotype reminiscent of "brown" adipocytes residing in the BAT when exposed to cold or certain agents (149,179-181). Unlike white adipocytes, beige and brown adipocytes dissipate energy as heat. That Ad-FLD mice have elevated OCR in the iWAT, where beige precursor cells are prevalent (182), suggests that increasing systemic FLD levels induces beige/brown conversion in the iWAT. Supporting this contention, we found that the mRNA levels of thermogenic genes [*Ppargc1a* (a.k.a. *Pgc1α*), *Cidea* and *Ucp1*], were significantly elevated in iWAT of Ad-FLD mice housed at 23ºC (Figures 6E and F, left).

We also assessed tissue levels of uncoupling protein-1 (Ucp1), which is encoded by the *Ucp1* gene and is indicative of thermogenic activation in beige and brown adipocytes. We saw that Ad-FLD mice had a striking increase over Ad-LacZ mice in the expression Ucp1 in the iWAT, but not the eWAT or BAT (Figure 6F, right). Taken together, our data indicate that systemically increasing FLD levels promotes beige/brown conversion and thermogenic activation within the iWAT, and strongly suggests that this mechanism is chiefly responsible for driving energy expenditure in Ad-FLD mice.

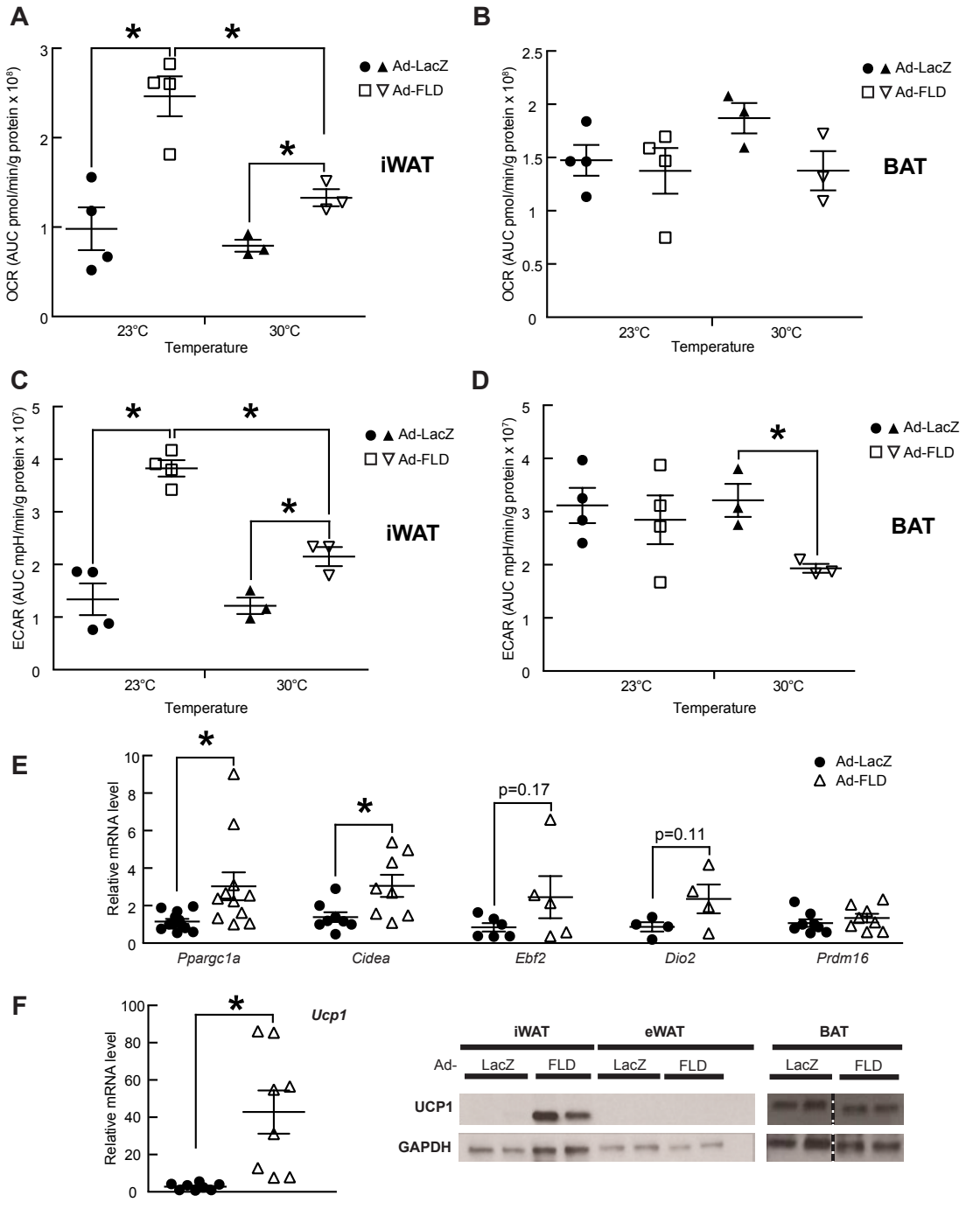

Figure 6. Increasing circulating levels of FLD in isolation induces beige/brown conversion in mice fed a HFD. A. OCR measured from iWAT samples taken from Ad-LacZ and Ad-FLD mice fed a HFD for 3 weeks. **B.** OCR measured from the BAT, **C.** ECAR measured from the iWAT, and **D.** ECAR measured from the BAT of the same mice as in A. **E.** qPCR data, showing markedly increased mRNA levels of thermogenic genes involved in the iWAT of Ad-FLD mice fed a HFD as in A **F.** qPCR data, showing markedly increased mRNA levels of *Ucp1* (left) and representative immunoblots (right, blots are cropped), showing a sharp induction of Ucp1 (U6382; Sigma) in the iWAT of Ad-FLD mice vs. Lac-Z mice fed a HFD as in A. GAPDH used as internal control (ab9483; Abcam) (n = 5-6 mice per group, and *p<0.05 vs. Ad-LacZ for all experiments).

Ad-FLD mice have improved glucose intolerance under conditions promoting DIO

Reduced adiposity and increased energy expenditure are frequently accompanied by improved glucose homeostasis. We thus performed glucose tolerance tests on Ad-LacZ and Ad-FLD mice fed a HFD for 3 weeks. Indeed, Ad-FLD mice under these dietary circumstances have markedly improved glucose tolerance, despite also having an ~50% reduction in fasting plasma insulin levels (Figures 7A and 7B). Gene expression analysis showed that the mRNA levels of genes encoding gluconeogenic enzymes, such as phosphoenolpyruvate carboxykinase (*Pck1*) and glucose-6-phosphatase catalytic subunit (*G6pc*), were lower in livers of Ad-FLD mice than those of Ad-LacZ mice (Figure 7C), suggesting that reduced hepatic glucose production contributes to the improved glucose tolerance seen in Ad-FLD mice fed a HFD.

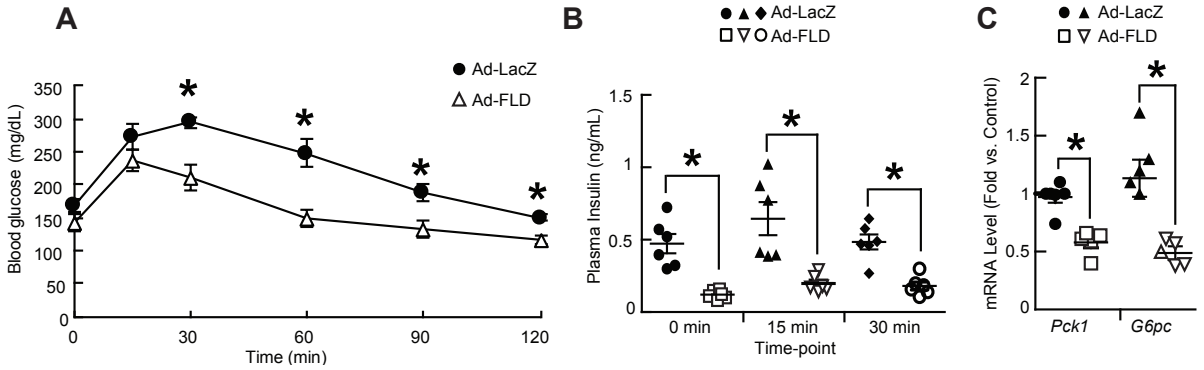

Figure 7. Increasing circulating FLD levels in isolation improves measures of glucose homeostasis in mice fed a HFD. A. Lower serum glucose levels and **B.** lower plasma insulin levels vs. Ad-LacZ controls during glucose tolerance testing in Ad-FLD mice fed a HFD for 14 days (n = 6 mice per group). **C.** Reduced hepatic mRNA levels of genes encoding the gluconeogenic enzymes PEPCK (*Pepck*) and G6Pase (*G6pc*) in Ad-FLD mice fed a HFD for 3 weeks (n = 5-6 mice per group). *p<0.05 vs. Ad-LacZ in all cases.

Discussion

Angptl4 mobilizes FFAs from the WAT by promoting adipocyte lipolysis, and limits uptake of circulating TG into the WAT by inhibiting extracellular LPL activity (183). The N-terminal CCD of Angptl4 is responsible for its ability to inhibit LPL. We show here that the C-terminal FLD of Angptl4 is responsible for stimulating adipocyte lipolysis, a finding that has important physiological and pharmacological implications for obesity and type 2 diabetes.

Angptl4 circulates in full-length and truncated forms, including its CCD and FLD, respectively. Therefore, stimuli such as fasting and glucocorticoids by definition increase circulating levels of full-length Angptl4 together with its individual CCD and FLD components, which then coordinately regulate lipid homeostasis. Supporting this concept, we noted that the FLAG-tagged proteins circulating in Ad-ANGPTL4 and Ad-FLD mice were of a similar size. This indicates either that most, if not all, circulating Angptl4 is cleaved into CCD and FLD components, or that the ability of Ad-Angptl4 mice to secrete full-length protein had waned by the time we drew plasma samples, leaving only long-lived truncated forms in the circulation.

While artificially increasing circulating levels of full-length Angptl4 should reduce adiposity, this process would also be expected to produce marked hypertriglyceridemia, and potentially widespread non-adipose tissue steatosis. On the other hand, if FLD levels could be systemically increased without concomitantly increasing CCD levels, then it might be possible to mitigate DIO without risking hyperlipidemia or ectopic steatosis. However, the FLD of Angptl4 had not been studied in isolation, and its impact on lipid, energy, and glucose homeostasis had not been explored. We used an adenoviral system to overexpress FLD in the livers of mice, thus markedly increasing its levels in the circulation. Remarkably, this strategy reduced adiposity in mice without raising circulating TG levels. Although a previous report showed that injecting FLD into the brains of mice reduces food intake (76), we did not observe such a phenotype, suggesting that circulating FLD may not cross the blood-brain barrier. We estimated that the plasma levels of FLD achieved in our overexpression model was approximately 61.5 nM when measured 10 days following adenoviral infection. Interestingly, we previously estimated that plasma levels of intact full-length Angptl4 reach to 11.6 nM after a 24-hour fast (81). Thus, circulating FLD levels in our overexpression model may be at least 5.3 times higher than what might be achieved by prolonged fasting.

On the other hand, there are two factors to consider when evaluating FLD levels in the blood of Ad-FLD mice. First, the ELISA we performed previously used antibodies recognizing the CCD, rather than FLD, of Angptl4. Thus, we could have underestimated the plasma levels of FLD in our analysis of full-length Angptl4 levels. It is also possible that peak circulating FLD levels in Ad-FLD mice are higher than 61.5nM, based on the fact that peak adenovirus-mediated FLD expression could be either prior to or after the 10 day post-infection time point when our measurements were made. Future experiments should utilize the administration of purified FLD proteins in order to confirm the exact concentrations of plasma FLD needed to produce the types of metabolic effects we observed here.

In exploring the mechanism(s) underlying the promising metabolic phenotype of Ad-FLD mice, we discovered that Ad-FLD mice have an elevation in systemic energy expenditure at relatively cold ambient temperatures, an effect profoundly suppressed at thermoneutrality. These results indicate that FLD acts to potentiate adaptive thermogenesis. Probing this phenotype revealed that Ad-FLD mice have increased expression of several thermogenic genes, including *Ucp1*, and consume more oxygen and glucose specifically in the iWAT. These features combine to suggest that FLD may promote beige/brown conversion in the subcutaneous WAT. Interestingly, an earlier study showed that overexpressing full-length Angptl4 in the WAT and skeletal muscle increases *Ucp1* mRNA levels in the eWAT of mice, although the iWAT was not assessed (73). It is possible that elevating FLD levels for longer than the 3-week period in our study would have also induced *Ucp1* expression in eWAT. Nonetheless, subcutaneous WAT depots such as iWAT have more abundant beige precursors than do visceral WAT depots such as eWAT (181,184), In our experiments, Ucp1 expression and oxygen consumption in the BAT were not augmented by FLD, despite its ability to activate cAMP signaling in brown adipocytes. This is likely due to the fact that baseline *Ucp1* mRNA levels and oxygen consumption rates in the BAT are already quite upregulated, even in control mice.

We propose that FLD could promote thermogenic energy expenditure through two potential mechanisms (Fig. 8). First, it could do so through the stimulation of cAMP-dependent PKA

activation in adipocytes, leading to downstream transcriptional induction of thermogenic mediators (149,179-181) (Fig. 8). Supporting this idea, we saw that mRNA levels of *Ppargc1a,* which is transcriptionally regulated by cAMP-PKA signaling (124,182,185), were elevated in the iWAT of Ad-FLD mice. Induction of *Ppargc1α* would, in turn, activate transcription of other thermogenic genes, such as *Ucp1* and *Cidea*. For example, adipocyte specific knockout of *Ppargc1a* reduces Ucp1 expression and thermogenic capacity in WAT (186). Second, FLD could increase the availability of intracellular FFAs mobilized through the cAMP-dependent stimulation of adipocyte lipolysis. These FFAs could then be oxidized by mitochondria to generate heat, and also serve as critical required factors for the stimulation of Ucp1 activity (127,187). Future work should focus on determining the relative contribution of these two possibilities to FLD-induced thermogenesis.

While lipolysis has been targeted to reduce body weight (144), unchecked lipolysis can lead to ectopic lipid accumulation and insulin resistance (138,139). Indeed, overexpression of full-length ANGPTL4 was shown to cause hepatic steatosis in mice (70). How does increased adipocyte lipolysis in Ad-FLD mice avoid this outcome? One potential explanation is based on our finding that Ad-FLD mice have suppressed mRNA levels of genes involved in in fat uptake, synthesis, and storage in both the liver and skeletal muscle. This downregulation may reduce the rate at which FAs fluxing from the WAT to the liver and muscle are incorporated into TG, thus preventing steatosis.

Alternatively, FAs in the liver and skeletal muscle could be consumed through FAO. Although gene expression analysis did not reveal FLD-regulation of genes involved in FAO, FLD could augment FAO by post-transcriptionally modifying FAO enzymes and/or molecules involved in mitochondrial respiration. Further studies should compare and contrast the relative roles of FAO, mitochondrial respiration, *de novo* lipogenesis, and TG synthesis on the impact of FLD on hepatic and muscle TG homeostasis. In any case, what is clear is that the tissue steatosis produced when full-length Angptl4 is overexpressed in mice requires the LPL-inhibitory action of CCD, since increasing systemic FLD levels without concomitantly increasing CCD levels prevents, rather than promotes, steatosis.

Overexpressing full-length ANGPTL4 in mice improved glucose tolerance (70,71), however our studies indicate that overexpressing FLD on its own is sufficient to improve glucose tolerance in mice fed a HFD. As may be true for energy expenditure, it is possible that FLD improves glucose homeostasis through mechanisms other than the enhancement of WAT lipolysis *per se*. For example, Ad-FLD mice fed a HFD had reduced hepatic mRNA levels of gluconeogenic genes, suggesting that FLD may enhance insulin sensitivity in the liver and reduce hepatic glucose production. Future work will need to determine the extent to which FLD directly regulates hepatic glucose metabolism vs. effects that result indirectly from its regulation of hepatic TG homeostasis.

We show that Angptl4 exerts metabolic effects through both its CCD and FLD, and that the FLD is specifically responsible for the ability of Angptl4 to stimulate adipocyte lipolysis. Moreover, FLD may be more appropriate than full-length Angptl4 when considering clinical translation, as FLD can stimulate lipolysis and reduce adiposity without inducing hypertriglyceridemia. Indeed, increasing the levels of FLD systemically in mice not only limits DIO, but also improves glucose homeostasis and protects against hepatic and muscular steatosis. Though this phenotypic

constellation may involve pleiotropic mechanisms, including enhanced adipocyte lipolysis, beige/brown conversion, and the potentiation of adaptive thermogenesis, our study highlights the potential value of FLD in ameliorating metabolic diseases linked to obesity.

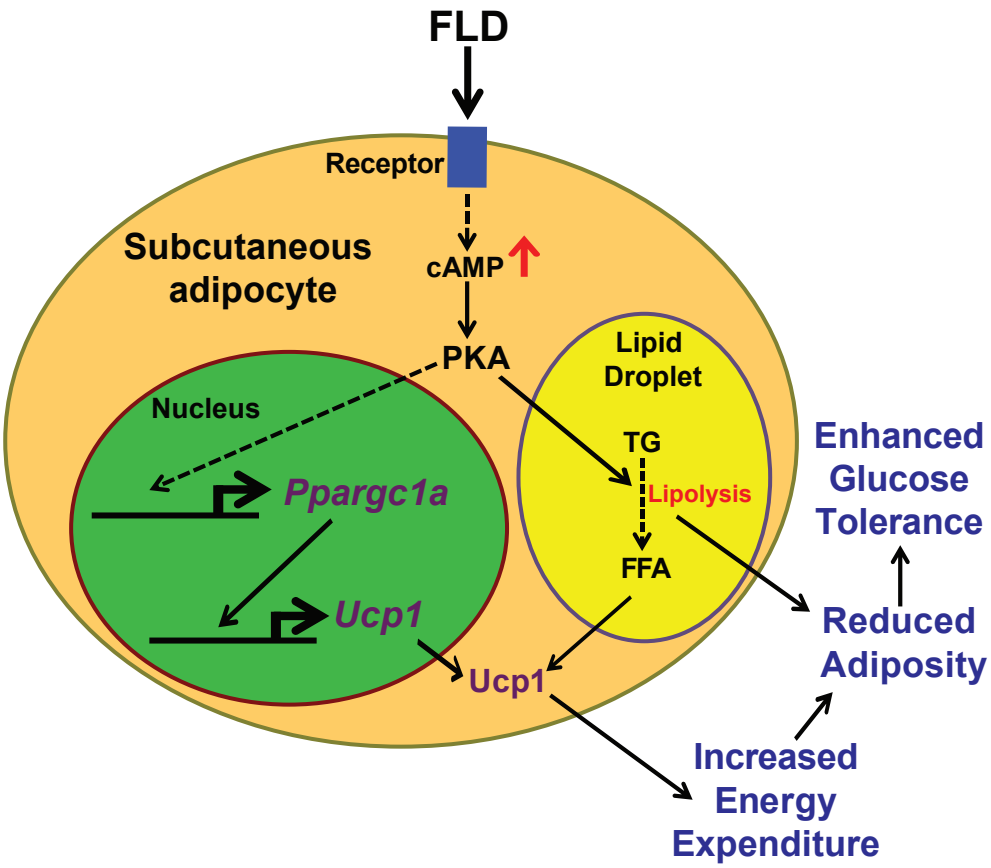

Figure 8. The model of FLD-induced energy expenditure. FLD acts through an unidentified receptor to increase intracellular cAMP levels in adipocytes, which promotes lipolysis. Fatty acids generated from lipolysis are required for Ucp1 activation. Increasing cAMP levels in adipocytes could also augment the expression of thermogenic genes, such as *Ppargc1a* and *Ucp1*, which promotes thermogenesis. Dash lines indicate multiple steps.

Experimental Procedures

Adenovirus Production

The adenoviral vector containing full-length human ANGPTL4 cDNA was provided by Dr. Ron Kahn (Joslin Diabetes Center, Boston, MA). To generate the FLD vector, the nucleotide sequence coding amino acids 38-165 of ANGPTL4 was deleted using the QuikChange Site-Directed Mutagenesis Kit (Agilent, Santa Clara, CA). Adenoviruses were produced, packaged and amplified by Vector Biolabs (Malvern, PA). Adenoviruses were injected via tail vein ($1x10^9$ PFU/mouse in PBS).

Mice

All animal experiments were conducted in accordance with the guidelines of the International Animal Care and Use Committees (IACUC) of the University of California, Berkeley. Eight week-old male C57BL/6J mice (Charles River, Wilmington, MA) were injected with adenovirus and fed either a standard low-fat chow diet or a HFD (42% Kcal from fat; Envigo, Indianapolis, IN) *ad libitum* for 21 days. Mice were either housed at 20-22ºC for the entire study, or switched to thermoneutral (30ºC) housing for the last five days.

Oxygen consumption (VO_2), carbon dioxide production (VCO_2) and respiratory exchange ratio (RER) were monitored in mice by a Comprehensive Lab Animal Monitoring System (CLAMS) 18 days after adenoviral injection. Data were normalized to body weight.

Immunoblotting

Tissues were lysed in RIPA buffer, and the proteins from lysates were separated by SDS-PAGE, transferred to nitrocellulose membrane and probed with the indicated antibodies.

To measure plasma FLAG-FLD and FLAG-ANGPTL4 levels, 40μL of plasma from Ad-ANGPTL4, Ad-FLD, or Ad-LacZ mice was diluted to 1mL with lysis buffer and incubated two hours at 4°C. Lysates were run through an anti-FLAG M2 affinity gel (A2220, Sigma) to pull down FLAG-tagged proteins. The resin was washed with TBS, boiled for 5 minutes at 100°C in sample buffer, and the eluent subjected to SDS-PAGE. Additionally, 3μl of plasma from Ad-FLD or Ad-LacZ mice fed a HFD, along with 20.5 ng of purified FLAG-FLD proteins were diluted 10-fold in saline, incubated at 95°C in sample buffer [31mM Tris-HCl, pH 6.8; 1%(wt/vol) glycerol], and then run on SDS-PAGE. After immunoblotting using FLAG antibodies (F3165, Sigma; 1:1000 in 5% BSA), ImageJ software (http://rsbweb.nih.gov/ij) was used to measure the intensity of the resulting bands. The relative concentration of FLAG-FLD in plasma of Ad-FLD mice was then calculated.

RNA isolation and quantitative real-time PCR (qPCR)

Total RNA was isolated from mouse inguinal WAT, epididymal WAT, liver and gastrocnemius muscle using Trizol Reagent (15596026, Ambion/ThermoFisher, Waltham, MA). To synthesize randomly primed cDNA, 0.6 μg of total RNA, 4 μl of 2.5 mM dNTP, and 2 μl of 15 μM random primers (New England Biolabs, Ipswich, MA) were mixed in a volume of 16 μl and incubated at 70°C for 10 min. Then, a 4-μl cocktail containing 25 units of Moloney murine leukemia virus (M-MuLV) Reverse Transcriptase (New England Biolabs), 10 units of RNasin (Promega, Sunnyvale, CA), and 2 μl of 10× reaction buffer (New England Biolabs) was added, and the samples were incubated at 42°C for 1 hour and then at 95°C for 5 min. The cDNA was diluted and used to perform real-time quantitative PCR (qPCR) using the EVA QPCR SuperMix Kit (Biochain, Newark, CA), following manufacturer's protocol. qPCR was performed in a StepOne PCR System (Applied Biosystems, Foster City, CA) and analyzed by the ΔΔ-Ct method, as supplied by the manufacturer (Applied Biosystems/Thermo Fisher). Rpl19 gene expression was used for internal normalization. Primer sequences for qPCR are listed in Table 1.

Plasma TG and FFA measurement

Plasma TG levels were measured using a Serum Triglyceride Determination Kit (TR0100, Sigma) according to the manufacturer's recommended protocol, and Plasma FFA levels were measured using a colorimetric kit (Sigma, MAK044) according to manufacturer's recommended protocol.

Body composition analysis

Body composition was analyzed by dual energy X-ray absorptiometry (DEXA) with a PIXImus2 scanner (GE Healthcare Lunar, Madison, WI).

Tissue TG measurement

Liver samples were weighed and homogenized in a buffer containing 50 mM Tris-HCl (pH 7.4) and 250 mM sucrose. Lipids were extracted in chloroform/methanol (2:1) and separated by TLC on silica gel G-60 plates with the solvent hexane/ethyl ether/acetic acid (v/v/v, 80:20:1). The TG bands were visualized by exposure to iodine and then scraped and analyzed as described (81), with triolein (T7140, Sigma) as a standard, and expressed per tissue weight.

Seahorse XF24e Analysis

Tissue explants were collected and minced in Krebs-Henseleit buffer (188). 3-5mg pieces were transferred to Seahorse XF24e Islet Capture Microplates with 500uL KHB per well. These microplates were then incubated for 1 hour at 37ºC in absence of CO_2, read using an XF24e Analyzer (Seahorse Bioscience, Billerica, MA), and then homogenized in RIPA buffer. Oxygen consumption rate (OCR) and extracellular acidification rate (ECAR) data were normalized to protein concentration.

Measuring lipolysis from isolated adipocytes

C57BL/6J mice were euthanized and iWAT was dissected out and minced in Krebs-Ringer buffer (KRB; 12 mM HEPES, 121 mM NaCl, 4.9 mM KCl, 1.2 mM MgSO4 and 0.33 mM CaCl2) containing collagenase (Sigma) supplemented with 3mM glucose and 1% FA-free BSA. The mixture was transferred to conical tubes and shaken at 37°C for 1 hour. After digestion, the mixture was filtered through nylon mesh and spun for 5 minutes at 200rpm. Isolated adipocytes were collected from the upper phase and washed three times with KRB. Cells were resuspended in DMEM containing 10% stripped FBS. 300uL aliquots of cells were placed in microcentrifuge tubes containing medium at a final volume of 500uL for further treatment. These cells were then treated with either 20nM Angptl4, 20nM FLD, 20nM E40K or buffer (control). Glycerol release in response to each treatment was measured from aliquots taken from the incubation buffer using Free Glycerol reagent (Sigma). iWAT cAMP levels was measured from cell lysates in KRB. Lysates were centrifuged at 13000 x g for 10 minutes at 4 °C and the cAMP content of the tissue supernatants was measured by ELISA (Enzo Life Sciences, Farmingdale, NY). cAMP levels were measured by ELISA (Enzo Life Sciences, Farmingdale NY). Measurements normalized to protein concentration (BioRad).

Purification of FLAG-tagged proteins

AD293 cells cultured in medium with 10% FBS and 1% penicillin/streptomycin were infected with adenovirus expressing FLAG-ANGPTL4, FLAG-FLD or FLAG-E40K for 1 hour, after which the medium was refreshed. After an additional 72 hours, the medium was collected, and FLAG-tagged proteins were purified from it using an anti-FLAG M2 affinity gel (Sigma) according to manufacturer's protocol. The purified proteins were then dialyzed and concentrated using Slide-A-Lyzer dialyzing cassettes and concentrating solution (Thermo Scientific). Immunoblotting and coomassie staining confirmed protein purity. The affinity gel elution buffer (Tris-buffered saline) was also dialyzed and concentrated to serve as a control.

Measuring glucose tolerance and plasma insulin levels in mice

Mice were fasted for 6 hours and then given i.p. glucose (1g/kg body weight). To perform an intraperitoneal glucose tolerance test (IPGTT), tail blood collected at 0, 15, 30, 60, 90, 120 minutes after glucose administration was used measure glucose levels by glucometer (Contour, Bayer). Fasting plasma insulin levels were measured by an Ultra Sensitive Mouse Insulin ELISA Kit (Crystal Chem, Downers Grove, IL).

Statistical analyses

Data are expressed as means ± standard error (S.E.M.). Statistically significant differences between two groups were assessed by Student's t-test. IPGTT, CLAMS and Seahorse results were also analyzed by calculating the area-under-the-curve (AUC).

Acknowledgements

We thank Drs. C. Ronald Kahn and Sara Vienberg for the adenoviral vector harboring full-length human ANGPTL4 cDNA; Donghui Wang from the UCSF Helen Diller Cancer Center for performing tail vein injections; Dr. Christophe Paillart and the UCSF Nutrition and Obesity Research Center Mouse Metabolism Core (NIDDK P30 DK098722-01A1) for help with CLAMS experiments; and Dr. Jon Dempersmier for critical reading of the manuscript. JCW and SKK are guarantors of this work and, as such, had full access to all the data in the study and take responsibility for the integrity of the data and the accuracy of the data analysis. The NIH (R01DK084591 to JCW) and The American Heart Association (15GRNT22920008 to JCW) supported this work.

Table 1: List of Primers for RT-qPCR

Gene	Forward Primer (5'-3')	Reverse Primer (3'-5')
Rpl19	AGCCTGTGACTGTCCATTCC	GGCAGTACCCTTCCTCTTCC
G6pc	TCCTGGGACAGACACACAAG	CAACTTTAATATACGCTATTGG
Pck1	AGATGGCAAGTTCCTCTGGC	TGTCTTCCCCTTCAATCCGC
Dgat2	AGTGGCAATGCTATCATCATCGT	AAGGAATAAGTGGGAACCCAGATCA
Lpin1	TGACTCGTTTCAGACGGA	GGCTTTCCATTCTCGCAGCTCCT
Agpat2	GCAACGACAATGGGGACCTG	ACAGCATCCAGCACTTGTACC
Cd36	CCTCCAGAATCCAGACAACC	CACAGGCTTTCCTTCTTTGC
Fasn	GGCATCATTGGGCACTCCTT	GCTGCAAGCACAGCCTCTCT
Mlxipl	CGACACTCACCCACCTCTTC	TTGTTCAGCCGGATCTTGTC
Srebf1	TGACCCTACGAAGTGCACAC	CATGCCCTCCATAGACACATC
Dio2	CCACCTGACCACCTTTCACT	TGGTTCCGGTGCTTCTTAAC
Cidea	GCCTGCAGGAACTTATCAGC	CCATTTCTGTCCCTTTTCCA
Ucp1	GCCTTCAGATCCAAGGTGAA	TAAGCCGGCTGAGATCTTGT
Ppargc1a	ATGTGTCGCCTTCTTGCTCT	ATCTACTGCCTGGGGACCTT
Prdm16	GCCATTCATATGCGAGGTCT	CCAGGCGTGTAATGGTTCTT
Ebf2	GGGATTCAAGATACGCTAGGAAG	GGAGGTTGCTTTCAAAATGGG

Chapter 2: Characterizing the Role of the Angiopoietin-like 4 Fibrinogen-like Domain in Hepatic Gluconeogenesis

Chapter 2: Characterizing the Role of the Angiopoietin-like 4 Fibrinogen-like Domain in Hepatic Gluconeogenesis

Abstract

Angiopoietin-like 4 (Angptl4) is a secreted protein that inhibits lipoprotein lipase (LPL) activity and promotes lipolysis in adipocytes. Previous studies have shown that the N-terminal coiled-coil domain of Angptl4 alone can inhibit LPL. Previously, we reported that the C-terminal fibrinogen-like domain (FLD) of ANGPTL4 alone can elevate intracellular cAMP levels to promote lipolysis. Thus, the LPL inhibitory and the lipolytic activities of ANGPTL4 can be separated. Here, mice were infected with adenovirus that express either the ANGPTL4 FLD (Ad-FLD) or LacZ (Ad-LacZ, control) and then placed on high-fat diet (HFD) at thermoneutrality or chow diet (CD) at room temperature for three weeks. Ad-FLD mice on HFD gained markedly less weight and had reduced adiposity as well as improved glucose tolerance compared with Ad-LacZ controls. To more closely examine the role of FLD in the improvement of glucose tolerance of these mice, we then overexpressed FLD in mice on chow diet. While there was no difference in body weight or adiposity under chow conditions, Ad-FLD mice on chow diet did exhibit improved glucose tolerance. Gene expression analysis revealed that treatment of cultured hepatocytes with purified recombinant FLD protein reduced gluconeogenic gene expression, indicating that FLD may improve glucose tolerance through suppression of gluconeogenesis.

Introduction

Obesity and its associated metabolic disorders, including type two diabetes, have become an ever increasing public health problem in recent decades. However, many of the therapies developed to treat metabolic diseases have serious metabolic off-target effects. There is a burgeoning interest in identifying novel metabolic regulators that could offer beneficial metabolic effects in the context of obesity and type 2 diabetes while avoiding serious health consequences.

Angiopoietin-like 4 (Angptl4; also known as fasting induced adipose factor, FIAF; hepatic fibrinogen/angiopoietin-related protein, HFARP; PPARγ angiopoietin-related protein, PGAR) is a secreted glycoprotein expressed highly in white and brown adipose tissue (WAT and BAT, respectively) and liver (51-53). Angptl4 is highly conserved, consisting of an amino-terminal coiled coil domain (CCD) and a carboxy-terminal fibrinogen-like domain (FLD) connected by a cleavable linker region (54,172). Angptl4 is secreted to the plasma by both WAT and liver. From WAT, Angptl4 is mainly secreted in its full length form, while it is mainly secreted in its truncated form (either as the CCD or FLD alone) from the liver (57,61,65). ANGPTL4 expression is controlled by a variety of factors including nutritional status and environmental factors. *Angptl4* mRNA is upregulated during fasting and cold exposure and in response to glucocorticoids, thyroid hormone, free fatty acids and hypoxia (53,55-57,59-61). Its expression is also directly regulated by the peroxisome proliferator-activated receptor (PPAR) family of transcription factors—specifically PPARα and PPARβ/δ which are regulated by free fatty acids (50,61).

Angptl4 was initially characterized for its role in lipid metabolism. Prior work has shown that the CCD of Angptl4 inhibits extracellular lipoprotein lipase (LPL), the enzyme responsible for hydrolyzing triacylglycerol (TAG) to glycerol and free fatty acids (FFA) in circulation for their

uptake into tissues (67,69,79). Intravenous injection of human recombinant full length ANGPTL4 in KK/San mice (an obese model with low plasma lipid levels) markedly increased plasma TG levels and hepatic steatosis, as did adenoviral overexpression of Angptl4 in C57BL/6 mice (68,69). By contrast, Angptl4 deficient (*Angptl4*$^{-/-}$) mice had decreased levels of plasma TG compared to wild-type (WT) mice and gained more weight compared with age-matched WT counterparts (21,76). In addition, treatment with human purified recombinant ANGPTL4 promotes lipolysis in adipocytes (81). Our lab has recently shown that this effect is mediated by the Angptl4 FLD (81,189). Originally, injection of recombinant full length ANGPTL4 in mice resulted in increased plasma non-esterified free fatty acid (NEFA) levels indicative of a lipolytic function. More recently, our lab showed that adenoviral overexpression of ANGPTL4 FLD alone increases plasma FFAs. We also showed that *ex vivo* treatment of primary white adipocytes isolated from mice with purified recombinant ANGPTL4 FLD promotes glycerol release via the cAMP-PKA signaling pathway (189).

A role for Angptl4 has also been identified in glucose homeostasis. Adenoviral overexpression of full length Angptl4 improves overall glucose tolerance despite causing hypertriglyceridemia and hepatic steatosis in both C57BL/6J mice on chow diet and in db/db diabetic mice (70). More recently, our lab has identified the Angptl4 FLD as responsible for this effect on glucose homeostasis. Indeed, adenoviral overexpression of ANGPTL4 FLD in mice fed a high fat diet improves glucose tolerance and insulin sensitivity in addition to protecting against high fat diet induced obesity and ectopic accumulation of TGs and increasing energy expenditure (189).

Though the receptors through which the metabolic functions of Angptl4 FLD are mediated are currently unknown, other groups have shown that the FLD interacts with β1, β3 and β5 integrins to mediate keratinocyte migration via an integrin-dependent focal adhesion kinase-Src–p21–activated kinase 1 dependent pathway during wound healing (101,176,177). Angptl4 FLD coordinates cell matrix communication in wound keratinocytes by interacting with fibronectin and vitronectin in the extracellular matrix to stimulate integrin-focal adhesion kinase (FAK), 14-3-3, and PKC-mediated signaling pathways essential for effective wound healing (101). By contrast the potential for the ANGPTL4 FLD interaction and signaling through integrins in liver and adipocytes has yet to be explored.

Here we show that ANGPTL4 FLD-mediated improvement in glucose tolerance can be separated from its effects on energy expenditure and weight gain. Rather, ANGPTL4 FLD effects on glucose homeostasis may be due to a cell autonomous effect on the liver leading to suppression of hepatic gluconeogenesis.

Results

FLD overexpression protects mice against high fat diet induced obesity at thermoneutrality

Previously, our lab has shown that adenoviral overexpression of ANGPTL4 FLD protects mice against high fat diet-induced obesity and glucose intolerance. This FLD effect is likely due to the increase of energy expenditure through beiging of inguinal white adipose tissue depots (189). To further examine the role of energy expenditure in FLD-improved metabolic profiles, Ad-FLD and Ad-LacZ mice were placed on high fat diet and housed at thermoneutrality (30°C) for three weeks.

Our previous work (Chapter 1, Figure 5) indicated that FLD overexpression no longer increased energy expenditure in mice at thermoneutrality (189). However, surprisingly, Ad-FLD mice fed a HFD still gained less weight than Ad-LacZ mice, with a divergence beginning after one week post-injection (Figure 9A). A closer look at the tissue specific effects of this protection against DIO revealed that Ad-FLD mice have reduced body fat. Epididymal WAT (eWAT) pad weights were reduced by 53% in Ad-FLD mice compared to controls (Figure 9B). Gastrocnemius (GA) muscle weights were also reduced by 3% in Ad-FLD mice compared to controls. There were no differences in weights in liver, heart, iWAT or BAT depots between Ad-FLD and Ad-LacZ mice, indicating that increasing plasma FLD levels promotes resistance to weight gain primarily by reducing adiposity.

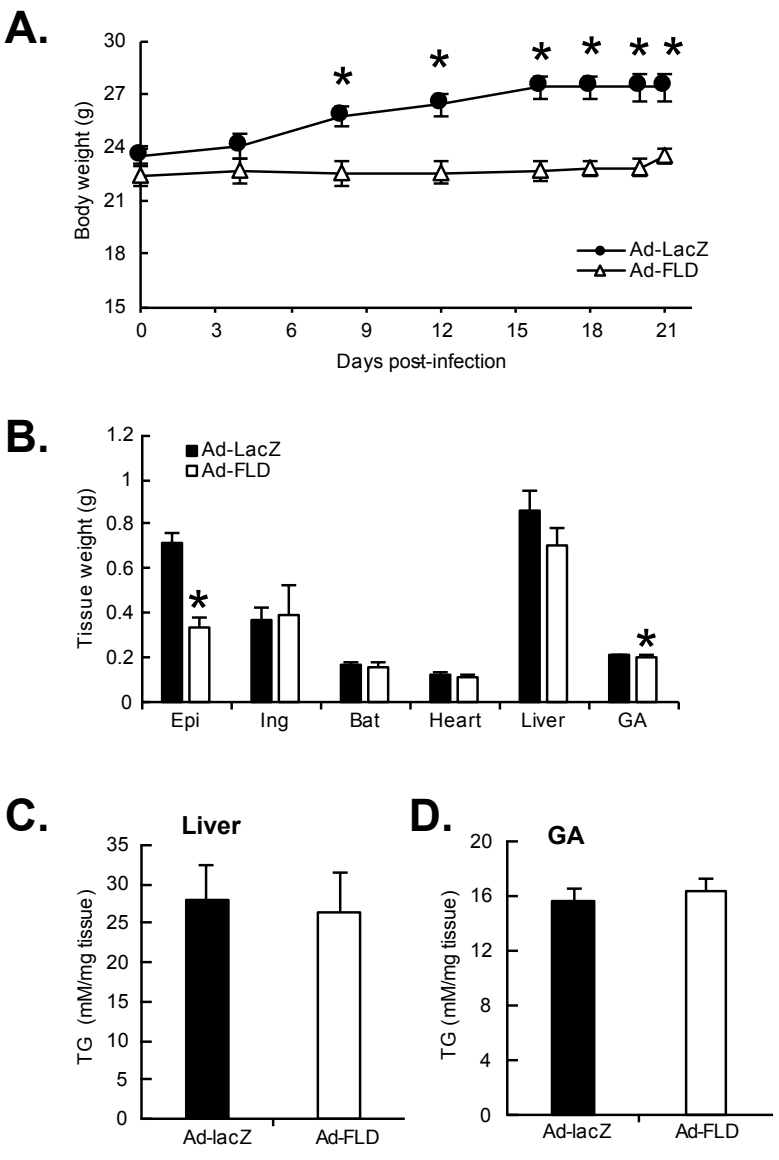

Given the *in vivo* FLD lipolytic effect we had previously observed (189), we expected that prolonged FLD-mediated lipolysis would cause flux of mobilized FFAs from WAT to various other tissues such as the liver and skeletal muscle, leading to ectopic TG storage. Quite surprisingly, we found that although elevated plasma FLD levels protected mice against high fat diet induced obesity at thermoneutrality, it did not result in liver and muscle steatosis. Measurement of TG levels in the livers (Figure 9C) and skeletal muscle (Figure 9D) of Ad-FLD mice were similar to those of Ad-LacZ mice.

Figure 9. FLD overexpression protects mice against high fat diet induced weight gain at thermoneutrality.
Body weights for Ad-LacZ and Ad-FLD mice fed a high fat diet at thermoneutrality (A). Tissue weights for Ad-LacZ and Ad-FLD mice fed a high fat diet at thermoneutrality (B). Triglyceride levels in liver (C) and gastrocnemius muscle (D) in Ad-LacZ and Ad-FLD mice. (n=6 mice/group) *p<0.05 vs. Ad-LacZ in all cases.

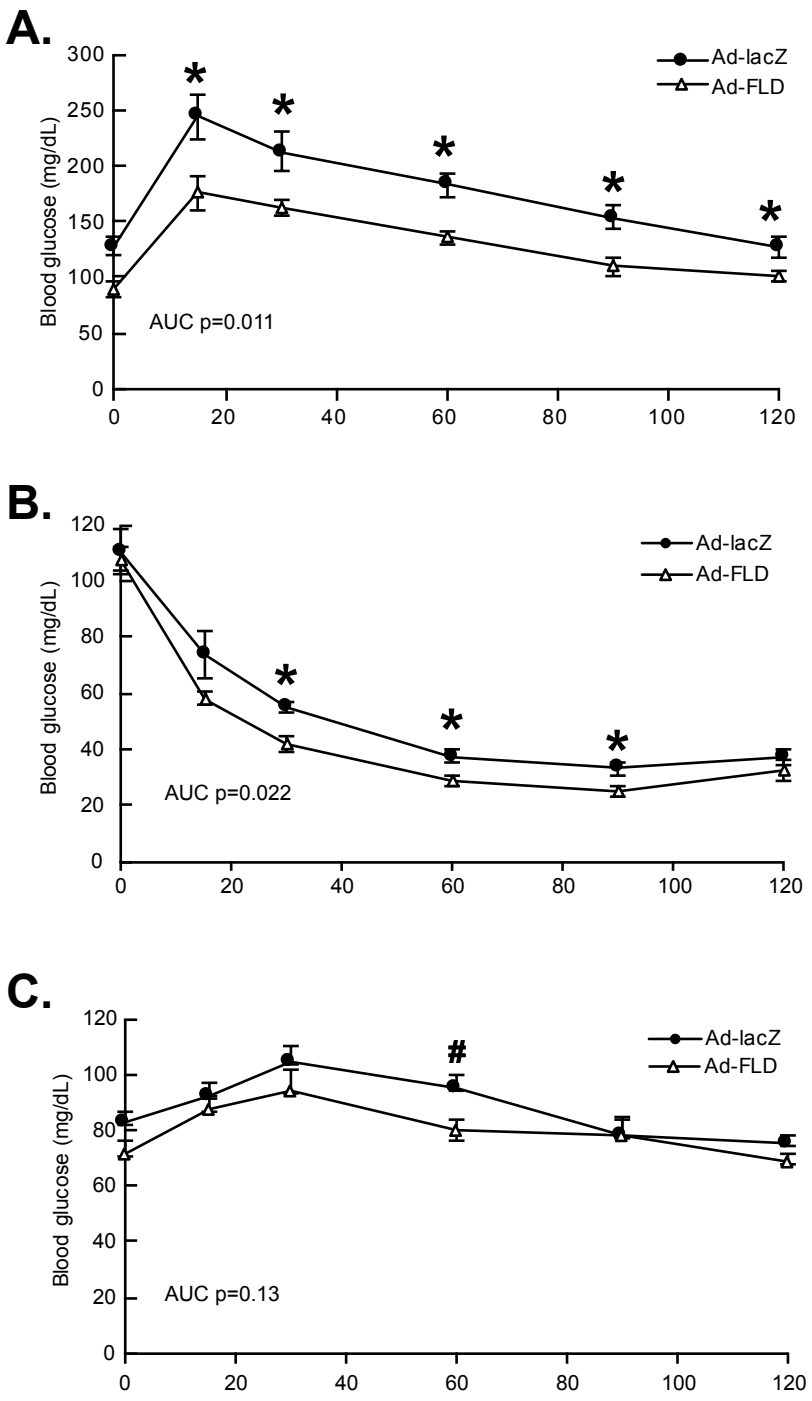

Figure 10. FLD overexpression improves glucose and insulin tolerance in HFD-fed mice at thermoneutrality. Lower plasma glucose levels during glucose tolerance test (A), insulin tolerance test (B), and pyruvate tolerance test (C) (#=0.09) vs. Ad-LacZ controls during glucose tolerance testing in Ad-FLD mice fed a HFD for 21 days (n = 6 mice per group) *p<0.05 vs. Ad-LacZ in all cases.

FLD overexpression improves glucose tolerance in HFD-fed mice at thermoneutrality

Quite often, reduced adiposity is accompanied by improved glucose homeostasis. To test this, we performed glucose, insulin and pyruvate tolerance tests on Ad-LacZ and Ad-FLD mice fed a HFD and housed at thermoneutrality for 3 weeks. Interestingly, Ad-FLD mice displayed markedly improved glucose tolerance (Figure 10A) and insulin sensitivity (Figure 10B). The pyruvate tolerance test also revealed slightly lower glucose production in Ad-FLD mice injected with sodium pyruvate one hour post-injection (Figure 10C).

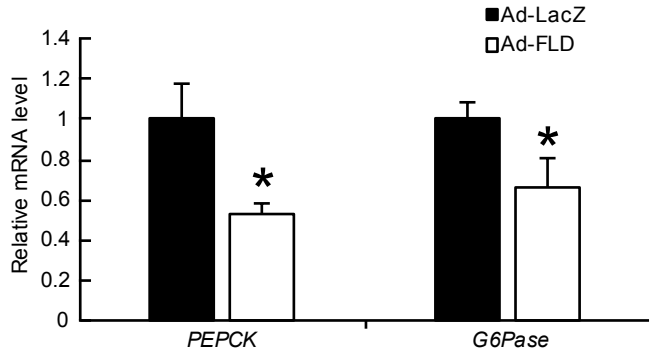

Figure 11. FLD overexpression decreases liver gluconeogenic gene expression. Gluconeogenic gene expression in liver in Ad-FLD mice fed a HFD and housed at thermoneutrality for 21 days (n = 6 mice per group) *p<0.05 vs. Ad-LacZ in all cases.

We previously showed that HFD-fed Ad-FLD mice housed at room temperature have improved glucose tolerance and reduced the expression of gluconeogenic genes (189). Here, gene expression analysis revealed that the mRNA levels of genes encoding gluconeogenic enzymes, such as phosphoenolpyruvate carboxykinase (*Pepck*) and glucose-6-phosphatase (*G6Pase*), were reduced in livers of Ad-FLD mice compared to those of Ad-LacZ mice by 47% and 34% respectively (Figure 11), suggesting that reduced hepatic glucose production may contribute to the improved glucose tolerance in this thermoneutral model. Overall these results demonstrated that increasing circulating FLD at thermoneutrality significantly improves metabolic profiles and insulin sensitivity without elevating energy expenditure in high fat diet fed mice.

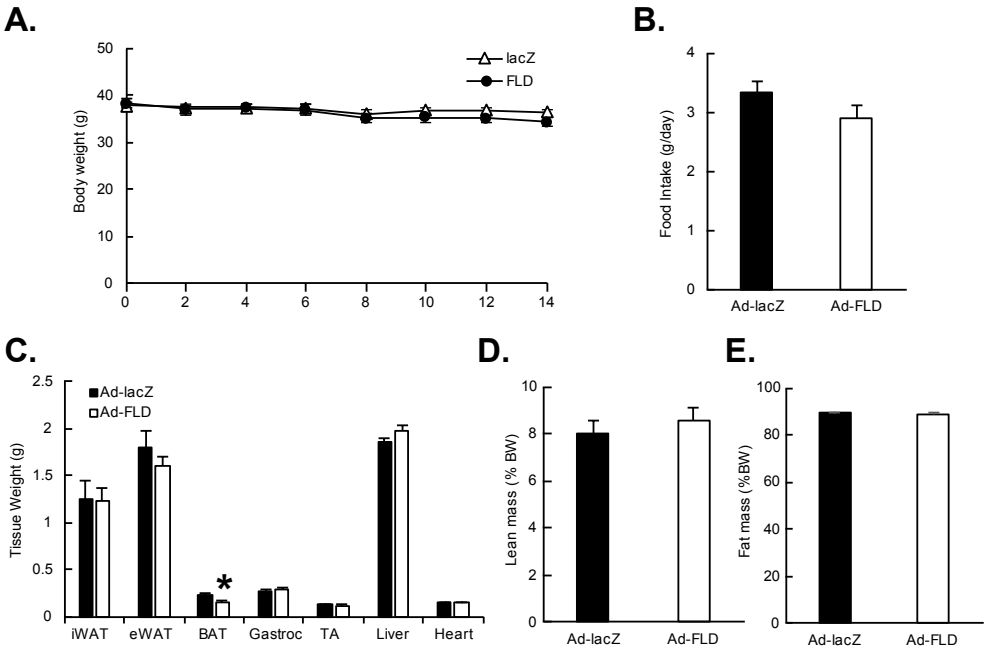

Figure 12. FLD overexpression in mice fed a chow diet does not affect weight gain or adiposity. Body weight (A) and food intake (B) for Ad-LacZ and Ad-FLD mice fed a standard chow diet for 14 days. Tissue weights (C) for Ad-LacZ and Ad-FLD mice fed a standard chow diet for 14 days. Lean body mass (D) and fat mass (E) measured by DEXA body scan. (n = 6 mice/group) *p<0.05 vs. Ad-LacZ in all cases.

FLD overexpression improves glucose tolerance in mice on chow diet

Next, we tested whether FLD improves glucose tolerance independent of its effect on adiposity. Ad-LacZ and Ad-FLD mice were placed on a standard chow diet and housed at room temperature for 14 days. Monitoring of body weight revealed no difference in weight gain (Figure 12A) or food intake (Figure 12B) between the two groups. Additionally, tissue weights were similar between the two groups except for the Ad-FLD BAT depot, which was reduced by ~35% (Figure 12C). Finally, EchoMRI analysis revealed no difference in lean body mass (Figure 12D) or fat mass (Figure 12E) between the two groups.

Despite the fact that FLD overexpression did not affect body weight on chow diet, a GTT revealed that Ad-FLD mice have improved glucose tolerance two weeks post-injection with adenovirus (Figure 13A). Plasma insulin levels were not different between the two groups (Figure 13B). Gene expression analysis of the liver once again revealed that gluconeogenic gene expression of both *PEPCK* and *G6Pase* were reduced by ~72% and ~70%, respectively, in Ad-FLD mice (Figure 13C).

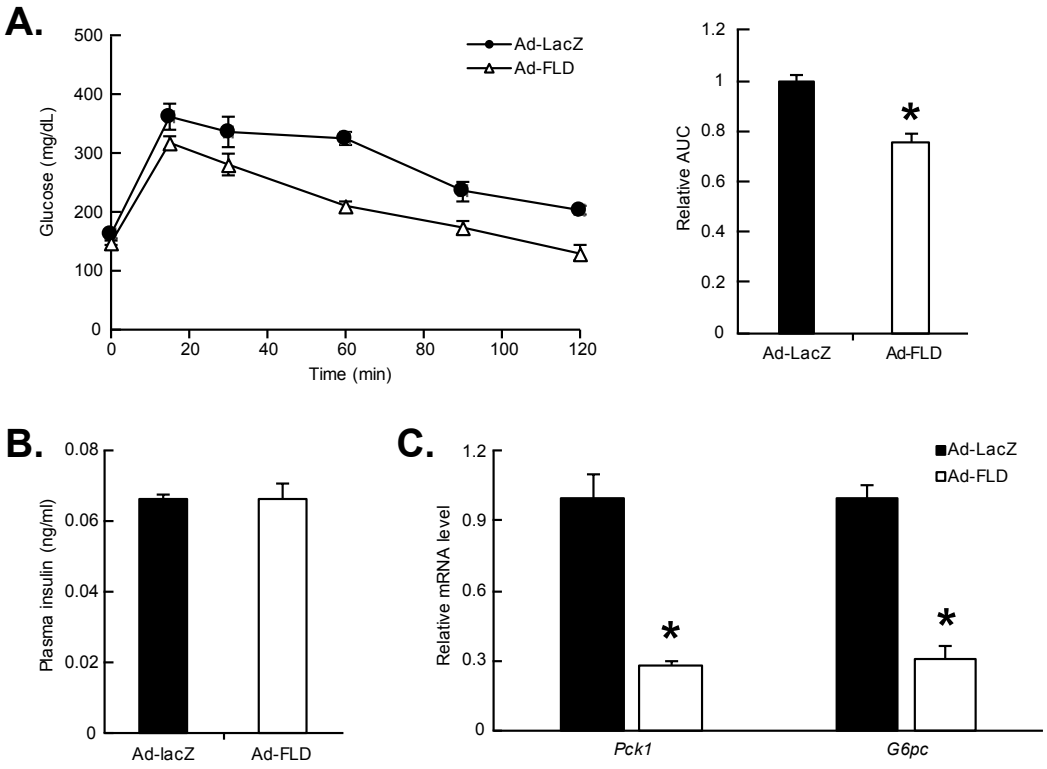

Figure 13. FLD overexpression improves glucose tolerance in mice fed a chow diet. Lower plasma glucose levels during a glucose tolerance test (A) vs. Ad-LacZ mice. (n = 6 mice per group) Plasma insulin levels for Ad-LacZ and Ad-FLD mice fed a standard chow diet for 14 days (B). qPCR showing reduced gluconeogenic gene expression in the livers of Ad-LacZ and Ad-FLD mice fed a standard chow diet for 14 days (C). (n=6 mice/group) *p<0.05 vs. Ad-LacZ in all cases.

FLD suppresses gluconeogenic gene expression in cultured hepatocytes

We hypothesized that FLD suppression of gluconeogenic gene expression is a cell autonomous effect. To test this, we treated rat H4IIE hepatoma cells with purified recombinant FLD protein or FLD protein plus dexamethasone. Dexamethasone is a synthetic glucocorticoid, which induces the expression of hepatic gluconeogenic genes. FLD treatment decreased basal and dexamethasone-induced *PEPCK* (Figure 14A) and *G6Pase* (Figure 14B) expression.

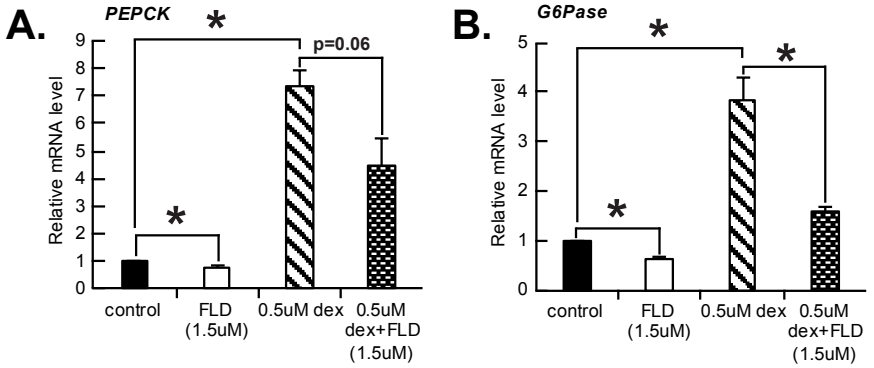

Figure 14. FLD suppresses gluconeogenic gene expression *in vitro*. PEPCK (A) and G6Pase (B) gene expression in H4IIE cells treated with purified recombinant FLD (1.5uM), dexamethasone (0.5uM) or dexamethasone +/- FLD for 6 hours.

Discussion

In this study, we show that overexpression of the ANGPTL4 FLD reduces adiposity and improves glucose tolerance in high fat diet-fed mice at thermoneutrality. Since these FLD overexpressing mice no longer have elevated energy expenditure, the reduction of adiposity is likely due mainly to increased FLD-mediated lipolysis. Thermoneutral conditions have not been reported to affect lipolysis. However, FLD overexpression only decreased eWAT but not iWAT and BAT depot size at thermoneutrality, which is unlike what we observed in Ad-FLD mice at room temperature (189). At room temperature, all fat depots have reduced adiposity in Ad-FLD mice (189). One potential explanation of these results is that there could be signals induced during thermoneutrality that suppress FLD action on lipolysis in iWAT. Alternatively, it is possible that signals that are required to act with FLD to enhance lipolysis are not present during thermoneutrality. Finally, it is also possible that upon secretion from the liver, circulating FLD only reaches eWAT but not iWAT during thermoneutrality.

Despite this eWAT-specific reduction in adiposity, we did not observe an accumulation of TG in either liver or gastrocnemius muscle. These results are reminiscent of our previous observation in high fat diet fed Ad-FLD mice at room temperature, for which TG levels in liver or gastrocnemius muscle are reduced rather than increased despite the elevated lipolysis in WAT (189). This observation in room temperature is attributed, at least in part, to reduced expression of genes encoding proteins involved in lipogenesis, triglyceride storage, and fatty acid uptake (189). We speculate that a similar mechanism is employed at thermoneutrality to reduce TG accumulation in liver and gastrocnemius muscle.

Elevating circulating FLD also improves high fat diet-induced glucose intolerance at thermoneutrality. These results indicate that augmentation of energy expenditure by FLD is unlikely the major contributor to improved glucose homeostasis observed in Ad-FLD mice.

Reducing adiposity is frequently associated with improved glucose homeostasis. However, we further show that overexpression of FLD in chow fed mice at room temperature does not reduce adiposity but still improves glucose tolerance. These results indicate that the beneficial metabolic effect of FLD on glucose homeostasis is independent of its ability to induce beiging and lipolysis of WAT. Xu et al previously reported that increasing circulating full length ANGPTL4 improves glucose tolerance (70). Thus, our data identifies FLD as the functional domain in ANGPTL4 that confers such a beneficial metabolic effect on glucose homeostasis. Interestingly, overexpression of full length ANGPTL4 in mice fed with a chow diet also concomitantly results in hepatic steatosis and hyperlipidemia (70), which are not seen in chow diet fed mice overexpressing FLD. These results suggest that the N-terminal CCD of ANGPTL4, which inhibits LPL, is responsible for lipid disorders seen in full length ANGPTL4 overexpression.

FLD overexpression results in reduced hepatic expression of *Pepck* and *G6pase*, two genes encoding rate-controlling enzymes in gluconeogenesis in both high fat diet- and chow-fed mice under thermoneutrality and room temperature. These results support a previous finding by Xu et al, in which they show that overexpression of full length ANGPTL4 in primary hepatocytes reduces the expression of *Pepck* and *G6pase* genes (70). To further support this observation, we found that treatment with purified ANGPTL4 FLD protein directly suppresses the expression of *Pepck* and *G6pase* genes in H4IIE rat hepatoma cells. These results further substantiate FLD as the functional domain for ANGPTL4 in modulating glucose metabolism. The mechanism underlying the inhibitory effect of FLD on gluconeogenic gene expression is unclear. However, previous studies have shown that ANGPTL4 interacts with integrin β1, β3 and β5 through FLD to activate focal adhesion kinase (FAK)-Src-PAK1 signaling pathway (102). Both FAK and Src kinase have been shown to act upstream of phosphoinositide-3 kinase (PI3K) and Akt, which suppress *PEPCK* and *G6Pase* gene expression (190-194). In fact, it has been shown that the inhibition of FAK causes insulin resistance *in vivo* (195,196). While we do not exclude the possibility of that other membrane receptors could mediate FLD actions in hepatocytes, the role of integrin-mediated signaling on gluconeogenic gene expression in response to FLD treatment will be the primary focus of our future studies.

Overall, in this study we were surprised to find that the augmentation of energy expenditure does not play a major role in the ability of FLD to reduce adiposity and improve glucose tolerance. The anti-obesity effect of FLD appears to be attributed mainly to lipolytic activity of FLD. While enhancing WAT lipolysis reduces adiposity, excess fatty acids generated from lipolysis could result in steatosis in peripheral tissues such as liver and skeletal muscle. However, these phonotypes are not seen in FLD overexpressing mice, which make FLD an attractive anti-obesity approach. The improvement of glucose homeostasis by FLD is likely due to, at least in part, the ability of FLD to directly suppress the expression of gluconeogenic genes. This likely results in the suppression of hepatic glucose production, which is one of the major therapeutic approaches currently used to tackle type 2 diabetes (197). Notably, elevating FLD also improves insulin tolerance in high fat diet fed mice under thermoneutrality. This suggests that FLD might also enhance insulin sensitivity. This notion, however, will require further investigation.

Experimental Procedures

Adenovirus Production

The adenoviral vector containing full-length human ANGPTL4 cDNA was provided by Dr. Ron Kahn (Joslin Diabetes Center, Boston, MA). To generate the FLD vector, the nucleotide sequence coding amino acids 38-165 of ANGPTL4 was deleted using the QuikChange Site-Directed Mutagenesis Kit (Agilent, Santa Clara, CA). Adenoviruses were produced, packaged and amplified by Vector Biolabs (Malvern, PA). Adenoviruses were injected via tail vein ($1x10^9$ PFU/mouse in PBS).

Mice

All animal experiments were conducted in accordance with the guidelines of the International Animal Care and Use Committees (IACUC) of the University of California, Berkeley. Eight week-old male C57BL/6J mice (Charles River, Wilmington, MA) were injected with adenovirus and fed either a high fat diet (HFD, 42% calories from fat, Envigo) or a standard low-fat chow diet *ad libitum* for 21 (HFD) or 14 (chow) days. The mice were housed at either room temperature (20–22°C) or at thermoneutrality (30°C) for the entire study (a 21 day period). Mice were weighed every two days throughout the duration of the study. Oxygen consumption (VO_2), carbon dioxide production (VCO_2) and respiratory exchange ratio (RER) were monitored in mice by a Comprehensive Lab Animal Monitoring System (CLAMS) 7 days after adenoviral injection. Data were normalized to body weight.

Tissue triglyceride measurement

Liver samples were weighed and homogenized in a buffer containing 50 mM Tris-HCl (pH 7.4) and 250 mM sucrose. Lipids were extracted in chloroform/methanol (2:1) and separated by TLC on silica gel G-60 plates with the solvent hexane/ethyl ether/acetic acid (v/v/v, 80:20:1). The TG bands were visualized by exposure to iodine, scraped and analyzed as described (81) with triolein (T7140; Sigma) as a standard, and expressed per tissue weight.

Measuring glucose, insulin and pyruvate tolerance and plasma insulin levels in mice

Mice were fasted for 6 hours and then given intraperitoneal (i.p.) glucose (1g/kg body weight) or sodium pyruvate (2g/kg body weight). For insulin tolerance test, fed mice were i.p. injected with 1 unit/kg body weight insulin (Sigma, I2643). To perform tests, tail blood collected at 0, 15, 30, 60, 90, 120 minutes after glucose, pyruvate or insulin administration was used measure glucose levels by glucometer (Contour, Bayer). Fasting plasma insulin levels were measured by an Ultra Sensitive Mouse Insulin ELISA Kit (Crystal Chem, Downers Grove, IL).

RNA isolation and quantitative real-time PCR (qPCR)

Total RNA was isolated from mouse inguinal WAT, epididymal WAT, liver and gastrocnemius muscle using Trizol Reagent (15596026, Ambion/ThermoFisher, Waltham, MA). To synthesize randomly primed cDNA, 0.6 μg of total RNA, 4 μl of 2.5 mM dNTP, and 2 μl of 15 μM random

primers (New England Biolabs, Ipswich, MA) were mixed in a volume of 16 µl and incubated at 70°C for 10 min. Then, a 4-µl cocktail containing 25 units of Moloney murine leukemia virus (M-MuLV) Reverse Transcriptase (New England Biolabs), 10 units of RNasin (Promega, Sunnyvale, CA), and 2 µl of 10× reaction buffer (New England Biolabs) was added, and the samples were incubated at 42°C for 1 hour and then at 95°C for 5 min. The cDNA was diluted and used to perform real-time quantitative PCR (qPCR) using the EVA QPCR SuperMix Kit (Biochain, Newark, CA), following manufacturer's protocol. qPCR was performed in a StepOne PCR System (Applied Biosystems, Foster City, CA) and analyzed by the ΔΔ-Ct method, as supplied by the manufacturer (Applied Biosystems/Thermo Fisher). Rpl19 gene expression was used for internal normalization. Primer sequences are listed (Table 2).

Body composition analysis

Body composition was analyzed by dual energy X-ray absorptiometry (DEXA) with a PIXImus2 scanner (GE Healthcare Lunar, Madison, WI).

Immunoblotting

Media from cells infected with Ad-LacZ and Ad-FLD adenovirus were collected and the proteins from lysates were separated by SDS-PAGE, transferred to nitrocellulose membrane. Blots were probed with anti-FLAG antibodies (1:1000; Sigma, F3165). Bands were visualized using a film developer.

Purification of FLAG-tagged proteins

AD293 cells cultured in medium with 10% FBS and 1% penicillin/streptomycin were infected with adenovirus expressing FLAG-FLD for 1 hour, after which the medium was refreshed. After an additional 72 hours, the medium was collected, and FLAG-tagged proteins were purified from it using an anti-FLAG M2 affinity gel (Sigma) according to manufacturer's protocol. The purified proteins were then dialyzed and concentrated using Slide-A-Lyzer dialyzing cassettes and concentrating solution (Thermo Scientific). Immunoblotting and coomassie staining confirmed protein purity. The affinity gel elution buffer (Tris-buffered saline) was also dialyzed and concentrated to serve as a control.

Cell culture

H4IIE cells were cultured in DMEM with 10% fetal bovine serum (FBS) and 1% penicillin/streptomycin in 12-well plates. Cells were treated with purified recombinant 1.5uM FLD protein or 1.5uM FLD with 0.5uM dexamethasone (Sigma, #D4902). After 5 hour incubation at 37°C, cells were collected in Trizol (Thermo Fisher, cat. #15596026) and RNA was isolated according to manufacturer's protocol.

Statistical analyses

Data are expressed as means ± standard error (S.E.M.). Statistically significant differences between two groups were assessed by Student's t-test. IPGTT, CLAMS and Seahorse results were

also analyzed by calculating the area-under-the-curve (AUC).

Acknowledgements

We thank Drs. C. Ronald Kahn and Sara Vienberg for the adenoviral vector harboring full-length human ANGPTL4 cDNA. The NIH (R01DK084591 to JCW) and The American Heart Association (15GRNT22920008 to JCW) supported this work.

Table 2: List of Primers for RT-qPCR

Gene	Forward Primer (5'-3')	Reverse Primer (3'-5')
mRpl19	AGCCTGTGACTGTCCATTCC	GGCAGTACCCTTCCTCTTCC
mPepck	AGATGGCAAGTTCCTCTGGC	TGTCTTCCCCTTCAATCCGC
mG6pase	TCCTGGGACAGACACACAAG	CAACTTTAATATACGCTATTGG
rRPL19	ACAAGCGGATTCTCATGGAG	TCCTTGGTCTTAGACCTGCG
rPEPCK	ATACGGTGGGAACTCACTGC	TGCCTTCGGGGTTAGTTATG
rG6pase	GGACCTCCTGTGGACTTTGG	AAACGGAATGGGAGCGACTT

Chapter 3: Angiopoietin-like 4 is required to defend body temperature and maintain energy expenditure upon cold exposure

Chapter 3: Angiopoietin-like 4 is required to defend body temperature and maintain energy expenditure upon cold exposure

Abstract

Angiopoietin-like 4 (Angptl4) is a secreted protein highly expressed in white adipose tissue (WAT) and liver that inhibits extracellular lipoprotein lipase and promotes adipocyte lipolysis. Previous work has shown that Angptl4 is required for shuttling lipids to brown adipose tissue (BAT) upon cold exposure. However, the role of ANGPTL4 in energy expenditure has not been reported. Here we show that when *Angptl4* null mice (*Angptl4*$^{-/-}$) are housed during cold exposure (4^{0}C), room temperature (23^{0}C) and thermoneutrality their oxygen consumption is lower than that of wild type mice. Under cold exposure, uncoupling protein 1 (Ucp1) protein levels are similar in BAT of wild type and *Angptl4*$^{-/-}$ mice. However, the levels of UCP1 proteins are lower in inguinal white adipose tissue (iWAT). These results indicate that the beiging of iWAT by cold exposure is impaired in *Angptl4*$^{-/-}$ mice. Overall, our results demonstrate the critical role of ANGPTL4 in plasma lipid and energy homeostasis during cold exposure.

Introduction

Obesity and its associated metabolic disorders have become an increasingly serious global health problem reflecting a lack of effective strategies for intervention and treatment. Given that obesity is the result of an energy imbalance in the body (namely, increased caloric intake relative to energy expenditure), one potential solution would be to increase energy expenditure. Adipose tissue is critical in maintaining a balance between lipid storage and lipid utilization for energy. Two types of adipose tissue have been identified—white adipose tissue (WAT) and brown adipose tissue (BAT). These two depots have been characterized as having differential functions: WAT is responsible for storage of excess triglycerides (TG) while BAT is a highly specialized organ that dissipates energy by producing heat. Increasing energy expenditure by increasing brown adipose tissue activity has been proposed as a potential therapeutic approach to reduce obesity and improve insulin sensitivity (162,198,199).

BAT is activated during cold exposure as additional heat production is required to maintain homeothermy (127). Thermogenesis is triggered when norepinephrine (NE), secreted from the sympathetic nervous system upon cold exposure, activates the β3 adrenergic receptor (AR) on the surface of brown adipocytes (127). This activates transmembrane adenylyl cyclase that converts ATP to cAMP, subsequently activating PKA to trigger lipolysis, a crucial process in the initiation of thermogenesis (124-126). Lipolysis occurs via the cAMP-PKA signaling pathway in both BAT and WAT (122,200,201). The free fatty acids (FFAs) liberated during lipolysis are then shuttled to the mitochondria to activate uncoupling protein 1 (UCP1) and be used as substrates for thermogenesis (202,203).

In addition to BAT, there are precursor cells within the WAT depots that possess an inducible brown-like phenotype, referred to as beige adipocytes (148,151,204,205). Conversion to a thermogenic phenotype or "beiging" in these cells can be triggered in response to either cold exposure or exposure to β3-AR or PPARγ agonists, promoting UCP1 expression and β-oxidation in these cells (149,150,152). These beige adipocytes are a potential therapeutic target as their

conversion can be manipulated to promote increased energy expenditure to counteract metabolic diseases such as obesity and type 2 diabetes (150,206). In fact, increased activity of beige (as well as BAT) adipose tissue has been linked to obesity resistance in a variety of mouse models (154-156,181).

In humans, it was long thought that BAT depots were substantial at birth and decrease during development (157). However, in recent years, considerably sized depots containing UCP1-expressing adipocytes have been identified by positron emission tomography (PET) imaging in human subjects (158,159,207). Importantly, BAT in humans more closely resembles mouse beige adipocytes as their thermogenic capacity is inducible (208,209). Further, the size and activity of these depots were decreased in obese individuals (210,211). Thus, there is evidence for BAT/beiging in humans and thus therapeutic potential for both BAT activation and beige recruitment in humans.

Angiopoietin-like 4 (Angptl4; also known as fasting induced adipose factor, FIAF) is a secreted protein expressed in liver and WAT as well as in BAT (50,55). Angptl4 plays a crucial role in lipid metabolism under a variety of conditions under the regulation of peroxisome proliferator-activated receptors (PPARs)—its expression is induced during fasting, exercise, under hypoxic conditions, and by glucocorticoids (50,52,53,55-57,60,61). As has been previously shown, Angptl4 inhibits lipoprotein lipase (LPL) via its N-terminal coiled coil domain (CCD) while it promotes intracellular lipolysis in WAT via its C-terminal fibrinogen-like domain (FLD), as described in Chapter 1 (67,77). Studies have shown that *Angptl4* transgenic mice have increased levels of both plasma TG and plasma FFAs (21). Whole body *Angptl4* knockout (*Angptl4*$^{-/-}$) mice, on the other hand, have decreased levels of both plasma TG and FFAs (61). While seemingly having two opposing effects, through its inhibition of LPL, Angptl4 appears to decrease lipid uptake to adipocytes while promoting efflux of FFAs from the adipocytes so that lipids may be shunted to peripheral tissues, such as muscle or liver, during fasting or other times of stress (81,183).

The role of Angptl4 in thermogenesis is not well established. Here I analyzed the energy expenditure of *Angptl4*$^{-/-}$ and wild type mice under cold exposure (4^0C), room temperature (23^0C) and thermoneutrality (30^0C). I found that whole body oxygen consumption was different between *Angptl4*$^{-/-}$ and wild type mice under all three conditions. I found that the levels of Ucp1 protein were elevated upon cold exposure in both BAT and inguinal WAT (iWAT) in wild type mice. This induction, however, was specifically impaired in iWAT of *Angptl4*$^{-/-}$ mice.

Unpublished data from our lab has shown that Angptl4 levels in BAT are higher than in eWAT and iWAT at room temperature. Following a 24 hour cold exposure, BAT Angptl4 levels are increased while Angptl4 levels in iWAT and eWAT are unchanged. Previous unpublished work has also shown that lipolysis is reduced in *Angptl4*$^{-/-}$ mouse WAT explants stimulated with β-adrenergic receptor agonists. Similarly, isoproterenol-stimulated lipolysis is reduced in BAT explants isolated from *Angptl4*$^{-/-}$ mice (unpublished data). Further, in *Angptl4*$^{-/-}$ mice, plasma triglyceride (TG) levels are drastically reduced compared to WT upon cold exposure (unpublished data). In addition, after cold exposure plasma FFA levels in *Angptl4*$^{-/-}$ mice are reduced compared to WT mice (unpublished data). This phenotype could be attributed to decreased lipolysis in BAT and WAT of due to a lack of Angptl4 and indicates a role for Angptl4 in regulating plasma TG and FFA levels during cold exposure.

Given that cold exposure can upregulate a thermogenic gene program, our lab also measured thermogenic gene expression in the BAT of both WT and *Angptl4*$^{-/-}$ mice after cold exposure. These genes—including *Ucp1*, *Dio2*, *Elovl3*, *Cidea*, *Pgc1-a*, *Prdm16*, and *Cpt1a*—were increased in the BAT of WT mice. However, the induction of all of these genes was reduced in the BAT of *Angptl4*$^{-/-}$ mice. Given that cold exposure can also induce a beige phenotype in WAT, we measured thermogenic gene expression in the inguinal WAT (iWAT) of cold exposed WT and *Angptl4*$^{-/-}$ mice. Once again, cold exposure increased thermogenic gene expression in the iWAT of WT mice but expression was blunted in the *Angptl4*$^{-/-}$ mice, indicating that Angptl4 is required for a complete increase in beiging in response to cold exposure.

These findings—that Angptl4 promotes lipolysis in BAT, alters lipid composition in circulation during cold exposure, and that a lack of Angptl4 reduces BAT and iWAT thermogenic gene expression cold exposure—indicate a critical role for Angptl4 in the regulation of thermogenesis and lipid homeostasis during cold exposure. Given this role for Angptl4 as well as the role of the Angptl4 FLD in energy expenditure as outlined in Chapter 1, we hypothesize that full length Angptl4 would be required to defend body temperature and normal energy expenditure levels.

Results

Angptl4$^{-/-}$ mice have lower body temperature than those of WT mice under cold exposure

Activation of lipolysis and the subsequent liberation of FFAs are required for the activation of Ucp1 which can then dissipate energy as heat. Given that the cAMP-PKA signaling pathway promotes lipolysis and our lab has previously shown that Angptl4 stimulates lipolysis via a cAMP-PKA pathway (81), we wanted to test whether Angptl4 could effect homeothermy. To test the impact of the absence of Angptl4 on thermogenesis, we measured core body temperature of mice over 24 hours at 4°C (Figure 15). Following an abrupt decrease in body temperature directly following housing at 4°C, after 5 hours of cold exposure, *Angptl4*$^{-/-}$ mice maintained a body temperature approximately 0.5-1°C lower than that of WT mice. These results suggest that Angptl4 is involved in maintaining thermogenesis under cold exposure *in vivo*.

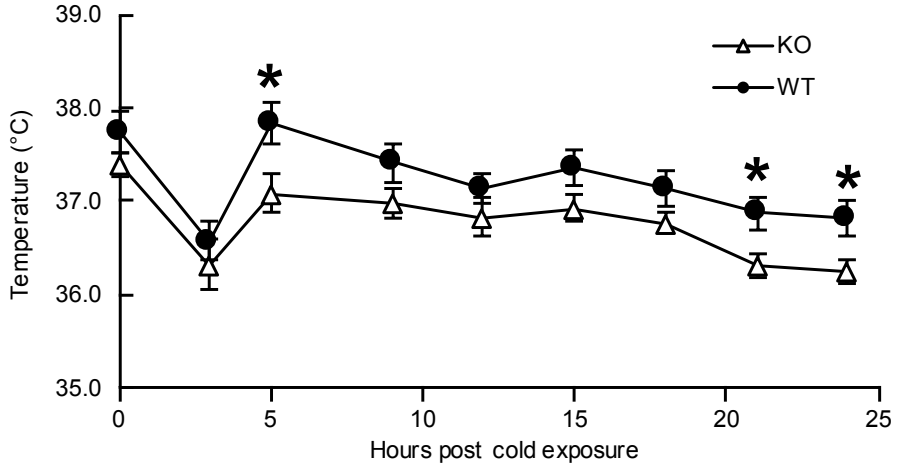

Figure 15. *Angptl4*$^{-/-}$ mice have lower body temperature than those of WT mice under cold exposure. Body temperature of mice was measured over a 24 hour cold exposure showing that *Angptl4*$^{-/-}$ mice maintained lower body temperature during cold exposure. n=13-15 mice/group. Mice were 10-11 weeks old. *p<0.05 vs. WT in all cases.

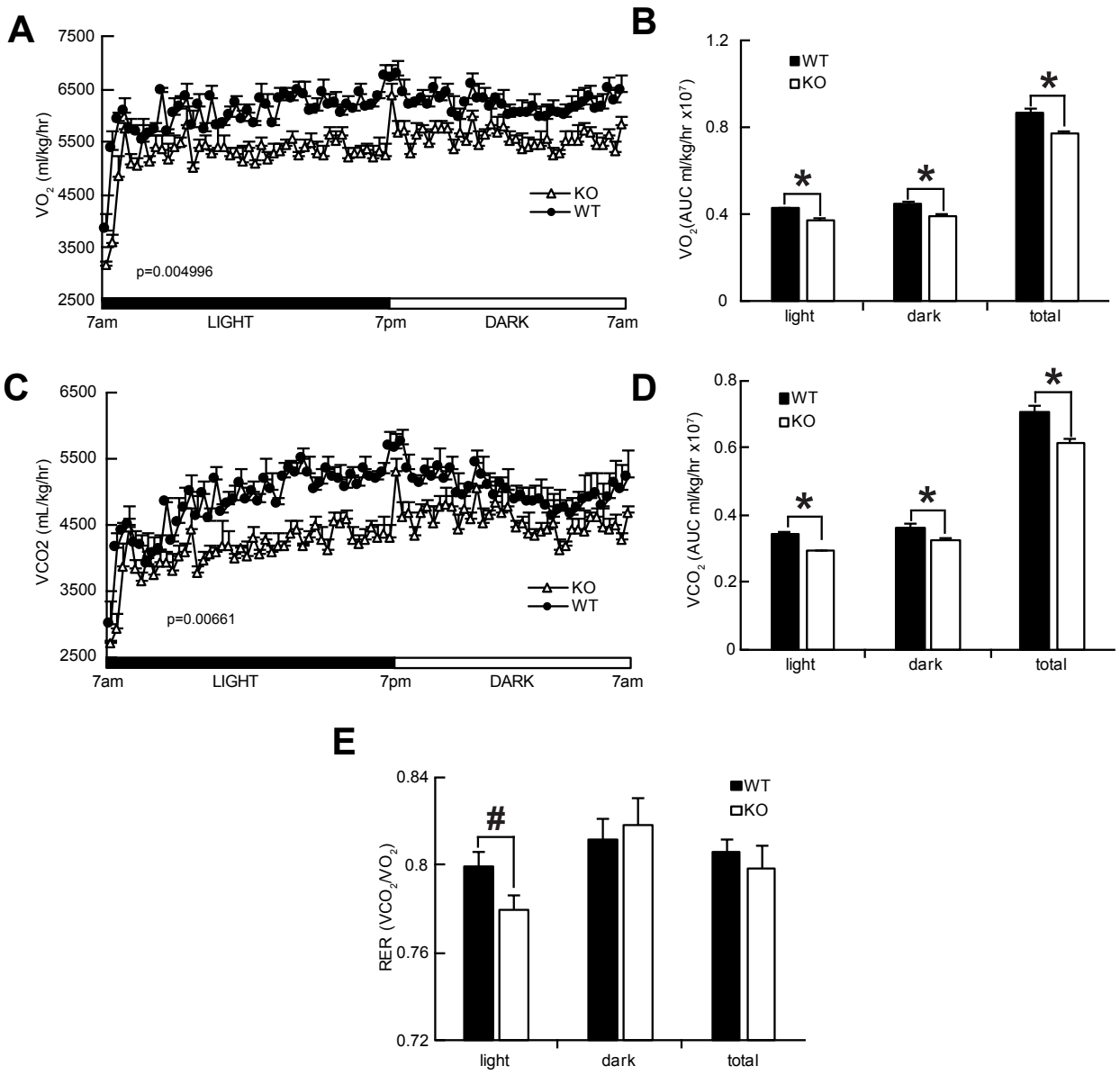

Figure 16. *Angptl4*$^{-/-}$ mice have reduced energy expenditure upon cold exposure. A. Whole-body oxygen consumption (VO2) measured at 4ºC over a 24-hour period in WT and *Angptl4*$^{-/-}$ mice (n = 6 per group). B. Average VO2 during the light and dark periods for the data in A. C. Carbon dioxide production (VCO2) measured over 24 hours from the mice in A. D. Average VCO2 during light and dark periods for the data in C. E. Respiratory exchange ratios (RERs) measured at 4ºC and during light and dark periods from the mice in A. (#=0.08) *p<0.05 vs. WT in all cases. Mice were 8-9 weeks old.

Angptl4$^{-/-}$ mice have lower energy expenditure than wild type mice under cold exposure

Given that *Angptl4*$^{-/-}$ mice were defending a lower core body temperature during cold exposure, we also monitored energy expenditure during a 24-hour 4°C cold challenge. *Angptl4*$^{-/-}$ mice displayed a 12% lower oxygen consumption (VO_2) and 15% lower carbon dioxide production (VCO_2) than WT mice during the light cycle at 4°C (Figure 16A-D). *Angptl4*$^{-/-}$ mice also displayed a 11% decrease in VO_2 and 10% decrease in VCO_2 during the dark cycle compared to WT mice (Figure 16A-D). Overall *Angptl4*$^{-/-}$ mice displayed an 11.5% reduction in VCO_2 and 10.5%

reduction in VCO_2 compared to WT mice (Figure 16A-D). Despite an overall reduction in respiration, RER was in fact reduced during the light cycle (p=0.08) in *Angptl4*$^{-/-}$ mice compared to WTs (Figure 16E), indicating a shift toward increased lipid utilization. RER was not different during the dark cycle.

Angptl4$^{-/-}$ mice have reduced Ucp1 levels in inguinal WAT upon cold exposure

Cold exposure induces "browning" of iWAT in which white adipocytes gain a similar phenotype to those of brown adipocytes, including a multilocular lipid droplet morphology and the induction of Ucp1 expression as well as other thermogenic genes. Given that we had previously observed reduced induction of thermogenic genes in iWAT and BAT after cold exposure in the *Angptl4*$^{-/-}$ mice (as outlined above), I wanted to further confirm the effect on Ucp1 protein levels.

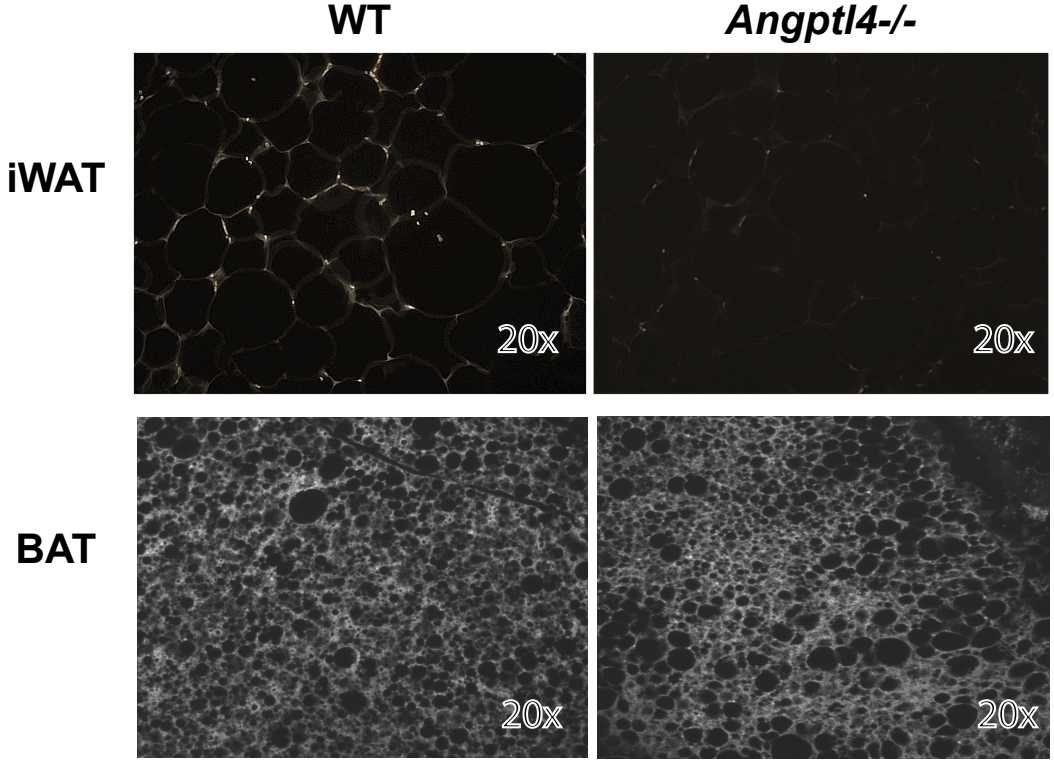

Figure 17. *Angptl4*$^{-/-}$ mice have reduced UCP1 levels in inguinal WAT but not BAT upon cold exposure. A. Immunostaining for UCP1 in sections of iWAT of 10 hour cold-exposed WT (left) and *Angptl4*$^{-/-}$ (right) mice. 20x B. Immunostaining for UCP1 in sections of BAT from WT (left) and *Angptl4*$^{-/-}$ (right) mice.

iWAT and BAT were collected from 10 hour cold-exposed WT and *Angptl4*$^{-/-}$ mice (Figure 17) and sectioned and stained for Ucp1 protein. Ucp1 protein levels were indeed decreased in iWAT of *Angptl4*$^{-/-}$ mice after 10 hours of cold exposure (Figure 17, top). Upon staining for UCP1 in BAT (Figure 17, bottom), there appeared to be no difference in Ucp1 levels between the WT and

Angptl4$^{-/-}$ mice, although the BAT of the *Angptl4* $^{-/-}$ mice appeared to have larger, more unilocular lipid droplets, suggesting, perhaps a reduction in lipolysis. These results suggest that Angptl4 is specifically required for a complete browning response in iWAT during cold exposure.

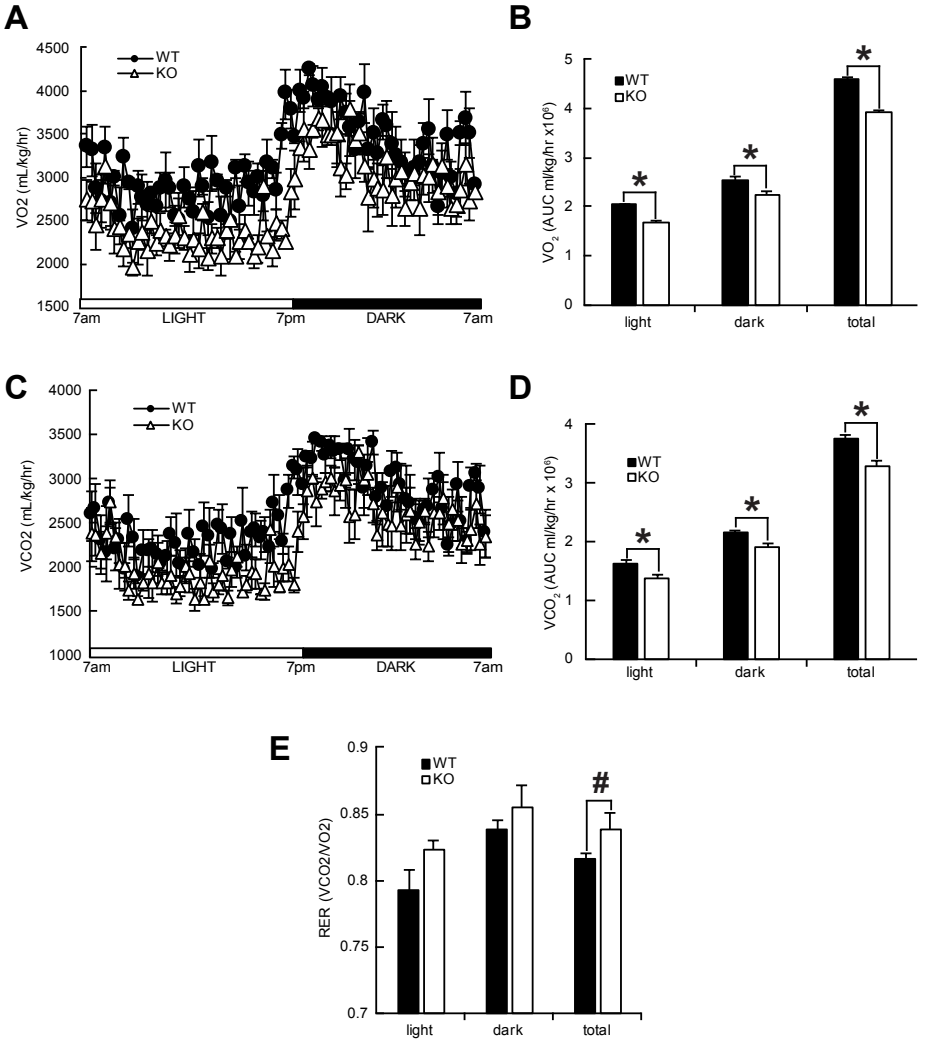

Figure 18. *Angptl4*$^{-/-}$ mice have reduced energy expenditure at room temperature. A. Whole-body oxygen consumption (VO2) measured at 23ºC over a 24-hour period in WT and *Angptl4*$^{-/-}$ mice (n = 6 per group). B. Average VO2 during the light and dark periods for the data in A. C. Carbon dioxide production (VCO2) measured over 24 hours from the mice in A. D. Average VCO2 during light and dark periods for the data in C. E. Respiratory exchange ratios (RERs) measured at 23ºC and during light and dark periods from the mice in A. (#=0.11) *p<0.05 vs. WT in all cases. Mice were 8-9 weeks old.

Angptl4$^{-/-}$ mice have lower energy expenditure at room temperature and at thermoneutrality

To further analyze the role of Angptl4 in energy homeostasis, I monitored the respiratory capacity of WT and *Angptl4*$^{-/-}$ mice at room temperature and at thermoneutrality (30°C). To do so, mice were singly housed in a Comprehensive Laboratory Animal Monitoring System (CLAMS) to perform indirect calorimetry. *Angptl4*$^{-/-}$ mice displayed 18% lower oxygen consumption (VO_2) and 15% lower carbon dioxide production (VCO_2) than WT mice during the light cycle when housed at room temperature (Figure 18A-D). *Angptl4*$^{-/-}$ mice also displayed a 12.4% decrease in VO_2 and 10.6% decrease in VCO_2 during the dark cycle (Figure 18A-D). Overall *Angptl4*$^{-/-}$ mice displayed an overall 15% reduction in VCO_2 and 12.4% reduction in VCO_2 (Figure 18A-D). Despite this,

RER did not differ between WT and *Angptl4*$^{-/-}$ mice at room temperature (Figure 18E), though total RER trended slightly higher in *Angptl4*$^{-/-}$ mice (p=0.11).

Finally, after establishing the requirement of Angptl4 to maintain energy expenditure at room temperature (22-23ºC), which prior studies indicate is sufficient to stimulate reactive thermogenesis in mice (178) and during a 4°C cold exposure, we examined *Angptl4*-/- mice at thermoneutrality (30°C) to eliminate any such thermogenic stress. Interestingly, despite a thermoneutral environment, *Angptl4* $^{-/-}$ maintained lower VO_2 and VCO_2 over a 24 hour cycle.

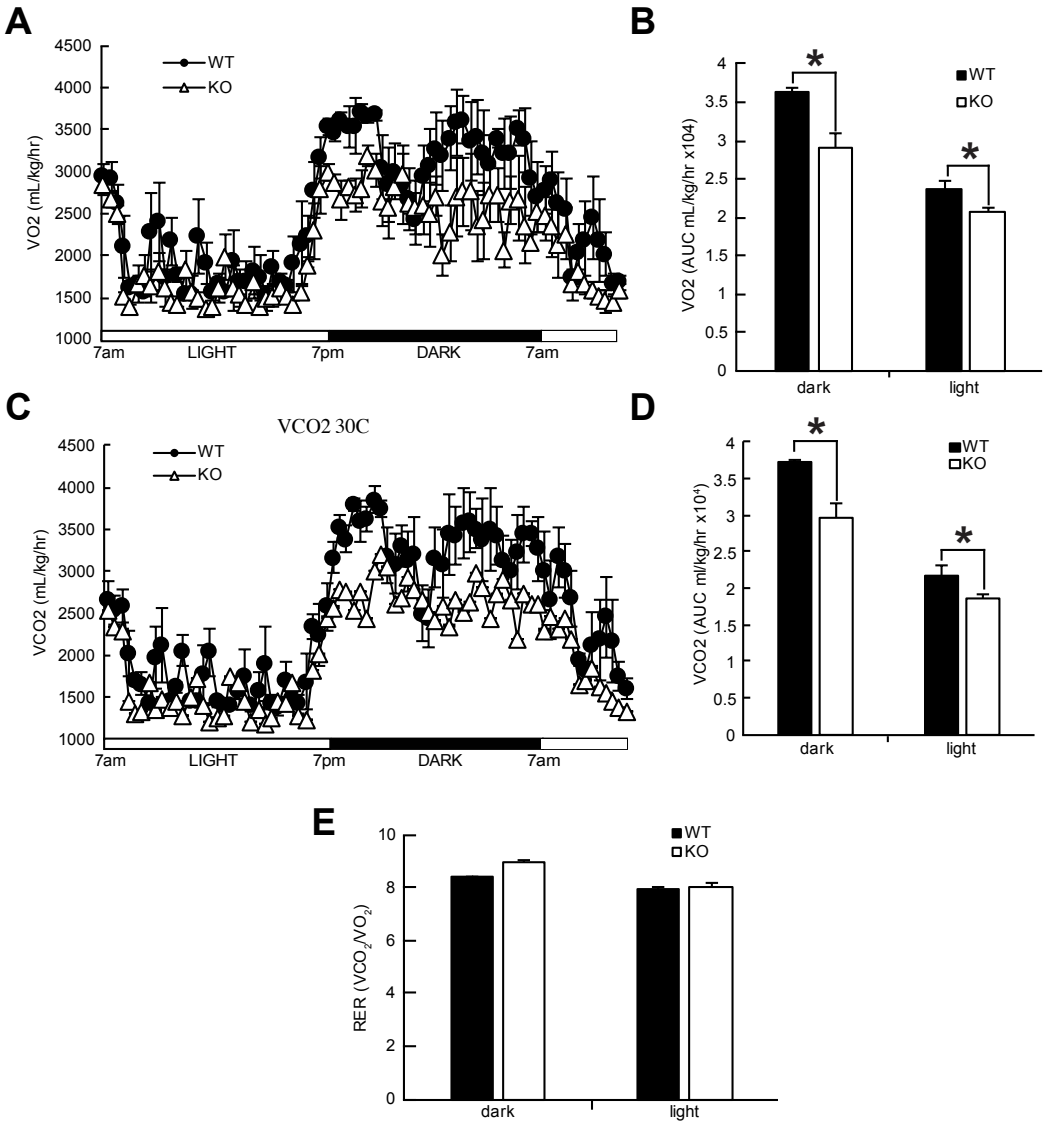

Figure 19. *Angptl4*$^{-/-}$ mice at thermoneutrality have lowered energy expenditure. A. Whole-body oxygen consumption (VO2) measured at 30ºC over a 24-hour period in WT and *Angptl4*$^{-/-}$ mice (n = 6 per group). B. Average VO2 during the light and dark periods for the data in A. C. Carbon dioxide production (VCO2) measured over 24 hours from the mice in A. D. Average VCO2 during light and dark periods for the data in C. E. Respiratory exchange ratios (RERs) measured at 30ºC and during light and dark periods from the mice in A. *p<0.05 vs. WT in all cases. Mice were 8-9 weeks old.

During the light cycle, *Angptl4*$^{-/-}$ mice had a 12.5% reduction in VO_2 and a ~15% reduction in VCO_2 (Figure 19A-D). During the dark cycle, VO2 is reduced by ~20% and VCO_2 is reduced by ~20% in *Angptl4*$^{-/-}$ mice (Figure 19A-D). Despite this reduction, there was no difference in RER during either light or dark cycles (Figure 19E). Together, these data suggest that Angptl4 contributes to normal thermogenic regulation and thus affects whole body metabolic rate during thermogenic stress.

Discussion

Previous work from Dijk et al (55) demonstrated that Angptl4 is required for shuttling lipids into BAT upon cold exposure. However, the role of Angptl4 in energy expenditure was not examined. Here we show that *Angptl4*$^{-/-}$ mice had lower oxygen consumption and carbon dioxide production than WT mice during cold exposure (4^0C), at room temperature (22-23^0C) and under thermoneutral (30^0C) conditions. If Angptl4 is only required for maintaining basal metabolic rate, we should observe equally reduced energy expenditure in *Angptl4*$^{-/-}$ mice compared to WT mice in all three conditions. However, the difference in energy expenditure levels between WT and *Angptl4*$^{-/-}$ mice was mitigated at both room temperature and at thermoneutrality compared with the difference in energy expenditure during cold exposure. This suggests that Angptl4 is also required for adaptive thermogenesis. Room temperature is considered a "cold" environment for mice, but this condition is not as extreme as 4^0C (178). Thus, mice do not rely on adaptive thermogenesis at room temperature as at 4^0C. This is likely the reason we observed a smaller difference in energy expenditure between WT and *Angptl4*$^{-/-}$ mice during room temperature than cold exposure.

The role of Angptl4 in adaptive thermogenesis is supported by the fact that cold-induced expression of *Ucp1* and other thermogenic genes are blunted in iWAT of *Angptl4*$^{-/-}$ mice. Interestingly, we find that cold-induced Ucp1 protein expression is reduced in iWAT but not BAT of *Angptl4*$^{-/-}$ mice. These findings are somewhat consistent with our observation in Chapter 1 that shows UCP1 levels are elevated in iWAT but not BAT upon increasing circulating ANGPTL4 FLD. Thus, Angptl4 is mainly involved in the beiging of iWAT instead of enhancing thermogenic activity of BAT. It is important to note that a previous report indicated that BAT UCP1 levels do not change during cold exposure, but that absolute levels of BAT tissue change during cold acclimatization (212). Also, levels of *Ucp1* mRNA in BAT do not necessarily directly correlate with BAT protein levels (212). By this view, it is necessary to measure oxygen consumption rate in iWAT and BAT of WT and *Angptl4*$^{-/-}$ mice to verify the role of Angptl4 energy metabolism in these two tissues.

Activation of cAMP-PKA signaling is one of the major pathways that induce the beiging of white adipose tissue (124,180). Upon cold exposure, norepinephrine is released from sympathetic nervous system or macrophages that infiltrate into BAT and WAT to activate β3-adrenergic receptor signaling, which in turn triggers a cAMP-PKA signaling pathway to induce Ucp1 expression (181,213). Moreover cAMP-PKA pathway triggers lipolysis in BAT and WAT that hydrolyzes triglycerides to glycerol and fatty acids, which are required for Ucp1 activity (148,214,215). Treating rodents with β3-AR agonist, such as CL316,243, chronically also increases their energy expenditure and promote the beiging of iWAT (149,216). Our previous studies showed that purified human ANGPTL4 protein can directly induce lipolysis whereas lipolysis induced by isoproterenol, a β-adrenergic receptor agonist, was attenuated in fat pads

isolated from *Angptl4*$^{-/-}$ mice (81). Thus, we speculate that the impaired beiging in iWAT of *Angptl4*$^{-/-}$ mice is due to the reduced cAMP-PKA signaling in this tissue during cold exposure and room temperature.

Interestingly, we observed that *Angptl4*$^{-/-}$ mice had lower body temperature during the course of a 24 hour cold exposure. By contrast, Dijk et al reported that they saw no difference in body temperatures between WT and *Angptl4*$^{-/-}$ mice over 10 days of cold exposure (55). However, there appears to be a trending lower body temperature in *Angptl4*$^{-/-}$ mice at days 2 and 6 of their cold exposure. Notably, in their report, 8-10 mice per group were used in the experiment whereas we used 15 mice per group. The high numbers of mice might allow us to observe a statistically significant reduction in body temperature.

The role of Angptl4 in maintaining basal metabolic rate is unclear. Without Angptl4, LPL activity is elevated in plasma, which could hamper the transport of lipids to certain tissues (72-74). Lipids are mainly transported and delivered to specific tissues as triglyceride-rich lipoproteins. In *Angptl4*$^{-/-}$ mice, elevated LPL activity would hydrolyze triglyceride-rich lipoproteins in plasma before they reach to target tissues, though plasma fatty acids are likely higher due to elevated LPL. This defective lipid mobilization could result in reduced basal metabolic rate in certain tissues, as they cannot use lipids as energy source. Alternatively, attenuated adipocyte lipolysis in *Angptl4*$^{-/-}$ mice could yield lower fatty acids to be oxidized that might also result in decreased metabolic rate in WAT. Overall, to understand the role of Angptl4 in supporting basal metabolism, it is important to identify the exact tissues that have lower metabolic rates in *Angptl4*$^{-/-}$ mice, which could be achieved by monitoring oxygen consumption rate in different tissues of WT and *Angptl4*$^{-/-}$ mice that are housed at thermoneutrality.

Experimental Procedures

Animals

All animal experiments were conducted in accordance with the guidelines of the International Animal Care and Use Committees (IACUC) of the University of California, Berkeley. *Angptl4*$^{-/-}$ mice were provided by the laboratories of Andras Nagy (Samuel Lunenfeld Research Institute, Mount Sinai Hospital) and Jeff Gordon (Washington University) (87). *Angptl4*$^{-/-}$ mice were generated on a mixed B6:129/Sv background. WT mice were the littermates of *Angptl4*$^{-/-}$ mice.

Angptl4 $^{-/-}$ and WT mice were fed a chow diet *ad libitum*. VO2 and VCO2 were measured using the Comprehensive Laboratory Animal Monitoring System (CLAMS). Cold exposure experiments involved individually housing each mouse at 4 degrees for 10 hours from 7am until 5pm. Body temperatures was were measured every hour using a rectal thermometer (Physitemp, Model BAT-12). After 10h animals were sacrificed and blood and tissue were taken for analysis. For fasting experiments mice were provided with food *ad libitum* for the first 24h and body temperature was measured at several points over the day. Food was removed and animals were fasted for a total of 24 hours with body temperatures being measured again after 6, 12, 18, and 24 hours.

Purification of FLAG-tagged proteins

AD293 cells cultured in DMEM plus 10% FBS and 1% penicillin/streptomycin were infected with adenovirus expressing a FLAG-tagged version of human ANGPTL4 (provided by Sara Vienberg and Ronald Kahn, Joslin Diabetes Center) for 1 hour, at which point the media was replaced. After 48 hours, the media was collected and Angptl4 protein was purified using an anti-FLAG M2 Affinity gel (Sigma). Purified protein was then dialyzed and concentrated using Slide-A-Lyzer dialyzing cassettes and concentrating solution (Thermo Scientific). Western Blot and Coomassie staining confirmed protein purity. The Affinity gel elution buffer (TBS) was also dialyzed and concentrated to serve as a control.

Staining of Inguinal White Adipose Tissue

Inguinal WAT was collected from mice that had been housed at 4°C for 10 hours. Tissue was fixed in 10% phosphate buffered formalin and embedded in paraffin. Tissues were then sectioned into 8 μm-thick sections, and stained for UCP1(Sigma).

Statistics

Data are expressed as standard error of the mean (S.E.M) for each group and comparisons were analyzed by Student's *t* test and area under curve (AUC).

Acknowledgements

The NIH (R01DK084591 to JCW) and The American Heart Association (15GRNT22920008 to JCW) supported this work.

Conclusion

Conclusion

Obesity and its associated metabolic diseases are currently one of the leading public health problems facing the world today. This growing epidemic reflects a lack of effective therapies and methods of treatment. Disrupting the imbalance of energy intake and expenditure that leads to development of obesity is one potential way to combat it. Increasing energy expenditure is one way to disrupt that imbalance. This can be done in a variety of ways though one of the most common methods currently is by increasing brown adipose tissue activity or by increasing beiging of white adipose tissue by increasing UCP1 activity or expression, respectively. While utilizing small molecules or other chemical therapeutics that confer a beiging effect have been explored, these can have serious off-target effects and currently efforts are being made to identify endogenous molecules that could potentially confer beiging or BAT-activating effects. Here I provide evidence that Angptl4 is one such molecule.

In Chapter 1, I have shown that increasing plasma FLD levels promoted lipolysis and lead to reduced weight gain and adiposity in mice fed a high fat diet. Surprisingly, although FLD increased plasma free fatty acid levels, I did not observe steatosis in either liver or muscle. Rather, FLD-expressing mice had reduced triglyceride levels accompanied by reduced expression of lipogenic genes. Increasing plasma FLD levels increased energy expenditure and expression of thermogenic genes in inguinal WAT. In addition, FLD expressing mice had improved glucose tolerance, an effect that could be mediated by suppression of gluconeogenic gene expression (*Pepck* and *G6pase*).

In Chapter 2, I have shown that elevating plasma FLD levels in mice fed a high fat diet at thermoneutrality reduced adiposity and improved glucose tolerance without affecting oxygen consumption or energy expenditure, indicating that the effect is mainly due to increased lipolysis, rather than beiging. Increasing plasma FLD levels in chow-fed mice, while not affecting adiposity, still improved glucose tolerance. Under both conditions, FLD suppressed hepatic gluconeogenic gene expression. In vitro, I confirmed that FLD has a cell autonomous effect as FLD suppressed both basal and dexamethasone-induced gluconeogenic gene expression.

In Chapter 3, I have shown that mice lacking Angptl4 have reduced body temperature upon cold exposure. In addition, I have shown that *Angptl4*$^{-/-}$ mice have reduced energy expenditure upon cold exposure, at room temperature and at thermoneutrality. *Angptl4*$^{-/-}$ mice have reduced levels of Ucp1 protein in iWAT upon cold exposure, indicating that the inability of *Angptl4*$^{-/-}$ mice to defend their body temperature and maintain normal oxygen consumption levels could be due to reduced beiging of iWAT. In addition, I have provided evidence that Angptl4 is required for complete thermogenic capacity, at least upon cold exposure.

Overall, I have provided evidence that separating the FLD from the CCD-mediated LPL-inhibitory activity of full-length Angptl4 reveals lipolytic and thermogenic properties. Further, by eliminating thermogenic stress and complicating high fat diet effects, I have shown that the lipolytic effect of the ANGPTL4 FLD may further be separated from its beneficial effects on glucose and insulin tolerance by identifying a liver-specific gluconeogenic suppressive effect. Finally, I have provided evidence that Angptl4 is required for a complete thermogenic effect upon cold exposure and at room temperature. While further work is required—namely identifying the receptor for FLD in

both adipose tissue and liver as well as elucidating the signaling pathway by which FLD confers its suppression of gluconeogenesis—I have identified a role for ANGPTL4 with therapeutic relevance, specifically highlighting the potential significance of FLD in ameliorating metabolic diseases linked to obesity.

References

1. Ward, N. L., and Dumont, D. J. (2017) The angiopoietins and Tie2/Tek: adding to the complexity of cardiovascular development - 1-s2.0-S1084952101902885-main.pdf.
2. Oike, Y., Yasunaga, K., and Suda, T. (2004) Angiopoietin-related/angiopoietin-like proteins regulate angiogenesis. *International journal of hematology* **80**, 21-28
3. Santulli, G. (2014) Angiopoietin-like proteins: a comprehensive look. *Front Endocrinol (Lausanne)* **5**, 4
4. Dhanabal, M., LaRochelle, W. J., Jeffers, M., Herrmann, J., Rastelli, L., McDonald, W. F., Chillakuru, R. A., Yang, M., Boldog, F. L., Padigaru, M., McQueeney, K. D., Wu, F., Minskoff, S. A., Shimkets, R. A., and Lichenstein, H. S. (2002) Angioarrestin: An Antiangiogenic Protein with Tumor-inhibiting Properties.
5. Kuo, T. C., Tan, C. T., Chang, Y. W., Hong, C. C., Lee, W. J., Chen, M. W., Jeng, Y. M., Chiou, J., Yu, P., Chen, P. S., Wang, M. Y., Hsiao, M., Su, J. L., and Kuo, M. L. (2013) Angiopoietin-like protein 1 suppresses SLUG to inhibit cancer cell motility. in *J Clin Invest*. pp 1082-1095
6. Yan, Q., Jiang, L., Liu, M., Yu, D., Zhang, Y., Li, Y., Fang, S., Li, Y., Zhu, Y.-H., Yuan, Y., and Guan, X. Y. (2017) ANGPTL1 interacts with integrin α1β1 to suppress HCC angiogenesis and metastasis by inhibiting JAK2/STAT3 signaling.
7. Chen, H., Xiao, Q., Hu, Y., Chen, L., Jiang, K., Tang, Y., Tan, Y., Hu, W., Wang, Z., He, J., Liu, Y., Cai, Y., Yang, Q., and Ding, K. (2017) ANGPTL1 attenuates colorectal cancer metastasis by up-regulating microRNA-138. in *J Exp Clin Cancer Res*. pp
8. Kim, I., Moon, S.-O., Koh, K. N., Kim, H., Uhm, C.-S., Kwak, H. J., Kim, N.-G., and Koh, G. Y. (1999) Molecular Cloning, Expression, and Characterization of Angiopoietin-related Protein.
9. Horio, E., Kadomatsu, T., Miyata, K., Arai, Y., Hosokawa, K., Doi, Y., Ninomiya, T., Horiguchi, H., Endo, M., Tabata, M., Tazume, H., Tian, Z., Takahashi, O., Terada, K., Takeya, M., Hao, H., Hirose, N., Minami, T., Suda, T., Kiyohara, Y., Ogawa, H., Kaikita, K., and Oike, Y. (2014) Role of endothelial cell-derived angptl2 in vascular inflammation leading to endothelial dysfunction and atherosclerosis progression. *Arteriosclerosis, thrombosis, and vascular biology* **34**, 790-800
10. Tabata, M., Kadomatsu, T., Fukuhara, S., Miyata, K., Ito, Y., Endo, M., Urano, T., Zhu, H. J., Tsukano, H., Tazume, H., Kaikita, K., Miyashita, K., Iwawaki, T., Shimabukuro, M., Sakaguchi, K., Ito, T., Nakagata, N., Yamada, T., Katagiri, H., Kasuga, M., Ando, Y., Ogawa, H., Mochizuki, N., Itoh, H., Suda, T., and Oike, Y. (2009) Angiopoietin-like protein 2 promotes chronic adipose tissue inflammation and obesity-related systemic insulin resistance. *Cell metabolism* **10**, 178-188
11. Tian, Z., Miyata, K., Kadomatsu, T., Horiguchi, H., Fukushima, H., Tohyama, S., Ujihara, Y., Okumura, T., Yamaguchi, S., Zhao, J., Endo, M., Morinaga, J., Sato, M., Sugizaki, T., Zhu, S., Terada, K., Sakaguchi, H., Komohara, Y., Takeya, M., Takeda, N., Araki, K., Manabe, I., Fukuda, K., Otsu, K., Wada, J., Murohara, T., Mohri, S., Yamashita, J. K., Sano, M., and Oike, Y. (2016) ANGPTL2 activity in cardiac pathologies accelerates heart failure by perturbing cardiac function and energy metabolism. *Nature communications* **7**, 13016
12. Piche, M. E., Thorin-Trescases, N., Auclair, A., Marceau, S., Martin, J., Fortier, A., Thorin, E., and Poirier, P. (2017) Bariatric Surgery-Induced Lower Angiopoietin-Like 2

Protein Is Associated With Improved Cardiometabolic Profile. *The Canadian journal of cardiology* **33**, 1044-1051
13. Yoshinaga, T., Shigemitsu, T., Nishimata, H., Kitazono, M., Hori, E., Tomiyoshi, A., Takei, T., and Yoshida, M. (2015) Angiopoietin-like protein 2 as a potential biomarker for colorectal cancer. in *Mol Clin Oncol*. pp 1080-1084
14. Drebert, Z., MacAskill, M., Doughty-Shenton, D., De Bosscher, K., Bracke, M., Hadoke, P. W., and Beck, I. M. (2017) Colon cancer-derived myofibroblasts increase endothelial cell migration by glucocorticoid-sensitive secretion of a pro-migratory factor. in *Vascul Pharmacol*. pp 19-30
15. Liu, X., Yu, X., Xie, J., Zhan, M., Yu, Z., Xie, L., Zeng, H., Zhang, F., Chen, G., Yi, X., and Zheng, J. (2015) ANGPTL2/LILRB2 signaling promotes the propagation of lung cancer cells. *Oncotarget* **6**, 21004-21015
16. Conklin, D., Gilbertson, D., Taft, D. W., Maurer, M. F., Whitmore, T. E., Smith, D. L., Walker, K. M., Chen, L. H., Wattler, S., Nehls, M., and Lewis, K. B. (1999) Identification of a mammalian angiopoietin-related protein expressed specifically in liver. *Genomics* **62**, 477-482
17. Ono, M., Shimizugawa, T., Shimamura, M., Yoshida, K., Noji-Sakikawa, C., Ando, Y., Koishi, R., and Furukawa, H. (2003) Protein region important for regulation of lipid metabolism in angiopoietin-like 3 (ANGPTL3): ANGPTL3 is cleaved and activated in vivo. *J Biol Chem* **278**, 41804-41809
18. Quagliarini, F., Wang, Y., Kozlitina, J., Grishin, N. V., Hyde, R., Boerwinkle, E., Valenzuela, D. M., Murphy, A. J., Cohen, J. C., and Hobbs, H. H. (2012) Atypical angiopoietin-like protein that regulates ANGPTL3. *Proceedings of the National Academy of Sciences of the United States of America* **109**, 19751-19756
19. Koishi, R., Ando, Y., Ono, M., Shimamura, M., Yasumo, H., Fujiwara, T., Horikoshi, H., and Furukawa, H. (2002) Angptl3 regulates lipid metabolism in mice. *Nat Genet* **30**, 151-157
20. Shan, L., Yu, X. C., Liu, Z., Hu, Y., Sturgis, L. T., Miranda, M. L., and Liu, Q. (2009) The Angiopoietin-like Proteins ANGPTL3 and ANGPTL4 Inhibit Lipoprotein Lipase Activity through Distinct Mechanisms*. in *J Biol Chem*. pp 1419-1424
21. Koster, A., Chao, Y. B., Mosior, M., Ford, A., Gonzalez-DeWhitt, P. A., Hale, J. E., Li, D., Qiu, Y., Fraser, C. C., Yang, D. D., Heuer, J. G., Jaskunas, S. R., and Eacho, P. (2005) Transgenic angiopoietin-like (angptl)4 overexpression and targeted disruption of angptl4 and angptl3: regulation of triglyceride metabolism. *Endocrinology* **146**, 4943-4950
22. Wang, Y., McNutt, M. C., Banfi, S., Levin, M. G., Holland, W. L., Gusarova, V., Gromada, J., Cohen, J. C., and Hobbs, H. H. (2015) Hepatic ANGPTL3 regulates adipose tissue energy homeostasis. *Proceedings of the National Academy of Sciences of the United States of America* **112**, 11630-11635
23. Willer, C. J., Sanna, S., Jackson, A. U., Scuteri, A., Bonnycastle, L. L., Clarke, R., Heath, S. C., Timpson, N. J., Najjar, S. S., Stringham, H. M., Strait, J., Duren, W. L., Maschio, A., Busonero, F., Mulas, A., Albai, G., Swift, A. J., Morken, M. A., Narisu, N., Bennett, D., Parish, S., Shen, H., Galan, P., Meneton, P., Hercberg, S., Zelenika, D., Chen, W. M., Li, Y., Scott, L. J., Scheet, P. A., Sundvall, J., Watanabe, R. M., Nagaraja, R., Ebrahim, S., Lawlor, D. A., Ben-Shlomo, Y., Davey-Smith, G., Shuldiner, A. R., Collins, R., Bergman, R. N., Uda, M., Tuomilehto, J., Cao, A., Collins, F. S., Lakatta, E., Lathrop, G.

M., Boehnke, M., Schlessinger, D., Mohlke, K. L., and Abecasis, G. R. (2008) Newly identified loci that influence lipid concentrations and risk of coronary artery disease. *Nat Genet* **40**, 161-169
24. Musunuru, K., Pirruccello, J. P., Do, R., Peloso, G. M., Guiducci, C., Sougnez, C., Garimella, K. V., Fisher, S., Abreu, J., Barry, A. J., Fennell, T., Banks, E., Ambrogio, L., Cibulskis, K., Kernytsky, A., Gonzalez, E., Rudzicz, N., Engert, J. C., DePristo, M. A., Daly, M. J., Cohen, J. C., Hobbs, H. H., Altshuler, D., Schonfeld, G., Gabriel, S. B., Yue, P., and Kathiresan, S. (2010) Exome sequencing, ANGPTL3 mutations, and familial combined hypolipidemia. *N Engl J Med* **363**, 2220-2227
25. Robciuc, M. R., Maranghi, M., Lahikainen, A., Rader, D., Bensadoun, A., Oorni, K., Metso, J., Minicocci, I., Ciociola, E., Ceci, F., Montali, A., Arca, M., Ehnholm, C., and Jauhiainen, M. (2013) Angptl3 deficiency is associated with increased insulin sensitivity, lipoprotein lipase activity, and decreased serum free fatty acids. *Arteriosclerosis, thrombosis, and vascular biology* **33**, 1706-1713
26. Ando, Y., Shimizugawa, T., Takeshita, S., Ono, M., Shimamura, M., Koishi, R., and Furukawa, H. (2003) A decreased expression of angiopoietin-like 3 is protective against atherosclerosis in apoE-deficient mice. *J Lipid Res* **44**, 1216-1223
27. Graham, M. J., Lee, R. G., Brandt, T. A., Tai, L. J., Fu, W., Peralta, R., Yu, R., Hurh, E., Paz, E., McEvoy, B. W., Baker, B. F., Pham, N. C., Digenio, A., Hughes, S. G., Geary, R. S., Witztum, J. L., Crooke, R. M., and Tsimikas, S. (2017) Cardiovascular and Metabolic Effects of ANGPTL3 Antisense Oligonucleotides. *N Engl J Med* **377**, 222-232
28. Zeng, L., Dai, J., Ying, K., Zhao, E., Jin, W., Ye, Y., Xu, J., Xie, Y., and Mao, Y. (2003) Identification of a novel human angiopoietin-like gene expressed mainly in heart. *Journal of human genetics* **48**, 159-162
29. Zhang, C. C., Kaba, M., Iizuka, S., Huynh, H., and Lodish, H. F. (2008) Angiopoietin-like 5 and IGFBP2 stimulate ex vivo expansion of human cord blood hematopoietic stem cells as assayed by NOD/SCID transplantation. in *Blood*. pp 3415-3423
30. Drake, A. C., Khoury, M., Leskov, I., Iliopoulou, B. P., Fragoso, M., Lodish, H., and Chen, J. (2011) Human CD34+ CD133+ hematopoietic stem cells cultured with growth factors including Angptl5 efficiently engraft adult NOD-SCID Il2rgamma-/- (NSG) mice. *PloS one* **6**, e18382
31. Blank, U., Ehrnstrom, B., Heinz, N., Nilsson, E., Brun, A., Baum, C., Schiedlmeier, B., and Karlsson, S. (2012) Angptl4 maintains in vivo repopulation capacity of CD34+ human cord blood cells. *European journal of haematology* **89**, 198-205
32. Liang, J., Lv, J., and Liu, Z. (2015) Identification of stage-specific biomarkers in lung adenocarcinoma based on RNA-seq data. *Tumour biology : the journal of the International Society for Oncodevelopmental Biology and Medicine* **36**, 6391-6399
33. Romeo, S., Yin, W., Kozlitina, J., Pennacchio, L. A., Boerwinkle, E., Hobbs, H. H., and Cohen, J. C. (2009) Rare loss-of-function mutations in ANGPTL family members contribute to plasma triglyceride levels in humans. in *J Clin Invest*. pp 70-79
34. Oike, Y., Ito, Y., Maekawa, H., Morisada, T., Kubota, Y., Akao, M., Urano, T., Yasunaga, K., and Suda, T. (2004) Angiopoietin-related growth factor (AGF) promotes angiogenesis. *Blood* **103**, 3760-3765
35. Oike, Y., Akao, M., Yasunaga, K., Yamauchi, T., Morisada, T., Ito, Y., Urano, T., Kimura, Y., Kubota, Y., Maekawa, H., Miyamoto, T., Miyata, K., Matsumoto, S., Sakai, J., Nakagata, N., Takeya, M., Koseki, H., Ogawa, Y., Kadowaki, T., and Suda, T. (2005)

Angiopoietin-related growth factor antagonizes obesity and insulin resistance. *Nature medicine* **11**, 400-408
36. Kang, S. G., Yi, H. S., Choi, M. J., Ryu, M. J., Jung, S., Chung, H. K., Chang, J. Y., Kim, Y. K., Lee, S. E., Kim, H. W., Choi, H., Kim, D. S., Lee, J. H., Kim, K. S., Kim, H. J., Lee, C. H., Oike, Y., and Shong, M. (2017) ANGPTL6 expression is coupled with mitochondrial OXPHOS function to regulate adipose FGF21. *The Journal of endocrinology* **233**, 105-118
37. Lim, J. A., Kim, H. J., Ahn, H. Y., Park, K. U., Yi, K. H., Park, D. J., Jang, H. C., and Park, Y. J. (2015) Influence of thyroid dysfunction on serum levels of angiopoietin-like protein 6. *Metabolism: clinical and experimental* **64**, 1279-1283
38. Hendricks, A. E., Bochukova, E. G., Marenne, G., Keogh, J. M., Atanassova, N., Bounds, R., Wheeler, E., Mistry, V., Henning, E., Korner, A., Muddyman, D., McCarthy, S., Hinney, A., Hebebrand, J., Scott, R. A., Langenberg, C., Wareham, N. J., Surendran, P., Howson, J. M., Butterworth, A. S., Danesh, J., Nordestgaard, B. G., Nielsen, S. F., Afzal, S., Papadia, S., Ashford, S., Garg, S., Millhauser, G. L., Palomino, R. I., Kwasniewska, A., Tachmazidou, I., O'Rahilly, S., Zeggini, E., Barroso, I., and Farooqi, I. S. (2017) Rare Variant Analysis of Human and Rodent Obesity Genes in Individuals with Severe Childhood Obesity. *Scientific reports* **7**, 4394
39. Katoh, Y., and Katoh, M. (2006) Comparative integromics on Angiopoietin family members. *International journal of molecular medicine* **17**, 1145-1149
40. Xiao, Y., Jiang, Z., Li, Y., Ye, W., Jia, B., Zhang, M., Xu, Y., Wu, D., Lai, L., Chen, Y., Chang, Y., Huang, X., Liu, H., Qing, G., Liu, P., Xu, B., Zhong, M., Yao, Y., Pei, D., and Li, P. (2015) ANGPTL7 regulates the expansion and repopulation of human hematopoietic stem and progenitor cells. *Haematologica* **100**, 585-594
41. Qian, T., Wang, K., Cui, J., He, Y., and Yang, Z. (2016) Angiopoietin-Like Protein 7 Promotes an Inflammatory Phenotype in RAW264.7 Macrophages Through the P38 MAPK Signaling Pathway. *Inflammation* **39**, 974-985
42. Liu, H. Y., and Zhang, C. J. (2017) Identification of differentially expressed genes and their upstream regulators in colorectal cancer. *Cancer gene therapy* **24**, 244-250
43. Guo, J. C., Li, C. Q., Wang, Q. Y., Zhao, J. M., Ding, J. Y., Li, E. M., and Xu, L. Y. (2016) Protein-coding genes combined with long non-coding RNAs predict prognosis in esophageal squamous cell carcinoma patients as a novel clinical multi-dimensional signature. *Molecular bioSystems* **12**, 3467-3477
44. Abu-Farha, M., Cherian, P., Al-Khairi, I., Madhu, D., Tiss, A., Warsam, S., Alhubail, A., Sriraman, D., Al-Refaei, F., and Abubaker, J. (2017) Plasma and adipose tissue level of angiopoietin-like 7 (ANGPTL7) are increased in obesity and reduced after physical exercise. *PloS one* **12**, e0173024
45. Fu, Z., Yao, F., Abou-Samra, A. B., and Zhang, R. (2013) Lipasin, thermoregulated in brown fat, is a novel but atypical member of the angiopoietin-like protein family. *Biochemical and biophysical research communications* **430**, 1126-1131
46. Ren, G., Kim, J. Y., and Smas, C. M. (2012) Identification of RIFL, a novel adipocyte-enriched insulin target gene with a role in lipid metabolism. *American journal of physiology. Endocrinology and metabolism* **303**, E334-351
47. Zhang, R. (2012) Lipasin, a novel nutritionally-regulated liver-enriched factor that regulates serum triglyceride levels. *Biochemical and biophysical research communications* **424**, 786-792

48. Mysore, R., Ortega, F. J., Latorre, J., Ahonen, M., Savolainen-Peltonen, H., Fischer-Posovszky, P., Wabitsch, M., Olkkonen, V. M., Fernandez-Real, J. M., and Nidhina Haridas, P. A. (2017) MicroRNA-221-3p regulates Angiopoietin-like 8 (ANGPTL8) expression in adipocytes. *The Journal of clinical endocrinology and metabolism*
49. Mysore, R., Liebisch, G., Zhou, Y., Olkkonen, V. M., and Nidhina Haridas, P. A. (2017) Angiopoietin-like 8 (Angptl8) controls adipocyte lipolysis and phospholipid composition. *Chemistry and physics of lipids*
50. Kersten, S., Lichtenstein, L., Steenbergen, E., Mudde, K., Hendriks, H. F., Hesselink, M. K., Schrauwen, P., and Muller, M. (2009) Caloric restriction and exercise increase plasma ANGPTL4 levels in humans via elevated free fatty acids. *Arteriosclerosis, thrombosis, and vascular biology* **29**, 969-974
51. Kim, I., Kim, H. G., Kim, H., Kim, H. H., Park, S. K., Uhm, C. S., Lee, Z. H., and Koh, G. Y. (2000) Hepatic expression, synthesis and secretion of a novel fibrinogen/angiopoietin-related protein that prevents endothelial-cell apoptosis. *Biochem J* **346 Pt 3**, 603-610
52. Kersten, S., Mandard, S., Tan, N. S., Escher, P., Metzger, D., Chambon, P., Gonzalez, F. J., Desvergne, B., and Wahli, W. (2000) Characterization of the fasting-induced adipose factor FIAF, a novel peroxisome proliferator-activated receptor target gene. *J Biol Chem* **275**, 28488-28493
53. Yoon, J. C., Chickering, T. W., Rosen, E. D., Dussault, B., Qin, Y., Soukas, A., Friedman, J. M., Holmes, W. E., and Spiegelman, B. M. (2000) Peroxisome proliferator-activated receptor gamma target gene encoding a novel angiopoietin-related protein associated with adipose differentiation. *Mol Cell Biol* **20**, 5343-5349
54. Zhu, P., Goh, Y. Y., Chin, H. F., Kersten, S., and Tan, N. S. (2012) Angiopoietin-like 4: a decade of research. *Bioscience reports* **32**, 211-219
55. Dijk, W., Heine, M., Vergnes, L., Boon, M. R., Schaart, G., Hesselink, M. K., Reue, K., van Marken Lichtenbelt, W. D., Olivecrona, G., Rensen, P. C., Heeren, J., and Kersten, S. (2015) ANGPTL4 mediates shuttling of lipid fuel to brown adipose tissue during sustained cold exposure. *Elife* **4**
56. Li, H., Ge, C., Zhao, F., Yan, M., Hu, C., Jia, D., Tian, H., Zhu, M., Chen, T., Jiang, G., Xie, H., Cui, Y., Gu, J., Tu, H., He, X., Yao, M., Liu, Y., and Li, J. (2011) Hypoxia-inducible factor 1 alpha-activated angiopoietin-like protein 4 contributes to tumor metastasis via vascular cell adhesion molecule-1/integrin beta1 signaling in human hepatocellular carcinoma. *Hepatology (Baltimore, Md.)* **54**, 910-919
57. Mandard, S., Zandbergen, F., Tan, N. S., Escher, P., Patsouris, D., Koenig, W., Kleemann, R., Bakker, A., Veenman, F., Wahli, W., Muller, M., and Kersten, S. (2004) The direct peroxisome proliferator-activated receptor target fasting-induced adipose factor (FIAF/PGAR/ANGPTL4) is present in blood plasma as a truncated protein that is increased by fenofibrate treatment. *J Biol Chem* **279**, 34411-34420
58. Abu-Farha, M., Al-Khairi, I., Cherian, P., Chandy, B., Sriraman, D., Alhubail, A., Al-Refaei, F., AlTerki, A., and Abubaker, J. (2016) Increased ANGPTL3, 4 and ANGPTL8/betatrophin expression levels in obesity and T2D. *Lipids in health and disease* **15**, 181
59. Yuan, C., Lin, J. Z., Sieglaff, D. H., Ayers, S. D., Denoto-Reynolds, F., Baxter, J. D., and Webb, P. (2012) Identical gene regulation patterns of T3 and selective thyroid hormone receptor modulator GC-1. *Endocrinology* **153**, 501-511

60. Wang, J., Zhu, X., Wang, Z., Yao, J., Zhao, B., and Liu, G. (2015) Non-esterified fatty acids promote expression and secretion of angiopoietin-like protein 4 in calf hepatocytes cultured in vitro. *Molecular and cellular biochemistry* **401**, 141-146
61. Koliwad, S. K., Kuo, T., Shipp, L. E., Gray, N. E., Backhed, F., So, A. Y., Farese, R. V., Jr., and Wang, J. C. (2009) Angiopoietin-like 4 (ANGPTL4, fasting-induced adipose factor) is a direct glucocorticoid receptor target and participates in glucocorticoid-regulated triglyceride metabolism. *J Biol Chem* **284**, 25593-25601
62. van Raalte, D. H., Brands, M., Serlie, M. J., Mudde, K., Stienstra, R., Sauerwein, H. P., Kersten, S., and Diamant, M. (2012) Angiopoietin-like protein 4 is differentially regulated by glucocorticoids and insulin in vitro and in vivo in healthy humans. *Experimental and clinical endocrinology & diabetes : official journal, German Society of Endocrinology [and] German Diabetes Association* **120**, 598-603
63. Dutton, S., and Trayhurn, P. (2008) Regulation of angiopoietin-like protein 4/fasting-induced adipose factor (Angptl4/FIAF) expression in mouse white adipose tissue and 3T3-L1 adipocytes. *The British journal of nutrition* **100**, 18-26
64. Belanger, A. J., Lu, H., Date, T., Liu, L. X., Vincent, K. A., Akita, G. Y., Cheng, S. H., Gregory, R. J., and Jiang, C. (2002) Hypoxia up-regulates expression of peroxisome proliferator-activated receptor gamma angiopoietin-related gene (PGAR) in cardiomyocytes: role of hypoxia inducible factor 1alpha. *Journal of molecular and cellular cardiology* **34**, 765-774
65. Lei, X., Shi, F., Basu, D., Huq, A., Routhier, S., Day, R., and Jin, W. (2011) Proteolytic processing of angiopoietin-like protein 4 by proprotein convertases modulates its inhibitory effects on lipoprotein lipase activity. *J Biol Chem* **286**, 15747-15756
66. Ge, H., Yang, G., Huang, L., Motola, D. L., Pourbahrami, T., and Li, C. (2004) Oligomerization and regulated proteolytic processing of angiopoietin-like protein 4. *J Biol Chem* **279**, 2038-2045
67. Yau, M. H., Wang, Y., Lam, K. S., Zhang, J., Wu, D., and Xu, A. (2009) A highly conserved motif within the NH2-terminal coiled-coil domain of angiopoietin-like protein 4 confers its inhibitory effects on lipoprotein lipase by disrupting the enzyme dimerization. *J Biol Chem* **284**, 11942-11952
68. Yoshida, K., Shimizugawa, T., Ono, M., and Furukawa, H. (2002) Angiopoietin-like protein 4 is a potent hyperlipidemia-inducing factor in mice and inhibitor of lipoprotein lipase. *J Lipid Res* **43**, 1770-1772
69. Ge, H., Yang, G., Yu, X., Pourbahrami, T., and Li, C. (2004) Oligomerization state-dependent hyperlipidemic effect of angiopoietin-like protein 4. *J Lipid Res* **45**, 2071-2079
70. Xu, A., Lam, M. C., Chan, K. W., Wang, Y., Zhang, J., Hoo, R. L., Xu, J. Y., Chen, B., Chow, W. S., Tso, A. W., and Lam, K. S. (2005) Angiopoietin-like protein 4 decreases blood glucose and improves glucose tolerance but induces hyperlipidemia and hepatic steatosis in mice. *Proceedings of the National Academy of Sciences of the United States of America* **102**, 6086-6091
71. Wang, Y., Liu, L. M., Wei, L., Ye, W. W., Meng, X. Y., Chen, F., Xiao, Q., Chen, J. Y., and Zhou, Y. (2016) Angiopoietin-like protein 4 improves glucose tolerance and insulin resistance but induces liver steatosis in high-fat-diet mice. *Mol Med Rep* **14**, 3293-3300

72. Vienberg, S. G., Kleinridders, A., Suzuki, R., and Kahn, C. R. (2015) Differential effects of angiopoietin-like 4 in brain and muscle on regulation of lipoprotein lipase activity. *Molecular metabolism* **4**, 144-150
73. Mandard, S., Zandbergen, F., van Straten, E., Wahli, W., Kuipers, F., Muller, M., and Kersten, S. (2006) The fasting-induced adipose factor/angiopoietin-like protein 4 is physically associated with lipoproteins and governs plasma lipid levels and adiposity. *J Biol Chem* **281**, 934-944
74. Adachi, H., Fujiwara, Y., Kondo, T., Nishikawa, T., Ogawa, R., Matsumura, T., Ishii, N., Nagai, R., Miyata, K., Tabata, M., Motoshima, H., Furukawa, N., Tsuruzoe, K., Kawashima, J., Takeya, M., Yamashita, S., Koh, G. Y., Nagy, A., Suda, T., Oike, Y., and Araki, E. (2009) Angptl 4 deficiency improves lipid metabolism, suppresses foam cell formation and protects against atherosclerosis. *Biochemical and biophysical research communications* **379**, 806-811
75. Desai, U., Lee, E. C., Chung, K., Gao, C., Gay, J., Key, B., Hansen, G., Machajewski, D., Platt, K. A., Sands, A. T., Schneider, M., Van Sligtenhorst, I., Suwanichkul, A., Vogel, P., Wilganowski, N., Wingert, J., Zambrowicz, B. P., Landes, G., and Powell, D. R. (2007) Lipid-lowering effects of anti-angiopoietin-like 4 antibody recapitulate the lipid phenotype found in angiopoietin-like 4 knockout mice. *Proceedings of the National Academy of Sciences of the United States of America* **104**, 11766-11771
76. Kim, H. K., Youn, B. S., Shin, M. S., Namkoong, C., Park, K. H., Baik, J. H., Kim, J. B., Park, J. Y., Lee, K. U., Kim, Y. B., and Kim, M. S. (2010) Hypothalamic angptl4/fiaf is a novel regulator of food intake and body weight. *Diabetes* **59**, 2772-2780
77. Yin, W., Romeo, S., Chang, S., Grishin, N. V., Hobbs, H. H., and Cohen, J. C. (2009) Genetic variation in ANGPTL4 provides insights into protein processing and function. *J Biol Chem* **284**, 13213-13222
78. Sukonina, V., Lookene, A., Olivecrona, T., and Olivecrona, G. (2006) Angiopoietin-like protein 4 converts lipoprotein lipase to inactive monomers and modulates lipase activity in adipose tissue. *Proceedings of the National Academy of Sciences of the United States of America* **103**, 17450-17455
79. Lafferty, M. J., Bradford, K. C., Erie, D. A., and Neher, S. B. (2013) Angiopoietin-like protein 4 inhibition of lipoprotein lipase: evidence for reversible complex formation. *J Biol Chem* **288**, 28524-28534
80. Lichtenstein, L., Berbee, J. F., van Dijk, S. J., van Dijk, K. W., Bensadoun, A., Kema, I. P., Voshol, P. J., Muller, M., Rensen, P. C., and Kersten, S. (2007) Angptl4 upregulates cholesterol synthesis in liver via inhibition of LPL- and HL-dependent hepatic cholesterol uptake. *Arterioscler Thromb Vasc Biol* **27**, 2420-2427
81. Gray, N. E., Lam, L. N., Yang, K., Zhou, A. Y., Koliwad, S., and Wang, J. C. (2012) Angiopoietin-like 4 (Angptl4) protein is a physiological mediator of intracellular lipolysis in murine adipocytes. *J Biol Chem* **287**, 8444-8456
82. Jonker, J. T., Smit, J. W., Hammer, S., Snel, M., van der Meer, R. W., Lamb, H. J., Mattijssen, F., Mudde, K., Jazet, I. M., Dekkers, O. M., de Roos, A., Romijn, J. A., Kersten, S., and Rensen, P. C. (2013) Dietary modulation of plasma angiopoietin-like protein 4 concentrations in healthy volunteers and in patients with type 2 diabetes. *The American journal of clinical nutrition* **97**, 255-260

83. Cushing, E. M., Chi, X., Sylvers, K. L., Shetty, S. K., Potthoff, M. J., and Davies, B. S. J. (2017) Angiopoietin-like 4 directs uptake of dietary fat away from adipose during fasting. *Molecular metabolism* **6**, 809-818
84. Wiesner, G., Brown, R. E., Robertson, G. S., Imran, S. A., Ur, E., and Wilkinson, M. (2006) Increased expression of the adipokine genes resistin and fasting-induced adipose factor in hypoxic/ischaemic mouse brain. *Neuroreport* **17**, 1195-1198
85. Lichtenbelt, W., Kingma, B., van der Lans, A., and Schellen, L. (2014) Cold exposure--an approach to increasing energy expenditure in humans. *Trends in endocrinology and metabolism: TEM* **25**, 165-167
86. Alex, S., Lichtenstein, L., Dijk, W., Mensink, R. P., Tan, N. S., and Kersten, S. (2014) ANGPTL4 is produced by entero-endocrine cells in the human intestinal tract. *Histochemistry and cell biology* **141**, 383-391
87. Backhed, F., Ding, H., Wang, T., Hooper, L. V., Koh, G. Y., Nagy, A., Semenkovich, C. F., and Gordon, J. I. (2004) The gut microbiota as an environmental factor that regulates fat storage. *Proceedings of the National Academy of Sciences of the United States of America* **101**, 15718-15723
88. Backhed, F., Manchester, J. K., Semenkovich, C. F., and Gordon, J. I. (2007) Mechanisms underlying the resistance to diet-induced obesity in germ-free mice. *Proceedings of the National Academy of Sciences of the United States of America* **104**, 979-984
89. Grootaert, C., Van de Wiele, T., Van Roosbroeck, I., Possemiers, S., Vercoutter-Edouart, A. S., Verstraete, W., Bracke, M., and Vanhoecke, B. (2011) Bacterial monocultures, propionate, butyrate and H2O2 modulate the expression, secretion and structure of the fasting-induced adipose factor in gut epithelial cell lines. *Environmental microbiology* **13**, 1778-1789
90. Brahe, L. K., Astrup, A., and Larsen, L. H. (2013) Is butyrate the link between diet, intestinal microbiota and obesity-related metabolic diseases? *Obesity reviews : an official journal of the International Association for the Study of Obesity* **14**, 950-959
91. Myocardial Infarction, G., Investigators, C. A. E. C., Stitziel, N. O., Stirrups, K. E., Masca, N. G., Erdmann, J., Ferrario, P. G., Konig, I. R., Weeke, P. E., Webb, T. R., Auer, P. L., Schick, U. M., Lu, Y., Zhang, H., Dube, M. P., Goel, A., Farrall, M., Peloso, G. M., Won, H. H., Do, R., van Iperen, E., Kanoni, S., Kruppa, J., Mahajan, A., Scott, R. A., Willenberg, C., Braund, P. S., van Capelleveen, J. C., Doney, A. S., Donnelly, L. A., Asselta, R., Merlini, P. A., Duga, S., Marziliano, N., Denny, J. C., Shaffer, C. M., El-Mokhtari, N. E., Franke, A., Gottesman, O., Heilmann, S., Hengstenberg, C., Hoffman, P., Holmen, O. L., Hveem, K., Jansson, J. H., Jockel, K. H., Kessler, T., Kriebel, J., Laugwitz, K. L., Marouli, E., Martinelli, N., McCarthy, M. I., Van Zuydam, N. R., Meisinger, C., Esko, T., Mihailov, E., Escher, S. A., Alvar, M., Moebus, S., Morris, A. D., Muller-Nurasyid, M., Nikpay, M., Olivieri, O., Lemieux Perreault, L. P., AlQarawi, A., Robertson, N. R., Akinsanya, K. O., Reilly, D. F., Vogt, T. F., Yin, W., Asselbergs, F. W., Kooperberg, C., Jackson, R. D., Stahl, E., Strauch, K., Varga, T. V., Waldenberger, M., Zeng, L., Kraja, A. T., Liu, C., Ehret, G. B., Newton-Cheh, C., Chasman, D. I., Chowdhury, R., Ferrario, M., Ford, I., Jukema, J. W., Kee, F., Kuulasmaa, K., Nordestgaard, B. G., Perola, M., Saleheen, D., Sattar, N., Surendran, P., Tregouet, D., Young, R., Howson, J. M., Butterworth, A. S., Danesh, J., Ardissino, D., Bottinger, E. P., Erbel, R., Franks, P. W., Girelli, D., Hall, A. S., Hovingh, G. K., Kastrati, A., Lieb, W.,

Meitinger, T., Kraus, W. E., Shah, S. H., McPherson, R., Orho-Melander, M., Melander, O., Metspalu, A., Palmer, C. N., Peters, A., Rader, D., Reilly, M. P., Loos, R. J., Reiner, A. P., Roden, D. M., Tardif, J. C., Thompson, J. R., Wareham, N. J., Watkins, H., Willer, C. J., Kathiresan, S., Deloukas, P., Samani, N. J., and Schunkert, H. (2016) Coding Variation in ANGPTL4, LPL, and SVEP1 and the Risk of Coronary Disease. *N Engl J Med* **374**, 1134-1144

92. Dewey, F. E., Gusarova, V., O'Dushlaine, C., Gottesman, O., Trejos, J., Hunt, C., Van Hout, C. V., Habegger, L., Buckler, D., Lai, K. M., Leader, J. B., Murray, M. F., Ritchie, M. D., Kirchner, H. L., Ledbetter, D. H., Penn, J., Lopez, A., Borecki, I. B., Overton, J. D., Reid, J. G., Carey, D. J., Murphy, A. J., Yancopoulos, G. D., Baras, A., Gromada, J., and Shuldiner, A. R. (2016) Inactivating Variants in ANGPTL4 and Risk of Coronary Artery Disease. *The New England journal of medicine* **374**, 1123-1133
93. Romeo, S., Pennacchio, L. A., Fu, Y., Boerwinkle, E., Tybjaerg-Hansen, A., Hobbs, H. H., and Cohen, J. C. (2007) Population-based resequencing of ANGPTL4 uncovers variations that reduce triglycerides and increase HDL. *Nat Genet* **39**, 513-516
94. Abid, K., Trimeche, T., Mili, D., Msolli, M. A., Trabelsi, I., Nouira, S., and Kenani, A. (2016) ANGPTL4 variants E40K and T266M are associated with lower fasting triglyceride levels and predicts cardiovascular disease risk in Type 2 diabetic Tunisian population. in *Lipids in health and disease*. pp
95. Mysling, S., Kristensen, K. K., Larsson, M., Kovrov, O., Bensadouen, A., Jorgensen, T. J., Olivecrona, G., Young, S. G., and Ploug, M. (2016) The angiopoietin-like protein ANGPTL4 catalyzes unfolding of the hydrolase domain in lipoprotein lipase and the endothelial membrane protein GPIHBP1 counteracts this unfolding. *Elife* **5**
96. Talmud, P. J., Smart, M., Presswood, E., Cooper, J. A., Nicaud, V., Drenos, F., Palmen, J., Marmot, M. G., Boekholdt, S. M., Wareham, N. J., Khaw, K. T., Kumari, M., and Humphries, S. E. (2008) ANGPTL4 E40K and T266M: effects on plasma triglyceride and HDL levels, postprandial responses, and CHD risk. *Arteriosclerosis, thrombosis, and vascular biology* **28**, 2319-2325
97. Tan, Z. W., Teo, Z., Tan, C., Choo, C. C., Loo, W. S., Song, Y., Tam, Z. Y., Ng, S. P., Koh, H. Z., Ng, Y. S., Shochat, S. G., Yau, Y. H., Zhu, P., and Tan, N. S. (2017) ANGPTL4 T266M variant is associated with reduced cancer invasiveness. *Biochimica et biophysica acta* **1864**, 1525-1536
98. Lichtenstein, L., Mattijssen, F., de Wit, N. J., Georgiadi, A., Hooiveld, G. J., van der Meer, R., He, Y., Qi, L., Koster, A., Tamsma, J. T., Tan, N. S., Muller, M., and Kersten, S. (2010) Angptl4 protects against severe proinflammatory effects of saturated fat by inhibiting fatty acid uptake into mesenteric lymph node macrophages. *Cell metabolism* **12**, 580-592
99. Phua, T., Sng, M. K., Tan, E. H., Chee, D. S., Li, Y., Wee, J. W., Teo, Z., Chan, J. S., Lim, M. M., Tan, C. K., Zhu, P., Arulampalam, V., and Tan, N. S. (2017) Angiopoietin-like 4 Mediates Colonic Inflammation by Regulating Chemokine Transcript Stability via Tristetraprolin. *Scientific reports* **7**, 44351
100. Aryal, B., Rotllan, N., Araldi, E., Ramirez, C. M., He, S., Chousterman, B. G., Fenn, A. M., Wanschel, A., Madrigal-Matute, J., Warrier, N., Martin-Ventura, J. L., Swirski, F. K., Suarez, Y., and Fernandez-Hernando, C. (2016) ANGPTL4 deficiency in haematopoietic cells promotes monocyte expansion and atherosclerosis progression. *Nature communications* **7**, 12313

101. Goh, Y. Y., Pal, M., Chong, H. C., Zhu, P., Tan, M. J., Punugu, L., Tan, C. K., Huang, R. L., Sze, S. K., Tang, M. B., Ding, J. L., Kersten, S., and Tan, N. S. (2010) Angiopoietin-like 4 interacts with matrix proteins to modulate wound healing. *J Biol Chem* **285**, 32999-33009
102. Goh, Y. Y., Pal, M., Chong, H. C., Zhu, P., Tan, M. J., Punugu, L., Lam, C. R., Yau, Y. H., Tan, C. K., Huang, R. L., Tan, S. M., Tang, M. B., Ding, J. L., Kersten, S., and Tan, N. S. (2010) Angiopoietin-like 4 interacts with integrins beta1 and beta5 to modulate keratinocyte migration. *Am J Pathol* **177**, 2791-2803
103. Arya, A. K., Tripathi, K., and Das, P. (2014) Promising role of ANGPTL4 gene in diabetic wound healing. *The international journal of lower extremity wounds* **13**, 58-63
104. Ito, Y., Oike, Y., Yasunaga, K., Hamada, K., Miyata, K., Matsumoto, S., Sugano, S., Tanihara, H., Masuho, Y., and Suda, T. (2003) Inhibition of angiogenesis and vascular leakiness by angiopoietin-related protein 4. *Cancer research* **63**, 6651-6657
105. Cazes, A., Galaup, A., Chomel, C., Bignon, M., Brechot, N., Le Jan, S., Weber, H., Corvol, P., Muller, L., Germain, S., and Monnot, C. (2006) Extracellular matrix-bound angiopoietin-like 4 inhibits endothelial cell adhesion, migration, and sprouting and alters actin cytoskeleton. *Circ Res* **99**, 1207-1215
106. Galaup, A., Cazes, A., Le Jan, S., Philippe, J., Connault, E., Le Coz, E., Mekid, H., Mir, L. M., Opolon, P., Corvol, P., Monnot, C., and Germain, S. (2006) Angiopoietin-like 4 prevents metastasis through inhibition of vascular permeability and tumor cell motility and invasiveness. *Proceedings of the National Academy of Sciences of the United States of America* **103**, 18721-18726
107. Le Jan, S., Amy, C., Cazes, A., Monnot, C., Lamande, N., Favier, J., Philippe, J., Sibony, M., Gasc, J. M., Corvol, P., and Germain, S. (2003) Angiopoietin-like 4 is a proangiogenic factor produced during ischemia and in conventional renal cell carcinoma. *Am J Pathol* **162**, 1521-1528
108. Katanasaka, Y., Kodera, Y., Kitamura, Y., Morimoto, T., Tamura, T., and Koizumi, F. (2013) Epidermal growth factor receptor variant type III markedly accelerates angiogenesis and tumor growth via inducing c-myc mediated angiopoietin-like 4 expression in malignant glioma. *Molecular cancer* **12**, 31
109. Kim, S. H., Park, Y. Y., Kim, S. W., Lee, J. S., Wang, D., and DuBois, R. N. (2011) ANGPTL4 induction by prostaglandin E2 under hypoxic conditions promotes colorectal cancer progression. *Cancer research* **71**, 7010-7020
110. Padua, D., Zhang, X. H., Wang, Q., Nadal, C., Gerald, W. L., Gomis, R. R., and Massague, J. (2008) TGFbeta primes breast tumors for lung metastasis seeding through angiopoietin-like 4. *Cell* **133**, 66-77
111. Li, B., Qian, M., Cao, H., Jia, Q., Wu, Z., Yang, X., Ma, T., Wei, H., Chen, T., and Xiao, J. (2017) TGF-beta2-induced ANGPTL4 expression promotes tumor progression and osteoclast differentiation in giant cell tumor of bone. *Oncotarget* **8**, 54966-54977
112. Liao, Y. H., Chiang, K. H., Shieh, J. M., Huang, C. R., Shen, C. J., Huang, W. C., and Chen, B. K. (2017) Epidermal growth factor-induced ANGPTL4 enhances anoikis resistance and tumour metastasis in head and neck squamous cell carcinoma. *Oncogene* **36**, 2228-2242
113. Sun, Y., Long, J., and Zhou, Y. (2014) Angiopoietin-like 4 promotes melanoma cell invasion and survival through aldolase A. *Oncology letters* **8**, 211-217

114. Akishima-Fukasawa, Y., Ishikawa, Y., Akasaka, Y., Uzuki, M., Inomata, N., Yokoo, T., Ishii, R., Shimokawa, R., Mukai, K., Kiguchi, H., Suzuki, K., Fujiwara, M., Ogata, K., Niino, H., Sugiura, H., Ichinose, A., Kuroda, Y., Kuroda, D., and Ishii, T. (2011) Histopathological predictors of regional lymph node metastasis at the invasive front in early colorectal cancer. *Histopathology* **59**, 470-481
115. Wilson, S. S., Wong, A., Toupadakis, C. A., and Yellowley, C. E. (2015) Expression of angiopoietin-like protein 4 at the fracture site: Regulation by hypoxia and osteoblastic differentiation. *Journal of orthopaedic research : official publication of the Orthopaedic Research Society* **33**, 1364-1373
116. Zheng, J., Umikawa, M., Cui, C., Li, J., Chen, X., Zhang, C., Huynh, H., Kang, X., Silvany, R., Wan, X., Ye, J., Canto, A. P., Chen, S. H., Wang, H. Y., Ward, E. S., and Zhang, C. C. (2012) Inhibitory receptors bind ANGPTLs and support blood stem cells and leukaemia development. *Nature* **485**, 656-660
117. Holm, C. (2003) Molecular mechanisms regulating hormone-sensitive lipase and lipolysis. *Biochemical Society transactions* **31**, 1120-1124
118. Villena, J. A., Roy, S., Sarkadi-Nagy, E., Kim, K. H., and Sul, H. S. (2004) Desnutrin, an adipocyte gene encoding a novel patatin domain-containing protein, is induced by fasting and glucocorticoids: ectopic expression of desnutrin increases triglyceride hydrolysis. *J Biol Chem* **279**, 47066-47075
119. Soni, K. G., Lehner, R., Metalnikov, P., O'Donnell, P., Semache, M., Gao, W., Ashman, K., Pshezhetsky, A. V., and Mitchell, G. A. (2004) Carboxylesterase 3 (EC 3.1.1.1) is a major adipocyte lipase. *J Biol Chem* **279**, 40683-40689
120. Gilham, D., Alam, M., Gao, W., Vance, D. E., and Lehner, R. (2005) Triacylglycerol hydrolase is localized to the endoplasmic reticulum by an unusual retrieval sequence where it participates in VLDL assembly without utilizing VLDL lipids as substrates. *Molecular biology of the cell* **16**, 984-996
121. Baulande, S., Lasnier, F., Lucas, M., and Pairault, J. (2001) Adiponutrin, a transmembrane protein corresponding to a novel dietary- and obesity-linked mRNA specifically expressed in the adipose lineage. *J Biol Chem* **276**, 33336-33344
122. Duncan, R. E., Ahmadian, M., Jaworski, K., Sarkadi-Nagy, E., and Sul, H. S. (2007) Regulation of lipolysis in adipocytes. *Annu Rev Nutr* **27**, 79-101
123. Tornqvist, H., and Belfrage, P. (1976) Purification and some properties of a monoacylglycerol-hydrolyzing enzyme of rat adipose tissue. *J Biol Chem* **251**, 813-819
124. Cao, W., Daniel, K. W., Robidoux, J., Puigserver, P., Medvedev, A. V., Bai, X., Floering, L. M., Spiegelman, B. M., and Collins, S. (2004) p38 mitogen-activated protein kinase is the central regulator of cyclic AMP-dependent transcription of the brown fat uncoupling protein 1 gene. *Mol Cell Biol* **24**, 3057-3067
125. Lass, A., Zimmermann, R., Oberer, M., and Zechner, R. (2011) Lipolysis - a highly regulated multi-enzyme complex mediates the catabolism of cellular fat stores. *Progress in lipid research* **50**, 14-27
126. Puigserver, P., Wu, Z., Park, C. W., Graves, R., Wright, M., and Spiegelman, B. M. (1998) A cold-inducible coactivator of nuclear receptors linked to adaptive thermogenesis. *Cell* **92**, 829-839
127. Cannon, B., and Nedergaard, J. (2004) Brown adipose tissue: function and physiological significance. *Physiological reviews* **84**, 277-359

128. Ahmadian, M., Abbott, M. J., Tang, T., Hudak, C. S., Kim, Y., Bruss, M., Hellerstein, M. K., Lee, H. Y., Samuel, V. T., Shulman, G. I., Wang, Y., Duncan, R. E., Kang, C., and Sul, H. S. (2011) Desnutrin/ATGL is regulated by AMPK and is required for a brown adipose phenotype. *Cell metabolism* **13**, 739-748
129. Matarese, V., and Bernlohr, D. A. (1988) Purification of murine adipocyte lipid-binding protein. Characterization as a fatty acid- and retinoic acid-binding protein. *J Biol Chem* **263**, 14544-14551
130. Coe, N. R., Simpson, M. A., and Bernlohr, D. A. (1999) Targeted disruption of the adipocyte lipid-binding protein (aP2 protein) gene impairs fat cell lipolysis and increases cellular fatty acid levels. *J Lipid Res* **40**, 967-972
131. Cohen, A. W., Razani, B., Schubert, W., Williams, T. M., Wang, X. B., Iyengar, P., Brasaemle, D. L., Scherer, P. E., and Lisanti, M. P. (2004) Role of caveolin-1 in the modulation of lipolysis and lipid droplet formation. *Diabetes* **53**, 1261-1270
132. Kim, C., Xuong, N. H., and Taylor, S. S. (2005) Crystal structure of a complex between the catalytic and regulatory (RIalpha) subunits of PKA. *Science (New York, N.Y.)* **307**, 690-696
133. Anthonsen, M. W., Ronnstrand, L., Wernstedt, C., Degerman, E., and Holm, C. (1998) Identification of novel phosphorylation sites in hormone-sensitive lipase that are phosphorylated in response to isoproterenol and govern activation properties in vitro. *J Biol Chem* **273**, 215-221
134. Marcinkiewicz, A., Gauthier, D., Garcia, A., and Brasaemle, D. L. (2006) The phosphorylation of serine 492 of perilipin a directs lipid droplet fragmentation and dispersion. *J Biol Chem* **281**, 11901-11909
135. Okazaki, H., Osuga, J., Tamura, Y., Yahagi, N., Tomita, S., Shionoiri, F., Iizuka, Y., Ohashi, K., Harada, K., Kimura, S., Gotoda, T., Shimano, H., Yamada, N., and Ishibashi, S. (2002) Lipolysis in the absence of hormone-sensitive lipase: evidence for a common mechanism regulating distinct lipases. *Diabetes* **51**, 3368-3375
136. Langin, D. (2006) Control of fatty acid and glycerol release in adipose tissue lipolysis. *Comptes rendus biologies* **329**, 598-607; discussion 653-595
137. Ragolia, L., and Begum, N. (1998) Protein phosphatase-1 and insulin action. *Molecular and cellular biochemistry* **182**, 49-58
138. Morigny, P., Houssier, M., Mouisel, E., and Langin, D. (2015) Adipocyte lipolysis and insulin resistance. *Biochimie*
139. Arner, P., and Langin, D. (2014) Lipolysis in lipid turnover, cancer cachexia, and obesity-induced insulin resistance. *Trends in endocrinology and metabolism: TEM* **25**, 255-262
140. Boden, G. (1997) Role of fatty acids in the pathogenesis of insulin resistance and NIDDM. *Diabetes* **46**, 3-10
141. McGarry, J. D. (2002) Banting lecture 2001: dysregulation of fatty acid metabolism in the etiology of type 2 diabetes. *Diabetes* **51**, 7-18
142. Kelley, D. E., and Mandarino, L. J. (2000) Fuel selection in human skeletal muscle in insulin resistance: a reexamination. *Diabetes* **49**, 677-683
143. Unger, R. H. (2002) Lipotoxic diseases. *Annual review of medicine* **53**, 319-336
144. Langin, D. (2006) Adipose tissue lipolysis as a metabolic pathway to define pharmacological strategies against obesity and the metabolic syndrome. *Pharmacological research : the official journal of the Italian Pharmacological Society* **53**, 482-491

145. Ahmadian, M., Duncan, R. E., Varady, K. A., Frasson, D., Hellerstein, M. K., Birkenfeld, A. L., Samuel, V. T., Shulman, G. I., Wang, Y., Kang, C., and Sul, H. S. (2009) Adipose overexpression of desnutrin promotes fatty acid use and attenuates diet-induced obesity. *Diabetes* **58**, 855-866
146. Jaworski, K., Ahmadian, M., Duncan, R. E., Sarkadi-Nagy, E., Varady, K. A., Hellerstein, M. K., Lee, H. Y., Samuel, V. T., Shulman, G. I., Kim, K. H., de Val, S., Kang, C., and Sul, H. S. (2009) AdPLA ablation increases lipolysis and prevents obesity induced by high-fat feeding or leptin deficiency. *Nature medicine* **15**, 159-168
147. Saha, P. K., Kojima, H., Martinez-Botas, J., Sunehag, A. L., and Chan, L. (2004) Metabolic adaptations in the absence of perilipin: increased beta-oxidation and decreased hepatic glucose production associated with peripheral insulin resistance but normal glucose tolerance in perilipin-null mice. *J Biol Chem* **279**, 35150-35158
148. Cousin, B., Cinti, S., Morroni, M., Raimbault, S., Ricquier, D., Penicaud, L., and Casteilla, L. (1992) Occurrence of brown adipocytes in rat white adipose tissue: molecular and morphological characterization. *Journal of cell science* **103 (Pt 4)**, 931-942
149. Himms-Hagen, J., Melnyk, A., Zingaretti, M. C., Ceresi, E., Barbatelli, G., and Cinti, S. (2000) Multilocular fat cells in WAT of CL-316243-treated rats derive directly from white adipocytes. *Am J Physiol Cell Physiol* **279**, C670-681
150. Seale, P., Conroe, H. M., Estall, J., Kajimura, S., Frontini, A., Ishibashi, J., Cohen, P., Cinti, S., and Spiegelman, B. M. (2011) Prdm16 determines the thermogenic program of subcutaneous white adipose tissue in mice. *J Clin Invest* **121**, 96-105
151. Cousin, B., Casteilla, L., Dani, C., Muzzin, P., Revelli, J. P., and Penicaud, L. (1993) Adipose tissues from various anatomical sites are characterized by different patterns of gene expression and regulation. *Biochem J* **292 (Pt 3)**, 873-876
152. Petrovic, N., Walden, T. B., Shabalina, I. G., Timmons, J. A., Cannon, B., and Nedergaard, J. (2010) Chronic peroxisome proliferator-activated receptor gamma (PPARgamma) activation of epididymally derived white adipocyte cultures reveals a population of thermogenically competent, UCP1-containing adipocytes molecularly distinct from classic brown adipocytes. *J Biol Chem* **285**, 7153-7164
153. Shabalina, I. G., Petrovic, N., de Jong, J. M., Kalinovich, A. V., Cannon, B., and Nedergaard, J. (2013) UCP1 in brite/beige adipose tissue mitochondria is functionally thermogenic. *Cell reports* **5**, 1196-1203
154. Bostrom, P., Wu, J., Jedrychowski, M. P., Korde, A., Ye, L., Lo, J. C., Rasbach, K. A., Bostrom, E. A., Choi, J. H., Long, J. Z., Kajimura, S., Zingaretti, M. C., Vind, B. F., Tu, H., Cinti, S., Hojlund, K., Gygi, S. P., and Spiegelman, B. M. (2012) A PGC1-alpha-dependent myokine that drives brown-fat-like development of white fat and thermogenesis. *Nature* **481**, 463-468
155. Ghorbani, M., and Himms-Hagen, J. (1997) Appearance of brown adipocytes in white adipose tissue during CL 316,243-induced reversal of obesity and diabetes in Zucker fa/fa rats. *International journal of obesity and related metabolic disorders : journal of the International Association for the Study of Obesity* **21**, 465-475
156. Guerra, C., Koza, R. A., Yamashita, H., Walsh, K., and Kozak, L. P. (1998) Emergence of brown adipocytes in white fat in mice is under genetic control. Effects on body weight and adiposity. *J Clin Invest* **102**, 412-420

157. Hany, T. F., Gharehpapagh, E., Kamel, E. M., Buck, A., Himms-Hagen, J., and von Schulthess, G. K. (2002) Brown adipose tissue: a factor to consider in symmetrical tracer uptake in the neck and upper chest region. *European journal of nuclear medicine and molecular imaging* **29**, 1393-1398
158. Soderlund, V., Larsson, S. A., and Jacobsson, H. (2007) Reduction of FDG uptake in brown adipose tissue in clinical patients by a single dose of propranolol. *European journal of nuclear medicine and molecular imaging* **34**, 1018-1022
159. van Marken Lichtenbelt, W. D., Vanhommerig, J. W., Smulders, N. M., Drossaerts, J. M., Kemerink, G. J., Bouvy, N. D., Schrauwen, P., and Teule, G. J. (2009) Cold-activated brown adipose tissue in healthy men. *N Engl J Med* **360**, 1500-1508
160. Cypess, A. M., Lehman, S., Williams, G., Tal, I., Rodman, D., Goldfine, A. B., Kuo, F. C., Palmer, E. L., Tseng, Y. H., Doria, A., Kolodny, G. M., and Kahn, C. R. (2009) Identification and importance of brown adipose tissue in adult humans. *N Engl J Med* **360**, 1509-1517
161. Lidell, M. E., Betz, M. J., Dahlqvist Leinhard, O., Heglind, M., Elander, L., Slawik, M., Mussack, T., Nilsson, D., Romu, T., Nuutila, P., Virtanen, K. A., Beuschlein, F., Persson, A., Borga, M., and Enerback, S. (2013) Evidence for two types of brown adipose tissue in humans. *Nature medicine* **19**, 631-634
162. Sidossis, L., and Kajimura, S. (2015) Brown and beige fat in humans: thermogenic adipocytes that control energy and glucose homeostasis. *J Clin Invest* **125**, 478-486
163. Lee, P., Smith, S., Linderman, J., Courville, A. B., Brychta, R. J., Dieckmann, W., Werner, C. D., Chen, K. Y., and Celi, F. S. (2014) Temperature-acclimated brown adipose tissue modulates insulin sensitivity in humans. *Diabetes* **63**, 3686-3698
164. Yoneshiro, T., Aita, S., Matsushita, M., Kayahara, T., Kameya, T., Kawai, Y., Iwanaga, T., and Saito, M. (2013) Recruited brown adipose tissue as an antiobesity agent in humans. *J Clin Invest* **123**, 3404-3408
165. Saito, M., Okamatsu-Ogura, Y., Matsushita, M., Watanabe, K., Yoneshiro, T., Nio-Kobayashi, J., Iwanaga, T., Miyagawa, M., Kameya, T., Nakada, K., Kawai, Y., and Tsujisaki, M. (2009) High incidence of metabolically active brown adipose tissue in healthy adult humans: effects of cold exposure and adiposity. *Diabetes* **58**, 1526-1531
166. Qian, S. W., Tang, Y., Li, X., Liu, Y., Zhang, Y. Y., Huang, H. Y., Xue, R. D., Yu, H. Y., Guo, L., Gao, H. D., Sun, X., Li, Y. M., Jia, W. P., and Tang, Q. Q. (2013) BMP4-mediated brown fat-like changes in white adipose tissue alter glucose and energy homeostasis. *Proceedings of the National Academy of Sciences of the United States of America* **110**, E798-807
167. Tseng, Y. H., Kokkotou, E., Schulz, T. J., Huang, T. L., Winnay, J. N., Taniguchi, C. M., Tran, T. T., Suzuki, R., Espinoza, D. O., Yamamoto, Y., Ahrens, M. J., Dudley, A. T., Norris, A. W., Kulkarni, R. N., and Kahn, C. R. (2008) New role of bone morphogenetic protein 7 in brown adipogenesis and energy expenditure. *Nature* **454**, 1000-1004
168. Tomlinson, E., Fu, L., John, L., Hultgren, B., Huang, X., Renz, M., Stephan, J. P., Tsai, S. P., Powell-Braxton, L., French, D., and Stewart, T. A. (2002) Transgenic mice expressing human fibroblast growth factor-19 display increased metabolic rate and decreased adiposity. *Endocrinology* **143**, 1741-1747
169. Fisher, F. M., Kleiner, S., Douris, N., Fox, E. C., Mepani, R. J., Verdeguer, F., Wu, J., Kharitonenkov, A., Flier, J. S., Maratos-Flier, E., and Spiegelman, B. M. (2012) FGF21

regulates PGC-1alpha and browning of white adipose tissues in adaptive thermogenesis. *Genes & development* **26**, 271-281
170. Madsen, L., Pedersen, L. M., Lillefosse, H. H., Fjaere, E., Bronstad, I., Hao, Q., Petersen, R. K., Hallenborg, P., Ma, T., De Matteis, R., Araujo, P., Mercader, J., Bonet, M. L., Hansen, J. B., Cannon, B., Nedergaard, J., Wang, J., Cinti, S., Voshol, P., Doskeland, S. O., and Kristiansen, K. (2010) UCP1 induction during recruitment of brown adipocytes in white adipose tissue is dependent on cyclooxygenase activity. *PloS one* **5**, e11391
171. Vegiopoulos, A., Muller-Decker, K., Strzoda, D., Schmitt, I., Chichelnitskiy, E., Ostertag, A., Berriel Diaz, M., Rozman, J., Hrabe de Angelis, M., Nusing, R. M., Meyer, C. W., Wahli, W., Klingenspor, M., and Herzig, S. (2010) Cyclooxygenase-2 controls energy homeostasis in mice by de novo recruitment of brown adipocytes. *Science (New York, N.Y.)* **328**, 1158-1161
172. Dijk, W., and Kersten, S. (2014) Regulation of lipoprotein lipase by Angptl4. *Trends in endocrinology and metabolism: TEM* **25**, 146-155
173. Catoire, M., Alex, S., Paraskevopulos, N., Mattijssen, F., Evers-van Gogh, I., Schaart, G., Jeppesen, J., Kneppers, A., Mensink, M., Voshol, P. J., Olivecrona, G., Tan, N. S., Hesselink, M. K., Berbee, J. F., Rensen, P. C., Kalkhoven, E., Schrauwen, P., and Kersten, S. (2014) Fatty acid-inducible ANGPTL4 governs lipid metabolic response to exercise. *Proceedings of the National Academy of Sciences of the United States of America* **111**, E1043-1052
174. Romeo, S., Yin, W., Kozlitina, J., Pennacchio, L. A., Boerwinkle, E., Hobbs, H. H., and Cohen, J. C. (2009) Rare loss-of-function mutations in ANGPTL family members contribute to plasma triglyceride levels in humans. *J Clin Invest* **119**, 70-79
175. Sanderson, L. M., Degenhardt, T., Koppen, A., Kalkhoven, E., Desvergne, B., Muller, M., and Kersten, S. (2009) Peroxisome proliferator-activated receptor beta/delta (PPARbeta/delta) but not PPARalpha serves as a plasma free fatty acid sensor in liver. *Mol Cell Biol* **29**, 6257-6267
176. Gomez Perdiguero, E., Liabotis-Fontugne, A., Durand, M., Faye, C., Ricard-Blum, S., Simonutti, M., Augustin, S., Robb, B. M., Paques, M., Valenzuela, D. M., Murphy, A. J., Yancopoulos, G. D., Thurston, G., Galaup, A., Monnot, C., and Germain, S. (2016) ANGPTL4-alphavbeta3 integrin interaction counteracts hypoxia-induced vascular permeability by modulating Src signalling downstream of VEGFR2. *J Pathol*
177. Zhu, P., Tan, M. J., Huang, R. L., Tan, C. K., Chong, H. C., Pal, M., Lam, C. R., Boukamp, P., Pan, J. Y., Tan, S. H., Kersten, S., Li, H. Y., Ding, J. L., and Tan, N. S. (2011) Angiopoietin-like 4 protein elevates the prosurvival intracellular O2(-):H2O2 ratio and confers anoikis resistance to tumors. *Cancer cell* **19**, 401-415
178. Cannon, B., and Nedergaard, J. (2011) Nonshivering thermogenesis and its adequate measurement in metabolic studies. *J Exp Biol* **214**, 242-253
179. Dickson, L. M., Gandhi, S., Layden, B. T., Cohen, R. N., and Wicksteed, B. (2016) Protein kinase A induces UCP1 expression in specific adipose depots to increase energy expenditure and improve metabolic health. *Am J Physiol Regul Integr Comp Physiol* **311**, R79-88
180. Wu, J., Cohen, P., and Spiegelman, B. M. (2013) Adaptive thermogenesis in adipocytes: is beige the new brown? *Genes & development* **27**, 234-250
181. Harms, M., and Seale, P. (2013) Brown and beige fat: development, function and therapeutic potential. *Nature medicine* **19**, 1252-1263

182. Wang, W., and Seale, P. (2016) Control of brown and beige fat development. *Nat Rev Mol Cell Biol* **17**, 691-702
183. Koliwad, S. K., Gray, N. E., and Wang, J. C. (2012) Angiopoietin-like 4 (Angptl4): A glucocorticoid-dependent gatekeeper of fatty acid flux during fasting. *Adipocyte* **1**, 182-187
184. Vitali, A., Murano, I., Zingaretti, M. C., Frontini, A., Ricquier, D., and Cinti, S. (2012) The adipose organ of obesity-prone C57BL/6J mice is composed of mixed white and brown adipocytes. *J Lipid Res* **53**, 619-629
185. Inagaki, T., Sakai, J., and Kajimura, S. (2016) Transcriptional and epigenetic control of brown and beige adipose cell fate and function. *Nat Rev Mol Cell Biol* **17**, 480-495
186. Kleiner, S., Mepani, R. J., Laznik, D., Ye, L., Jurczak, M. J., Jornayvaz, F. R., Estall, J. L., Chatterjee Bhowmick, D., Shulman, G. I., and Spiegelman, B. M. (2012) Development of insulin resistance in mice lacking PGC-1alpha in adipose tissues. *Proceedings of the National Academy of Sciences of the United States of America* **109**, 9635-9640
187. Fedorenko, A., Lishko, P. V., and Kirichok, Y. (2012) Mechanism of fatty-acid-dependent UCP1 uncoupling in brown fat mitochondria. *Cell* **151**, 400-413
188. Dempersmier, J., Sambeat, A., Gulyaeva, O., Paul, S. M., Hudak, C. S., Raposo, H. F., Kwan, H. Y., Kang, C., Wong, R. H., and Sul, H. S. (2015) Cold-inducible Zfp516 activates UCP1 transcription to promote browning of white fat and development of brown fat. *Mol Cell* **57**, 235-246
189. McQueen, A. E., Kanamaluru, D., Yan, K., Gray, N. E., Wu, L., Li, M. L., Chang, A., Hasan, A., Stifler, D., Koliwad, S., and Wang, J. C. (2017) The C-terminal Fibrinogen-like Domain of Angiopoietin-like 4 Stimulates Adipose Tissue Lipolysis and Promotes Energy Expenditure. *J Biol Chem*
190. Reif, S., Lang, A., Lindquist, J. N., Yata, Y., Gabele, E., Scanga, A., Brenner, D. A., and Rippe, R. A. (2003) The role of focal adhesion kinase-phosphatidylinositol 3-kinase-akt signaling in hepatic stellate cell proliferation and type I collagen expression. *J Biol Chem* **278**, 8083-8090
191. Chen, J. (2010) The Src/PI3K/Akt pathway may play a key role in the production of IL-17 in obesity.
192. Boucher, J., Kleinridders, A., and Kahn, C. R. (2014) Insulin Receptor Signaling in Normal and Insulin-Resistant States. in *Cold Spring Harb Perspect Biol*. pp
193. Cheng, Z., Tseng, Y., and White, M. F. (2010) Insulin signaling meets mitochondria in metabolism. *Trends in endocrinology and metabolism: TEM* **21**, 589-598
194. Rui, L. (2014) Energy metabolism in the liver. *Comprehensive Physiology* **4**, 177-197
195. Bisht, B., Srinivasan, K., and Dey, C. S. (2008) In vivo inhibition of focal adhesion kinase causes insulin resistance. *The Journal of physiology* **586**, 3825-3837
196. Bisht, B., and Dey, C. S. (2008) Focal Adhesion Kinase contributes to insulin-induced actin reorganization into a mesh harboring Glucose transporter-4 in insulin resistant skeletal muscle cells. *BMC cell biology* **9**, 48
197. Ferrannini, E. (2014) The target of metformin in type 2 diabetes. *N Engl J Med* **371**, 1547-1548
198. Poher, A. L., Altirriba, J., Veyrat-Durebex, C., and Rohner-Jeanrenaud, F. (2015) Brown adipose tissue activity as a target for the treatment of obesity/insulin resistance. *Front Physiol* **6**, 4

199. Lee, P., and Greenfield, J. R. (2015) Non-pharmacological and pharmacological strategies of brown adipose tissue recruitment in humans. *Mol Cell Endocrinol*
200. Jaworski, K., Sarkadi-Nagy, E., Duncan, R. E., Ahmadian, M., and Sul, H. S. (2007) Regulation of triglyceride metabolism. IV. Hormonal regulation of lipolysis in adipose tissue. *Am J Physiol Gastrointest Liver Physiol* **293**, G1-4
201. Young, S. G., and Zechner, R. (2013) Biochemistry and pathophysiology of intravascular and intracellular lipolysis. *Genes & development* **27**, 459-484
202. Robidoux, J., Martin, T. L., and Collins, S. (2004) Beta-adrenergic receptors and regulation of energy expenditure: a family affair. *Annu Rev Pharmacol Toxicol* **44**, 297-323
203. Collins, S., Cao, W., and Robidoux, J. (2004) Learning new tricks from old dogs: beta-adrenergic receptors teach new lessons on firing up adipose tissue metabolism. *Mol Endocrinol* **18**, 2123-2131
204. Rosenwald, M., Perdikari, A., Rulicke, T., and Wolfrum, C. (2013) Bi-directional interconversion of brite and white adipocytes. *Nature cell biology* **15**, 659-667
205. Wu, J., Bostrom, P., Sparks, L. M., Ye, L., Choi, J. H., Giang, A. H., Khandekar, M., Virtanen, K. A., Nuutila, P., Schaart, G., Huang, K., Tu, H., van Marken Lichtenbelt, W. D., Hoeks, J., Enerback, S., Schrauwen, P., and Spiegelman, B. M. (2012) Beige adipocytes are a distinct type of thermogenic fat cell in mouse and human. *Cell* **150**, 366-376
206. Bachman, E. S., Dhillon, H., Zhang, C. Y., Cinti, S., Bianco, A. C., Kobilka, B. K., and Lowell, B. B. (2002) betaAR signaling required for diet-induced thermogenesis and obesity resistance. *Science (New York, N.Y.)* **297**, 843-845
207. Vijgen, G. H., Sparks, L. M., Bouvy, N. D., Schaart, G., Hoeks, J., van Marken Lichtenbelt, W. D., and Schrauwen, P. (2013) Increased oxygen consumption in human adipose tissue from the "brown adipose tissue" region. *The Journal of clinical endocrinology and metabolism* **98**, E1230-1234
208. Lee, P., Werner, C. D., Kebebew, E., and Celi, F. S. (2014) Functional thermogenic beige adipogenesis is inducible in human neck fat. *International journal of obesity (2005)* **38**, 170-176
209. Sharp, L. Z., Shinoda, K., Ohno, H., Scheel, D. W., Tomoda, E., Ruiz, L., Hu, H., Wang, L., Pavlova, Z., Gilsanz, V., and Kajimura, S. (2012) Human BAT possesses molecular signatures that resemble beige/brite cells. *PloS one* **7**, e49452
210. Yoneshiro, T., and Saito, M. (2015) Activation and recruitment of brown adipose tissue as anti-obesity regimens in humans. *Annals of medicine* **47**, 133-141
211. Saito, M. (2013) Brown adipose tissue as a therapeutic target for human obesity. *Obesity research & clinical practice* **7**, e432-438
212. Nedergaard, J., and Cannon, B. (2013) UCP1 mRNA does not produce heat. *Biochimica et biophysica acta* **1831**, 943-949
213. Fukano, K., Okamatsu-Ogura, Y., Tsubota, A., Nio-Kobayashi, J., and Kimura, K. (2016) Cold Exposure Induces Proliferation of Mature Brown Adipocyte in a ss3-Adrenergic Receptor-Mediated Pathway. *PloS one* **11**, e0166579
214. Collins, S. (2011) β-Adrenoceptor Signaling Networks in Adipocytes for Recruiting Stored Fat and Energy Expenditure. *Front Endocrinol (Lausanne)* **2**
215. Bartelt, A., and Heeren, J. (2012) The holy grail of metabolic disease: brown adipose tissue. *Current opinion in lipidology* **23**, 190-195

216. Park, J. W., Jung, K. H., Lee, J. H., Quach, C. H., Moon, S. H., Cho, Y. S., and Lee, K. H. (2015) 18F-FDG PET/CT monitoring of beta3 agonist-stimulated brown adipocyte recruitment in white adipose tissue. *Journal of nuclear medicine : official publication, Society of Nuclear Medicine* **56**, 153-158